Mineralogical and porosity characterisation of potential aquifer and seal units for carbon capture and storage methodologies for the CASSEM Project

Responsive Strategic Surveys Scotland Programme

Commissioned Report CR/08/153

Mineralogical and porosity characterisation of potential aquifer and seal units for carbon capture and storage methodologies for the CASSEM Project

A E Milodowski and J E Rushton

BRITISH GEOLOGICAL SURVEY

The full range of our publications is available from BGS shops at Nottingham, Edinburgh, London and Cardiff (Welsh publications only) see contact details below or shop online at www.geologyshop.com

The London Information Office also maintains a reference collection of BGS publications, including maps, for consultation.

We publish an annual catalogue of our maps and other publications; this catalogue is available online or from any of the BGS shops.

The British Geological Survey carries out the geological survey of Great Britain and Northern Ireland (the latter as an agency service for the government of Northern Ireland), and of the surrounding continental shelf, as well as basic research projects. It also undertakes programmes of technical aid in geology in developing countries.

The British Geological Survey is a component body of the Natural Environment Research Council.

British Geological Survey offices

BGS Central Enquiries Desk

Tel   0115 936 3143   Fax   0115 936 3276
email   enquiries@bgs.ac.uk

Kingsley Dunham Centre, Keyworth, Nottingham NG12 5GG

Tel   0115 936 3241   Fax   0115 936 3488
email   sales@bgs.ac.uk

Murchison House, West Mains Road, Edinburgh EH9 3LA

Tel   0131 667 1000   Fax   0131 668 2683
email   scotsales@bgs.ac.uk

Natural History Museum, Cromwell Road, London SW7 5BD

Tel   020 7589 4090   Fax   020 7584 8270
Tel   020 7942 5344/45   email   bgslondon@bgs.ac.uk

Columbus House, Greenmeadow Springs, Tongwynlais, Cardiff CF15 7NE

Tel   029 2052 1962   Fax 029 2052 1963

Forde House, Park Five Business Centre, Harrier Way, Sowton EX2 7HU

Tel   01392 445271   Fax   01392 445371

Maclean Building, Crowmarsh Gifford, Wallingford OX10 8BB

Tel   01491 838800   Fax   01491 692345

Geological Survey of Northern Ireland, Colby House, Stranmillis Court, Belfast BT9 5BF

Tel   028 9038 8462   Fax   028 9038 8461

www.bgs.ac.uk/gsni/

Parent Body

Natural Environment Research Council, Polaris House, North Star Avenue, Swindon SN2 1EU

Tel   01793 411500   Fax   01793 411501
www.nerc.ac.uk

Website www.bgs.ac.uk
Shop online at   www.geologyshop.com

Foreword

This report is the published product of a study by the British Geological Survey (BGS) for the CASSEM consortium. It details the mineralogical and petrological characterisation of samples of Permo-Triassic reservoir (aquifer) and seal units from the Yorkshire-Lincolnshire-Nottinghamshire area in Eastern England, and Devonian-Carboniferous reservoir (aquifer) and seal units from the Forth area in eastern central Scotland that was undertaken in Work Package 1 of the CASSEM Project. This report should be read in conjunction with the two other BGS reports from Work Package 1 – Monaghan et al., CR/08/151 and Ford et al., CR/08/152. Use and release of this report to third parties is subject to the terms of the CASSEM collaboration agreement.

Acknowledgements

Contents

FIGURES

TABLES

Summary

This report describes the methods used and data collected in mineralogical and petrological characterisation of potential carbon capture and storage (CCS) aquifer and seal units in Yorkshire-Lincolnshire-Nottinghamshire and the Forth area of eastern central Scotland. It forms part of CASSEM work package 1 (WP1).

1 Introduction

Low-carbon use of fossil fuels requires capture of CO_2 at power stations, and storage in the pore space of rock units deep below ground. Volumetrically, CO_2 can be most efficiently stored underground because, with increasing pressure and temperature as CO_2 is injected deep into the subsurface, it undergoes a sharp increase in density (thereby reducing its volume) that is associated with phase change from gas to a liquid or supercritical fluid (Gale, 2004; Chadwick et al., 2004). The critical point of CO_2 is approximately 31 °C and 74 bar (Atkins, 1982). These conditions are generally reached at depths between 500 and 1000 m, principally dependant on the geothermal gradient (Chadwick et al., 2004). The basic requirement for the subsurface storage of CO_2 is the identification of porous candidate aquifer formations in the vicinity of CO_2 producing power stations, the sufficient volume to accommodate the CO_2 production, and suitable seal rocks and structural traps.

The CASSEM project will develop new methodologies, workflows and insights essential for the successful identification and evaluation of safe and effective CO_2 storage sites in offshore saline aquifers. The project will select on-shore and/or near-shore sites from which useful analogue data and information can be obtained in order to characterise important aquifer and cap rock systems. This will be done in the vicinity of two groupings of power stations in the Midland Valley of Scotland (Longannet, ScottishPower) and in the Yorkshire-Lincolnshire area of England (Ferrybridge, Scottish and Southern Energy). The CASSEM Project is a consortium led by Scottish Power Ltd. with Scottish and Southern Energy Plc., AMEC, Schlumberger Oilfield UK Plc., Marathon Oil, Heriott-Watt University, University of Edinburgh and the British Geological Survey (BGS).

The BGS component of the CASSEM Project is funded by the Department for Business, Enterprise and Regulatory Reform (now DECC), through the Engineering and Physical Sciences Research Council (EPSRC). It contributes to Phase 1 of the project 2008-2009, which includes stratigraphical and structural surveys and modelled surfaces leading to evaluation of injection pathways, geochemical reactivity, rock mechanics and physics of the aquifer and seal rocks and options for monitoring. The research activities aim to deliver up to date summaries, 3D analysis and sample descriptions of the underpinning geological units and structures present in the subsurface in the vicinity of the selected onshore and coastal power generation sites. These data are required to underpin and deliver the research activities of the other partners. This report deals with the acquisition, selection and analysis of representative samples of aquifer/reservoir and seal units from the two study areas, to provide background data on their modal mineralogical composition and porosity characteristic that are required for reservoir modelling and evaluation that is being carried out by project partners at Heriott-Watt and Edinburgh universities.

2 Sample location and selection

2.1   GENERAL

Budget provision within the CASSEM Project allowed for the analysis of a total of 80 samples of aquifer reservoir rocks and seal lithologies during the lifetime of the project, to include requirements for WP1 and subsequent drilling and characterisation of new borehole core previously planned under WP5. This meant that between 30-35 samples were envisaged to be analysed from each the two target areas − the Yorkshire-Lincolnshire area and Forth area ─ within WP1 (i.e. a total of approximately 60─75 samples). A subset of the samples examined for mineralogy was also collected for and supplied to Heriott-Watt University for geomechanical and petrophysical testing.

Thin sections were taken from samples in the vertical plane, approximately perpendicular to bedding where possible. All BGS-held borehole/well core material over the areas of interest was considered. The sampling strategy and background sample information are described in the following sections.

2.2   YORKSHIRE-LINCOLNSHIRE-NOTTINGHAMSHIRE AREA

The focus of interest in this area is the Ferrybridge Power Station in Yorkshire. The geology of the region is described by Ford et al. (2008) and the stratigraphy is summarised in Table 1.

The primary target reservoir unit is the Triassic Sherwood Sandstone Group. This comprises a thick sequence of porous and permeable fluvial and aeolian sandstones and represents a major onshore aquifer, plus it hosts important oil and gas reservoirs offshore in the southern North Sea (Downing et al., 1986; Allen et al., 1997). The Sherwood Sandstone Group in the east of the region reaches appropriate depths and temperatures (Ford et al., 2008), and appears to have sufficient volume and porosity for the potential storage of CO_2 as a supercritical fluid. It is overlain by the Mercia Mudstone Group which represents a thick sequence of argillaceous strata that offer a potential caprock seal.

A secondary target aquifer/seal pair exists at greater depth, represented by the sandstone-dominated Permian Rotliegendes Group and overlying Marl Slate, Cadeby and succeeding evaporite seal formations. These strata underlie the area at progressively increasing depth to the east, attaining depths appropriate for supercritical CO_2 stage onshore in Lincolnshire and Humberside (Ford et al., 2008). Although the Permian strata offer smaller storage capacity than the Sherwood Sandstone Group, the broad spatial coincidence of the primary and secondary target sequences suggests that secondary aquifer may add to the potential capacity of the primary target, and the primary seal may also contribute to the overall containment of secondary aquifer (Ford et al., 2008).

The availability of suitably deep (>500 m) samples of target aquifer and seal rocks from this area within the BGS reference collections and core archives is limited. Most of the archived material is either from outcrop or from relatively shallow boreholes (<400 m) in the freshwater aquifer zone. Previous detailed petrological investigations by Bath et al. (1986) and Milodowski et al. (1987) showed that the mineralogy, porosity and permeability of the Sherwood Sandstone Group and Permian sandstones at outcrop and in the shallow aquifer are strongly influenced by leaching and alteration associated with weathering and meteoric groundwater invasion. This has possibly been ongoing since the Pleistocene, and extends down-gradient for up to 20 km eastwards into confined aquifer. Consequently, CASSEM sampling strategy sought to avoid sampling material from outcrop and the unconfined shallow aquifer, since these rocks are unlikely to have

mineralogical, porosity and permeability characteristics that will be analogous to those encountered in the deep Sherwood Sandstone Group aquifer.

Deep hydrocarbon exploration wells drilled to access hydrocarbons with reservoirs in the Carboniferous in the Eakring, Hatfield, Welton and Saltfleetby oilfields (cf. Rothwell and Quinn, 1987; Scott and Colter, 1987; Storey and Nash, 1993; Hodge, 2003; Ward et al., 2003), penetrate the Permo-Triassic rocks at target depths. Unfortunately, these wells did not core the Permo-Triassic strata, and the only archived core material available represents the Carboniferous reservoir rocks. Therefore, the CASSEM sampling strategy focussed on the only available deep core material for the Sherwood Sandstone Group, Basal Permian aquifer lithologies and Marl Slate Formation, from the Cleethorpes No.1 Geothermal Well (Figure 1), drilled as part of the UK Department of Energy (DoE now DECC)-BGS Investigation of the Geothermal Potential of the UK research programme (Downing et al., 1985).

The Cleethorpes No.1 borehole recovered three short intervals of core from the deep saline (brine) aquifer in the Sherwood Sandstone Group (Core No.1:1112–1121 m, Core No.2:1203–1209 m, and Core No.3:1304–1322 m). One short cored interval (Core No.4 from 1855 m to about 1891 m) contains the Basal Permian aquifer sequence, including the Yellow Sands Formation and a local basal breccia, from the base of the Marl Slate Formation (caprock), to its unconformity with the underlying Carboniferous (Coal Measures). A total of 39 samples were examined from the Cleethorpes No.1 Geothermal Well, comprising: 13 samples from the Yellow Sands Formation and basal breccia and sandstones (Basal Permian aquifer); 2 samples from the Marl Slate Formation; and 24 samples from the Sherwood Sandstone Group (Table 2). These samples included 30 archived polished thin sections of from the original geothermal research project (Milodowski et al., 1987) identified by sample numbers CLSH01 to CLSH21 (Sherwood Sandstone Group) and CLBP01 to CLBP11 (Basal Permian sandstones and breccias) in the digital datasets (provided on the CDROM enclosure). Fourteen samples were also examined for comparison from the confined freshwater aquifer in the Sherwood Sandstone Group. These include 11 samples taken from depths between 32–212 m in the Gamston research borehole (Brown, 1970); 2 samples from between 212–215 m deep in the Cropwell Bishop (Cropwell Bridge) borehole; and 1 sample from a depth of 378 m in the Fulbeck Airfield No.1 borehole (Figure 1, Table 2). The Gamston borehole samples include 6 archived polished thin sections originally prepared for the geothermal research project (Milodowski et al., 1987). These are identified by the sample numbers G105 to G509 in the digital datasets.

The Mercia Mudstone Group was sampled from the Cropwell Bishop (8 samples) and Fulbeck Airfield No.1 (2 samples) borehole cores. The Cropwell Bishop borehole provided a series of samples representing the sequence from the Tarporley Siltstone Formation (formerly Keuper Waterstones), Sidmouth Mudstone Formation — Radcliffe Member, Sidmouth Mudstone Formation - Gunthorpe Member, Sidmouth Mudstone Formation — Edwalton Member, and Branscombe Mudstone Formation (Howard et al., 2008; Table 2). As in the eastern part of the region (cf. Ford et al., 2008), the Mercia Mudstone Group in Fulbeck Airfield No.1 is undifferentiated.

The sampling strategy sought to be representative of the principal lithologies observed in core, as well as provide examples of the range in lithologies. In addition, samples were selected to cover the depth range of the main sequences of aquifer units in Cleethorpes No.1 and Gamston boreholes, and of the Mercia Mudstone Group in the Cropwell Bishop borehole. This objective was reasonably well-met for these units. However, the complexity of lithological variation within the Mercia Mudstone Group meant that often only one sample of differentiated formation could be examined within the constraints of project resources. Furthermore, the Mercia Mudstone Group in these shallow boreholes exhibits complex deformation, alteration and secondary gypsum mineralisation that is associated with fracturing, hydration and alteration of primary anhydrite fabrics. Project limitations also excluded these features from the present study.

Table 1. Lithological summary of the bedrock succession in the region of study (from Ford et al., 2008). Shaded and red borders show level of subdivision represented by the bedrock geology model defined by the BGS (Ford et al., 2008).

	Group/SubPeriod	Formations		Dominant lithology
CRETACEOUS	Chalk Group (Upper Cretaceous)	Undivided		Chalk and marly-chalk, flint as nodules and persistent horizons
	Lower Cretaceous	Undivided		Sandstones, mudstones, ironstones and chalk
JURASSIC	Upper Jurassic	Undivided (Inc. Lincs. Limestone Formation ━━━)		Mudstone with minor sandstones, limestones and siltstones
	Middle Jurassic	Undivided		Limestones, sandstones, shales and ironstones
	Lias Group (Lower Jurassic)	Undivided		Mudstones with subordinate limestones, siltstones, sandstones and ironstones
TRIASSIC	**Penarth Group**	Not fully divisible in area		Grey and greenish grey calcareous mudstone
	Mercia Mudstone Group	Not fully divisible in area		Red-brown calcareous mudstone and siltstone with anhydrite and gypsum
	Sherwood Sandstone Group	Not fully divisible in area		Red-brown sandstone with calcareous mudstone and mud-flake conglomerate.
PERMIAN	Zechstein Group	**Roxby Formation Equivalents**	Roxby Formation (including Littlebeck Anhydrite Formation)	Red-brown calcareous and anhydritic or gypsiferous mudstone
				Anhydrite with minor gypsum
				Red-brown calcareous and anhydritic or gypsiferous mudstone
			Sherburn Anhydrite Formation	Grey and red-brown anhydrite, minor gypsum and mudstone
			Roxby Formation (part)	Red-brown calcareous and anhydritic or gypsiferous mudstone
			Boulby Halite Formation	Salt
			Billingham Anhydrite Formation	Grey anhydrite with minor gypsum
		Brotherton Formation		Light grey fine-grained dolomitic limestone
		Edlington Formation Equivalents	Edlington Formation (including Grauer Salzton and Fordon Evaporite fms)	Salt and mudstone
				Red-brown calcareous and anhydritic mudstone with minor gypsum
				Salt with mudstone
			Kirkham Abbey Formation	Grey dolostone
			Hayton Anhydrite Formation	Grey anhydrite with minor gypsum
		Cadeby Formation		Grey and light yellowish brown dolostone
		Marl Slate Formation		Dark grey laminated dolomitic pyritic mudstone
	Rotliegendes Group	Yellow Sands Formation		Grey fine-grained aeolian sand
		Permian Basal Breccia		Sandstones and matrix supported conglomerate

4
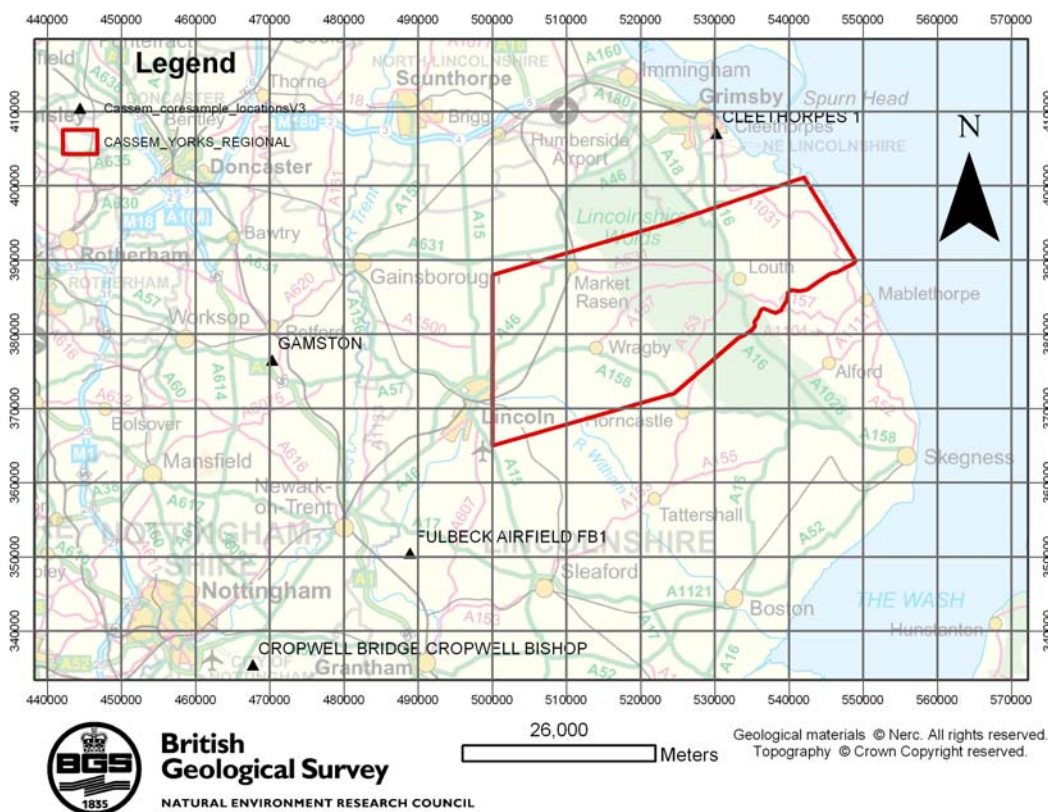
Figure 1. Map showing the location of cored boreholes from which samples of Permo-Triassic strata were obtained in the Yorkshire-Lincolnshire-Nottinghamshire area.

Table 2. Summary of sample numbers and distribution by formation or group in sampled boreholes from the Yorkshire-Lincolnshire-Nottinghamshire

Lithological unit		Borehole and no. of samples
Mercia Mudstone Gp.	Branscombe Mdstn Fm.	Cropwell Bishop [1 sample]
	Sidmouth Mdstn Fm. – Edwalton Member	Cropwell Bishop [1 sample]
	Sidmouth Mdstn Fm. – Gunthorpe Member	Cropwell Bishop [1 sample]
	Sidmouth Mdstn Fm. – Radcliffe Member	Cropwell Bishop [1 sample]
	Tarporley Siltstone Formation	Cropwell Bishop [4 samples]
	Undifferentiated stratigraphy	Fulbeck Airfield No.1 [2 samples]
Sherwood Sandstone Group		Cleethorpes No.1 [24 samples]
		Cropwell Bishop [2 samples]
		Fulbeck Airfield No.1 [1 sample]
Roxby Formation (mudstone lithology)		North Selby No.2 [1 sample]
		Whitemoor [1 sample]
Sherburn Anhydrite Formation (Roxby Equivalent)		Whitemoor [1 sample]
Marl Slate Formation		Cleethorpes No.1 [2 samples]
Yellow Sands Fm. and Basal Permian breccias (Rotliegendes Gp.)		Cleethorpes No.1 [13 samples]

The Marl Slate, Cadeby and succeeding evaporite seal formations overlying the Basal Permian aquifer are poorly-represented. This is partly because of the lack of availability of suitable preserved core samples from these rocks, and partly because these formations are lithologically extremely variable. Thus due to the resource constraint on the number of samples which could be analysed within the CASSEM Project, representative sampling and analysis of these formations could not be achieved. Consequently, only 2 examples of Roxby Formation mudstones and 1 example of the Sherburn Anhydrite Formation (Roxby Equivalent) were sampled from the Whitemoor and North Selby No.2 boreholes in the Selby Coalfield area in order to provide at least some information on these rocks. These borehole samples come from an area to the north of the western part of Figure 1.

2.3   FORTH AREA, SCOTLAND, UK

The focus of interest in Midland Valley of Scotland is to investigate methodologies for saline aquifer carbon capture and storage (CCS) in the vicinity of the Longannet Power Station. This geology of this region is very complex, with a series of Devonian, Carboniferous and Permian basins containing up to 5 km of largely fluvio-lacustrine and marginal marine sedimentary rocks (Monaghan et al., 2008 and references therein). The strata are highly heterogeneous, comprising a variety of intercalated mudstones, siltstones, sandstones, coals and limestones, with extrusive and intrusive igneous rocks. Consequently, there is a complex assemblage of potential aquifers and seal rocks hosted within the Carboniferous and Devonian stratigraphical sequence, which are summarised in Table 3. Minor accumulations of oil have been found within small anticlinal structures (Hallett et al., 1985; Scott and Colter, 1987) showing that the sequence contains potential reservoir units with effective seal rocks. The geology of the Forth area is described in detail by Monaghan et al. (2008).

The main target aquifers are the aeolian sandstones of the Knox Pulpit Sandstone Formation (Late Devonian) and the fluvial-dominated sandstones of the Kinnesswood Formation (Early Carboniferous). The main target seal is the Ballagan Formation (Early Carboniferous), which comprises intercalated mudstones, siltstones and fine sandstones. In addition, a number of other minor aquifer and seal units that may contribute to the CO_2 storage capacity of potential sites in the region (Monaghan et al., 2008).

The availability of suitably deep (>500 m) core samples of target aquifer and seal rocks was limited. No archived polished thin sections suitable for backscattered scanning electron microscopy (BSEM) analysis were available from the BGS collections for this area. Therefore, all the samples analysed were taken from borehole cores and outcrop material specifically sampled for the CASSEM Project. A total of 32 samples of aquifer and seal rocks were examined from the Forth area. The sampling strategy focussed on the relatively deep Glenrothes borehole (samples from 186–584 m; Figure 2), which was originally drilled under the BGS-DoE geothermal project. This provided samples from the Pathhead Formation (1 sample), Ballagan Formation (4 samples), transitional strata between the Ballagan Formation and Kinnesswood Sandstone Formation (1 sample), Kinnesswood Sandstone Formation (2 samples), Knox Pulpit Sandstone Formation (5 samples) (Table 3).

A smaller number of samples were also taken from relatively deep borehole cores from: the Kinkardine East borehole ─ Passage Formation (1 sample) and Upper Limestone Formation (2 samples); Milton of Balgonie No.2 borehole ─ Pathhead Formation (2 samples); Cousland Borehole No.6 ─ West Lothian Oil Shale Formation (1 sample); and Briathorne No.4 Seabore (NCB) ─ Upper Coal Measures (1 sample). Additional samplesof the Kinnesswood Sandstone Formation (2 samples), Knox Pulpit Sandstone Formation (4 samples); Burnside Sandstone Formation (2 samples), and Lower Coal Measures (4 samples) were also taken from a series of outcrop sites and shallow (< 60 m) water boreholes (Figure 2, Table 3).

6

Table 3. Potential aquifer and seal rocks for CCS in the Forth area, eastern central Scotland (from Monaghan et al., 2008).

Geological unit – potential aquifer	Age	Description	Borehole/site and number of samples
Passage Formation (PGP) and upper part of Upper Limestone Formation (ULGS) above Calmy Limestone (CAL)	Namurian - middle part of Carboniferous	Can be sandstone dominated	Kincardine East BH [PGP 1 sample; ULGS - 2 samples]
Strathclyde Group (SYG) Pathhead (PDB) Sandy Craig (SCB) Pittenweem (PMB) Anstruther (ARBS) Fife Ness (FNB)	Visean - Early Carboniferous	Sandstones in the fluvio-deltaic sedimentary rocks	Glenrothes BH [PDB – 1 sample] Milton of Balgonie No.2 BH [2 samples]
Aberlady Formation (ABY) Gullane Formation (GUL)	Visean	Sandstones in the fluvio-deltaic sedimentary rocks	Cousland BH No.6 [1 sample from the West Lothian Oil Shale Formation = Aberlady Formation]
Clyde Sandstone Formation (CYD)			No samples
Kinnesswood Formation (KNW)	Early Carboniferous	With Knox Pulpit and Glenvale sandstones – fluvial.	Glenrothes BH [4 samples] Balreavie No.3 Water BH [1 samples] Marspie Den outcrop [1 sample]
Knox Pulpit Sandstone Formation (KPF)	Late Devonian	Mainly aeolian sandstones	Glenrothes BH [5 samples] Balreavie No.3 Water BH [1 sample] Easter Lathrisk Water No.6 [1 sample] Arraty Crags outcrop [2 samples]
Glenvale Sandstone Formation (GEF)	Late Devonian	With Kinnesswood and Knox Pulpit sandstones– fluvial.	No samples
Burnside Sandstone Formation (BRN)	Late Devonian	Fluvial sandstone, conglomerate and mudstone	Mawcarse Station Water BH [2 samples]
Geological unit – potential seal	**Age**	**Description**	**Borehole/site and number of samples**
Lower (LCMS), Middle (MCMS), Upper (UCMS) Coal Measures	Late Carboniferous	Intercalated mudstone, siltstone, sandstone and coal well over 150m thick	Earlseat Opencast Site [4 samples]
Claystone unit in Early Carboniferous			No samples
Ballagan Formation (BGN)	Early Carboniferous	Intercalated mudstone, siltstone, fine grained sandstone, dolostone and limestone (though Ballagan Fm can be sand-rich in Lothians)	Glenrothes BH [4 samples]
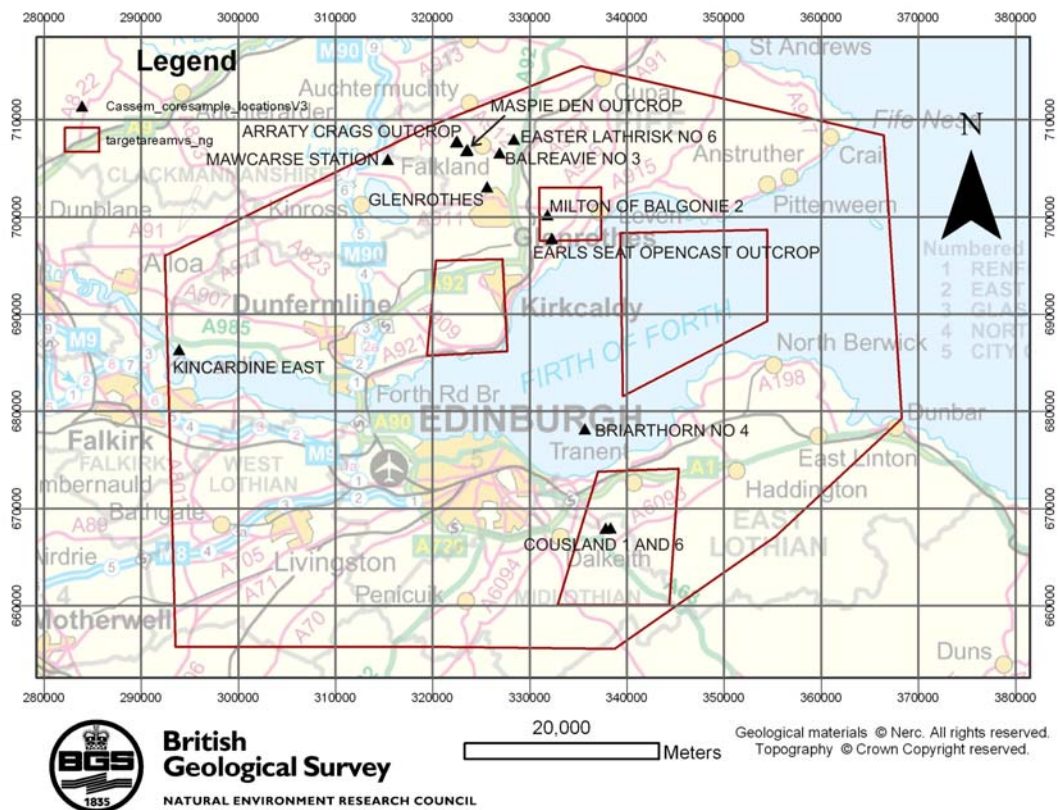
Figure 2. Map showing the location outcrop sampling points and cored boreholes examined in the Forth area, central Eastern Scotland.

Further sample details are given in the datasets provided the digital datasets (provided on the CDROM enclosure).

The scope of the project did allow for a sampling campaign to examine the detailed lithological variations. However, as far as possible within the resource limitations, samples were selected to be representative of the dominant lithologies of the main target strata: the Knox Pulpit Sandstone, Kinnesswood Sandstone and Ballagan formations. However, these strata are quite variable and not all of the lithologies could be represented. For the other minor aquifer and seal units, a very limited number of samples were taken, where suitable outcrop and borehole material was readily available, in order to provide examples of some of the lithologies. In these cases, the examples sampling tried to represent the dominant lithology.

3 Methods

3.1   MINERALOGICAL AND PETROGRAPHICAL ANALYSIS

3.1.1   Petrographical section preparation

Mineralogical and petrographical analysis was undertaken on 30 µm thick, 45 x 28 mm polished thin sections prepared from samples selected to represent principal potential aquifer (reservoir) rocks, and caprock and basal seal lithologies from the two study areas.

The new rock samples collected specifically for the CASSEM Project (see Section 2) were initially impregnated with epoxy-resin under vacuum in order to stabilise friable or unstable material. A blue dye was added to the epoxy-resin to enable any natural porosity to be readily identified and distinguished under the optical petrological microscope. Previous BGS research on the Permo-Triassic rocks from the Yorkshire Lincolnshire had shown that these rocks may contain significant amounts of water-soluble minerals (e.g. anhydrite, gypsum and halite) as important pore-filling cements. Therefore, in order to ensure preservation of these minerals all the polished thin sections (for both study areas) were lapped and polished under alcohol to prevent mineral dissolution and the production of artefacts that might otherwise be interpreted as porosity. A similar protocol had been used previously in the preparation of the polished thin sections which were re-examined for the CASSEM Project from the earlier BGS investigations on the Sherwood Sandstone Group and Basal Permian aquifer rocks from the Yorkshire-Lincolnshire-Nottinghamshire area (Milodowski et al., 1987; Bath et al., 1987). This ensures that observations from the archived thin sections will be comparable with any information recorded from the new CASSEM Project sections.

3.1.2   Optical petrography

Prior to detailed petrographical observations and modal analysis by backscattered scanning electron microscopy and energy-dispersive X-ray microanalysis, the polished thin sections were briefly examined in transmitted light using a Zeiss Axioplan 2 optical petrographic (polarising) microscope. Low magnification images of whole thin sections were also recorded by digitally scanning of the thin section using an Epsom Perfection 1240U flatbed scanner equipped with a transmitted light (transparency) scanning attachment. Scanned whole-section images were recorded at a resolution of 1200 dpi.

3.1.3   Backscattered scanning electron microscopy

Detailed mineralogical and petrographic observations were made on the polished thin sections using backscattered scanning electron microscopy (BSEM). BSEM was largely carried out using either:

- A LEO 435VP variable pressure digital scanning electron microscope (SEM) fitted with a solid-state 4-element (diode) backscattered electron detector, and equipped with an Oxford Instruments INCA Energy 350 energy-dispersive X-ray microanalysis (EDXA) system with a thin window Si-Li X-ray detector capable of detecting elements from boron to uranium. This analytical facility was used in preference for a larger proportion of the analyses because of its capability to record higher resolution images and greater computing power that enabled more efficient and higher quality (lower noise) EDXA X-ray elemental maps.

- A Cambridge Stereoscan S360 SEM instrument fitted with a solid-state 4-element (diode) backscattered electron detector, and equipped with an Oxford Instruments INCA Energy 450 energy-dispersive X-ray microanalysis (EDXA) system with a Ge-Li (GEM) X-ray detector capable of detecting elements from boron to uranium. This instrument was used to provide additional analytical support but because of its lower resolution and its more limited capacity to record high quality EDXA X-ray maps, fewer samples were analysed using this system.

The polished sections were coated with a thin layer (250–350 Å) of carbon by carbon evaporation under vacuum, in order to make their surface electrically conductive for high-resolution BSEM examination under conventional high vacuum mode ($<1 \times 10^{-4}$ torr).

For general petrographical observations, the SEM instrument was operated using a 20 kV electron beam accelerating potential, a beam current between 200-800 pA, and a working distance of 18–20 mm (LEO 435 VP instrument) or 25 mm (Cambridge S360 instrument), as required. Phase identification was aided by microchemical information obtained from observation of semi-quantitative EDXA spectra recorded from features of interest. BSEM images for routine observation purposes were recorded digitally via the SEM instrument at a resolution of 1024 x 768 pixels. However, BSEM images that were used for subsequent computerised petrographical image analysis to quantify the porosity characteristics (see Section 3.2) were collected at 1024 x 704 or higher 2048 x 1408 pixel resolutions via the Oxford INCA Energy EDXA system.

3.1.4   Mineralogical modal analysis

3.1.4.1 IMAGE PROCESSING AND ANALYSIS

Modal mineralogical analysis was carried out by image analysis of digital EDXA elemental X-ray maps recorded from the polished thin sections using the SEM instrument described above (Section 3.1.3). Section areas for EDXA element mapping were selected to be representative of each polished thin section as a whole, on the basis of expert petrographer's judgment, taking into account the variability and heterogeneity observed during optical and BSEM microscopy. Areas for X-ray elemental mapping were imaged by BSEM at a magnification chosen to include approximately 400 image objects (including mineral grains and intergranular pore regions) within each image field of view (Figure 3). For generally homogenous samples, two fields of view (minimum) were recorded. However, where more than one lithology comprised a significant proportion of the thin section at least two images were recorded from each of the lithologies, and the modal mineralogy of each lithology was determined separately.

EDXA element maps were recorded using the 'Mapping' programme within the Oxford Energy INCA Suite Version 4.08 (2006) software package. EDXA X-ray spectral data were recorded from each pixel the field of view at a resolution of 512 x 512 pixels, using a 20 kV electron beam, 1 nA (1000 pA) beam currents and at a working distance of 19 mm (LEO 435VP, to give optimum X-ray count rates of between 1200 and 1600 counts per second. X-ray element maps were produced by summation of data recorded from multiple frame scans to produce maps with sufficient X-ray counts per pixel to enable key elements, required for the differentiation of the mineral species present, to be detected above background noise. In general, maps were recorded over a minimum of 20 frame scans were recorded to achieve sufficient analytical sensitivity within a practical time limit of about 1 hour per map area, using the LEO435VP SEM instrument. However, in the case of the Cambridge S360 SEM instrument it was only possible to capture EDXA element maps over 8–15 frame scans per map area due to computer memory limitations. Consequently, the noise in the EDXA maps recorded using the Cambridge S360 SEM was higher, resulting in poorer element detection, and thereby reducing the ability to differentiate mineral phases as clearly during subsequent processing of the EDXA element map data.

BSEM image acquired from representative area, selected to include c.400 image objects

Continuous EDXA spectra are recorded from each pixel within the image area and summed over a number of frame scans (e.g. 20 frame scans)

Detected elements characteristic of minerals of interest are selected from Periodic Table menu

Distribution of selected elements displayed as concentration maps indicated by colour-contoured rainbow X-ray intensity scale

Groups of 3 element maps characteristic of key phases are selected, and the ratios of their X-ray intensity within each pixel in the image are plotted on a triangular ratio plot.

The clusters of data differentiate phases on the basis of different chemical composition

The boundary of each compositional cluster is defined interactively by expert judgement, and the pixel distribution and total pixel percentage area corresponding to each cluster is defined and displayed as a specific 'phase'.

The fit of the chemically-defined 'phase' is compared with the BSEM image, and the compositional limits of the phase data cluster manually modified iteratively to give the best visual fit of phase boundaries to the BSEM image

Figure 3. Work flow diagram for image processing of EDXA element maps for mineralogical modal analysis

EDXA element maps were processed to differentiate mineral/phase distributions and area percentages using the 'PhaseMap' programme within the Oxford Energy INCA Suite Version 4.08 (2006) software package (Figure 3). Groups of three elements were selected, as appropriate to define specific minerals or other components phases on the basis of their chemistry. For example, maps of K, Al and Si concentration can be used to differentiate between quartz, K-feldspar and muscovite, on the basis of the difference in the ratios of these elements within these minerals. Similarly, maps for C, O and Si differentiated between most minerals and the epoxy-resin-filled porosity in thin section. The ratio of X-ray count intensities for the characteristic X-ray line (K, L or M line) for each element within each pixel element of the map area was compared and plotted as a triangular ratio plot of the three elements. From this clusters of pixels could be identified with element concentration ratios corresponding to different phases. The compositional boundaries of each cluster of element ratios were defined by expert judgment, and the spatial distribution of pixels within these clusters displayed by the software as a map of that particular phase. The pixel area corresponding specific phase compositions could then be measured and its modal composition calculated in terms of the percentage of the total image area (Figure 3). Three elements were sufficient to define many of the minerals which were significantly different in chemistry. However, in some cases this process had to be repeated using several combinations of three elements to differentiate phases with more subtle differences in chemistry or where X-ray maps had not been acquired with sufficient X-ray counts to reliably detect some key elements (e.g. for light elements such as Na and Mg, where the quality of the EDXA data was noisier and poorer when recorded using smaller numbers of frame scans with the Cambridge Stereoscan S360 instrument). Where appropriate, some phases were calculated by difference between phase maps produced with different element combinations.

The BSEM recorded from the same area were subsequently used for the detailed quantification of porosity characteristics described in Section 3.2.

3.1.4.2 SOURCES OF ERROR AND UNCERTAINTY

There are a number of potential sources of error in the determination of the modal mineralogy, including the following:

1. Image resolution and magnification interact to have a potentially significant effect on the resolution of mineral grains, which in turn, influences the mineralogical modal analysis. The EDXA element maps were recorded at a resolution of 512 x 512 pixels per field of view. EDXA data recorded for each pixel represents the average composition within the pixel area. However, the actual area of the petrographic section that each pixel covers is dependent on the magnification of the image. Pixels recorded at a higher magnification sample smaller areas of the thin section, and therefore are more likely to resolve and sample finer grained material as discrete single phases. In contrast, pixels recorded at lower magnification will potentially include several mineral grains where the particle size is close to or finer than the pixel area. For pixels where this is the case, the EDXA data recorded at each pixel will reflect the average of the chemistry of the phases included within the pixel area.

2. Particle size and X-ray generation volume: Errors arise in the definition of the X-ray emission from very fine particles. X-rays may be generated by the electron beam from a region up to several micrometres deep in the sample, depending on mineral density and average atomic number. For fine particles (c. <5μm) X-ray emission may be generated from a region larger than the particle of interest and represent a mixture of phases.

3. Particle edge effects: Pixels at the edges of grains may overlap adjacent minerals. Consequently, pixels around grain margins may report mixed composition of the two adjacent phases.

4. X-ray detection limits for key elements place a major constraint on defining phases. Light elements including O, C, Na and Mg have particularly poor detection limits, and unless a significant number of frame scans are acquired can produce very noisy images. This can affect the discrimination of minerals where these key elements (e.g. albite (Na), porosity (C, O in epoxy resin)) are close to detection. This was a particular problem with data acquired on the Stereoscan S360 instrument, where only a small number of frame scans could be stored due to computing limitations.

5. Element X-ray line overlaps: Errors can arise where characteristic X-rays from different elements overlap. This may result in a high background and poorer element detection, or erroneous detection of elements (e.g. Ba L X-ray lines overlap with Ti K X-ray lines, making it difficult to differentiate between Ti and Ba phases on the basis of these elements alone.

6. Microporosity, pitting and scratching of the section surface and grain pluck sites within the polished section can produce anomalously low concentrations, as a result of the X-ray emission from pixels areas containing voids, returning a composition representing the average between void space and adjacent mineral substrate.

7. Operator definition of phase boundaries of the analysis clusters in compositional element triangular plots can be subjective, particularly if the compositions are gradational. This is very dependant on analyst experience. This was mitigated in the CASSEM project by (i) experienced expert mineralogist judgement; (ii) visually cross checking the goodness of fit between the boundaries of phases defined by X-ray mapping and the BSEM image; and (iii) only accepting measurements giving modal analysis totals between 95 and 105 % (before normalisation) — values outside these limits suggest significant missing components or major overlapping of defined phase boundaries.

8. Lithic clasts, chert and polymineralic grains. Conventional modal analysis by point-counting under a binocular microscope will differentiate lithic clasts (rock fragments), chert, polycrystalline quartz and monocrystalline quartz as discrete sedimentological components. This is based on expert judgment and the ability of the mineralogist to differentiate these components on the basis of their optical properties. However, modal analysis by SEM-EDXA phase mapping technique differentiates components on the basis of chemistry. Consequently, polymineralic lithic clasts will tend to be determined as their component minerals rather than as discrete particles, unless there is some distinctive chemical feature of the clast (such as sometimes produced by pervasive alteration). As a result, the modal analyses determined by SEM-EDXA phase mapping underestimate the significance of lithic components normally considered in sandstone classification (cf. Pettijohn et al., 1987; Hallsworth and Knox, 1999). Monocrystalline quartz, monocrystalline quartz and chert are all essentially composed of SiO_2, and are therefore simply grouped together as "quartz". Similarly, no differentiation can be made between primary sedimentary and secondary or authigenic generations of the same mineral using SEM-EDXA phase mapping.

These errors are difficult to estimate. Repeat analyses undertaken for a limited number of samples of Sherwood Sandstone Group from the Cleethorpes borehole suggest uncertainties for the principal minerals of the order of ±2-10 % for quartz, 10-25% for K-feldspar, dolomite-ankerite and anhydrite, 20-50% for albite and micas, and 10-30 % for kaolinite and clay.

3.2   TWO DIMENSIONAL POROSITY DATA

3.2.1   Image acquisition

The majority of the images used in this part of the study were acquired during the X-ray mapping process that was used for obtaining mineralogical modal analysis data (see Section 3.1), using

Oxford Instruments INCA software and hardware systems as 8 bit greyscale TIF format images. Images were obtained under backscatter electron imaging (BSEM) conditions. The brightness of a phase under BSEM is proportional to its mean atomic number. Porosity, which has been impregnated by a carbon-rich resin, is typically black or near-black with BSEM and consequently has a strong brightness contrast with most framework grain, matrix and cement phase minerals. The main exceptions to this are organic and coal fragments, also carbon-rich, which are typically of similar low levels of brightness. Images were collected at 2048 x 1408 or 1024 x 704 pixel resolutions.

To obtain some high resolution large field of view images, typically of approximately 3700 x 2900 pixel resolution and 3.7 mm field of view, images were acquired from a few samples from the Cleethorpes borehole using an automated macro-driven grid imaging approach. The inbuilt macro language of the LEO 435VP SEM was used. Montaging of the grid images was carried out using the Olympus AnalySIS Auto (v.5) petrographic image analysis (PIA) software package.

Both the single and montage images are calibrated from SEM image acquisition parameters that are recorded with the original images and retained through the montaging process. Image magnifications were selected so that the majority of the pore types within a field of view could be resolved and from an area that was considered representative of an identifiable sedimentary rock texture.

3.2.2   Image processing and analysis

Image processing and analysis were carried out on the images off-line, using the Olympus AnalySIS Auto (v.5) PIA software package. A similar methodology could be applied with many other image analysis packages available commercially or through share/freeware licences. Figure 4 summarises the work flow in this process.

The end product of the binarisation-and-detect processes is an image in which pore 'particles' have been identified. A range of parameters can be measured for these particles; in this study particle area, elongation and equivalent circular diameter (ECD) were recorded. Individual pores were also classified and colour coded on the basis of their ECD according to the Wentworth (Udden-Wentworth) standard grain size classification (Pettijohn et al. 1987; Hallsworth and Knox, 1999). This enables images at different magnifications to be readily compared whilst retaining an aspect of scale.

Total porosity is obtained by taking the proportion of the total field of view that has been identified as pore 'particles'. Pore particles of <2 pixels size were discarded as noise. Pores intersecting the image margins were included for porosity percentage determinations. After the first 'total porosity' detection step, a second step excluding mesopore and micropore particles was run, enabling separate quantification and characterisation of the macropores. A mesopore / macropore cut-off of 15μm ECD was used. The size of the cut-off pore particle size in pixels was calculated from the inherent image calibration, using the equation below:

$$\text{No. of pixels for 15μm ECD pore particle} = \pi*(15/2)^2/(\text{pixel size in μm})^2$$

The detection process was run a second time excluding particles smaller in total pixels than the calculated cut-off size. Again, pores intersecting image margins were included. Data obtained from this process included macroporosity, mean macropore size, mean macropore ECD and mean macropore elongation.
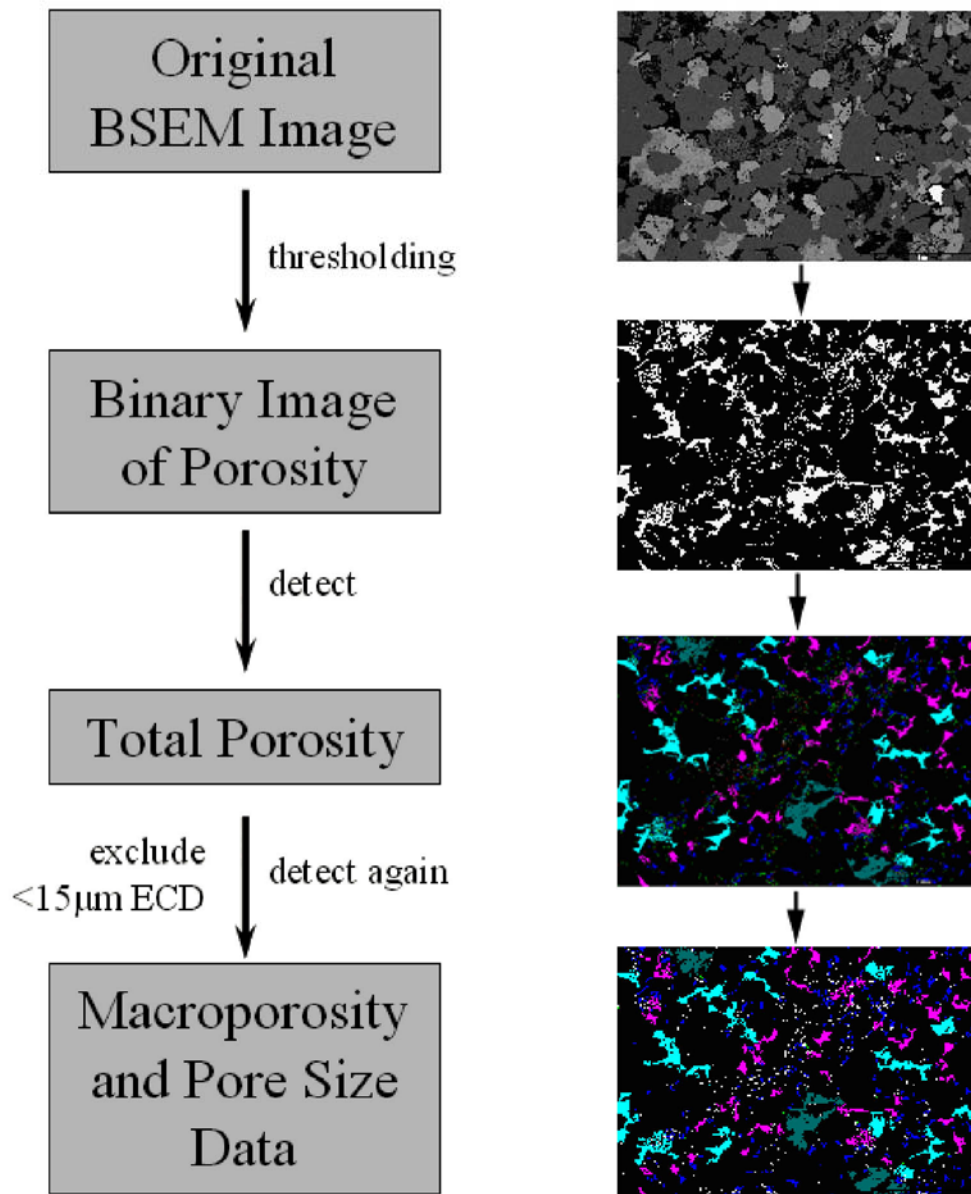
Figure 4. Work flow diagram for image processing and analysis

3.2.3   Pore area and elongation

Pore particles as identified by the image analysis process are areas of two-dimensionally continuously connected porosity. Pore particles can thus include several adjacent intergranular pores that interconnect through pore 'throats'. Pore particle size therefore increases both with the size of intergranular pores and with their degree of interconnection. As both of these factors have a strong influence on permeability, then the mean pore area of an area is expected to give a crude indication of the permeability of that area.

Elongation is a measurement that compares the shape of the perimeter of a particle with that of a circle. A circular particle perimeter has no elongation and thus returns an elongation value of 1. Increasing deviation from the circular form increases the elongation value such that the value approaches infinity as the shape approaches that of a straight line. For an idealised uncompacted sediment, comprising very well sorted high sphericity grains, pores would be expected to have an elongation of near to 1. The main factors that would be expected to increase the elongation of pore particles are compaction, elongate grain shapes and lamination (including elongate grain

alignment). Thus the mean pore elongation of an area is expected to give a guide to these textural factors. Additionally, mean pore elongation may give a guide to the horizontal – vertical heterogeneity of the pore system (since, where possible, thin sections have been taken in the vertical plane).

A limiting factor of the pore particle approach to deriving textural data is in the size of the field of view obtained for the porosity assessment. Initially, when obtaining porosity textural data, pores touching the edges of the field of view were excluded from the data set since they are undersized and will have false shapes. Fields of view containing few large macropores, however, caused problems since excluding these edge pores would exclude the bulk of the porosity. It was decided, therefore, to include edge pores and note the limitation. This effectively puts a cap on the sensitivity of the technique to the size and shape of the largest pores. For fields of view with high numbers of pore particles including edge pores will have little effect on the derived data.

3.2.4   Sources of error and uncertainty

Potential sources of porosity error include the following:

1. Pitting and scratching of the section surface

2. Grain pluck sites

3. Sample disruption

4. Presence of organic and / or coal fragments

5. Microporosity

Of these, sources 1 and 2 are random and unpredictable. Both result in areas that can be of similar BSEM brightness to the true porosity and are virtually impossible to exclude from the porosity quantification, and will increase the apparent porosity of an area. Sample disruption, source 3 in the list above, includes features such as shrinkage cracks (a common problem in clay-rich sediment), sampling-induced fractures and localised disaggregation. All three of these effects are primarily mitigated by avoidance where possible when selecting the imaging area.

Error source 4 is petrographically readily identifiable. In some cases (e.g. Glenrothes BH sample SSK2542; Kincardine East sample SSK2562) the content of organic and / or coal fragments is such that porosity measurement is not possible. In other samples it proved possible to differentiate these phases from porosity using multiple thresholding steps, or by manually selecting and excluding the appropriate detrital grains from the pore detection step (e.g. Easter Lathrisk sample BEB7481).

Error source 5, micropores (pores with an ECD <5μm) are typically underdetected by the process. There are two main causes for this. Firstly there is their size; depending on the magnification used, some micropores will be at or below the limits of detectability because they are of similar or lesser size to that of the individual pixels. Secondly, micropores tend to be brighter than larger pores because of edge effects. Pore edges are typically brighter as they include input from adjacent grain margins. These commonly slope beneath the surface of the section and produce some input into the BSEM signal since the SEM beam penetrates a significant depth into the sample. This issue is exacerbated with micropores since they are effectively all pore margin and additionally, because of their size, will typically have a mineral phase underlying the exposed pore surface. As micropores are of higher brightness they can be excluded by thresholding, or to be included significant areas of mineral material will also be included. Mitigation of this effect is difficult; a balance between under-detection of microporosity and inclusion of non-pore material has to be made as one of the thresholding decisions. In macropore-dominated samples, however, the effect of missed micropores is expected to be minor. It is only with highly microporous samples (e.g. Glenrothese sample SSK2546) that this effect will be significant.

The thresholding step is the main step that generates quantifiable uncertainty in the porosity detection and measurement process. This uncertainty can be broken down in to the following individual elements:

1. Selection of thresholding point

2. Repeatability

3. Imaging conditions (contrast, brightness variation, pixel resolution)

4. Operator

The last element has not been assessed here. A single operator with expert knowledge and experience performed all of the analyses to eliminate this factor from consideration.

The first element listed is the uncertainty involved in selecting the threshold point. There is not an absolute value above which mineral phases are selected and below which only porosity is selected. The main reason for this is the edge effect (as discussed in (5) – microporosity error). Micropores are an extreme example of the problems that this creates; all pores have this characteristic. The problems this creates are further exacerbated when there are thin grain-coating clays for example. Consequently there is typically a range of values over which porosity can be considered to have been selected, with a subjective element to judging the point at which pore margins and micropores are adequately selected, but grain contacts and other phase margins are not over-selected. The quantitative effect of this element was assessed on a subgroup of the study samples. On each image from the subgroup thresholds were selected, in a single session, bridging the full range from what was considered 'just enough' porosity (low limit threshold value) to 'nearly too much' mineral (high limit threshold value). The results of this low-high 'range' assessment are listed in detail in Table 4 below. These show that the mean range in total porosity created by low to high thresholding is 1.78% (0.62% standard deviation).

To assess (2) repeatability, fresh 'blind' optimal thresholds were repeated on a subgroup of images a significant period of time (weeks) after an initial thresholding had been performed. The results of this assessment are presented below, in Table 5. The uncertainty measured is less than that of the high to low thresholding; in other words no additional uncertainty has been identified from this effect. This implies that for a single operator repeatability is not of greater significance than the actual process of selecting a threshold point.

Images of different contrast and brightness were collected for the same field of view to assess the effect of variations in these imaging conditions (3). Optimal thresholds were performed on these, on the same day on several occasions, and the results compared between the two images. Results of these tests are presented below in Table 6. They show a variation that is greater than both of the thresholding and repeatability uncertainties. This suggests that additional uncertainty has been created and that care needs to be taken that images are captured under relatively consistent brightness and contrast conditions. One of the main things that will be affected by varying brightness and contrast is the degree of edge effect (as described above) and this will most likely have created some of the additional uncertainty.

Table 4. Statistical summary of variation in key values from threshold ranging

	Threshold range	Total Porosity	Macro-porosity	Meso+Micro-porosity	Mean Pore Area	Mean Elongation
	Grey Levels (8bit)	%	%	%	µm²	
Mean Low-High Range	17.9	1.78	1.54	0.28	358	0.033
Standard Deviation	3.7	0.62	0.63	0.15	392	0.025

Table 5. Test of repeatability of thresholding

Sample	Porosity 1	Porosity 2	Image	Threshold 1	Threshold 2	Threshold difference	Porosity difference
	%			Grey Level (8bit)			
CLSH7	14.48	13.21	Mosaic 1	59	45	14	1.26
CLSH7	13.01	11.05	Modal mapping 1	52	32	20	1.96
CLSH7	21.71	21.18	Modal mapping 2	40	34	6	0.54
CLSH8	14.23	14.44	Mosaic 1	22	24	2	0.21
CLSH8	17.03	14.48	Modal mapping 1	65	40	25	2.55
CLSH8	14.19	14.58	Modal mapping 2	42	46	4	0.39
CLSH9	24.07	23.47	Modal mapping 1	50	44	6	0.61
CLSH9	14.15	13.49	Modal mapping 2	42	35	7	0.67
CLSH10	11.68	11.23	Modal mapping 1	29	25	4	0.45
CLSH10	10.83	11.18	Modal mapping 2	32	35	3	0.35
				Mean		**9.1**	**0.899**
				Standard Deviation		**7.9**	**0.782**

Table 6. Test of brightness and contrast of imaging

Dark Image		Bright Image		Porosity Difference
Threshold	**Total Porosity**	**Threshold**	**Total Porosity**	
Levels (8bit grey)	%	Levels (8bit grey)	%	%
32	13.13	55	16.45	3.32
17	9.68	45	14.16	4.48
25	11.27	30	11.73	0.46
		Mean		2.751
		Standard Deviation		2.068

4 Results

4.1   MINERALOGY AND PETROGRAPHY

4.1.1   Yorkshire-Lincolnshire-Nottinghamshire area

The mineralogical analyses of the Permo-Triassic aquifer and seal samples from the Yorkshire-Lincolnshire-Nottinghamshire area are presented in the digital dataset *Modal Mineralogy-YORKS_LINCS_NOTTS v1.0.xls* (provided on the CDROM enclosure). An overview of the mineralogical and diagenetic characteristics of these rocks is described below. The grain size terminology (i.e. coarse, medium, fine) used in this report are based on the Wentworth (Udden-Wentworth) standard grain size classification (Pettijohn et al. 1987; Hallsworth and Knox, 1999).

4.1.1.1 SHERWOOD SANDSTONE GROUP – PRIMARY TARGET AQUIFER

Regionally, the Sherwood Sandstone Group comprises mainly fine- to coarse-grained, reddish brown, fluvial sandstones with occasional thin and laterally discontinuous marl seams (Ford et al., 2008). However, in the cores examined and sampled, the sandstones were represented dominantly by fine to medium grained fluvial sandstones (e.g. Plate 1). The sandstones are generally moderately sorted but some poorly-sorted sandstone and well-sorted sandstone are also encountered. Sandstone beds often fine upwards, from a coarse sandstone at the base (sometimes with scattered small pebbles or mudflake breccia), passing upwards through medium sandstone to fine and very fine sandstone tops, sometimes accompanied by a thin clay or mudstone.
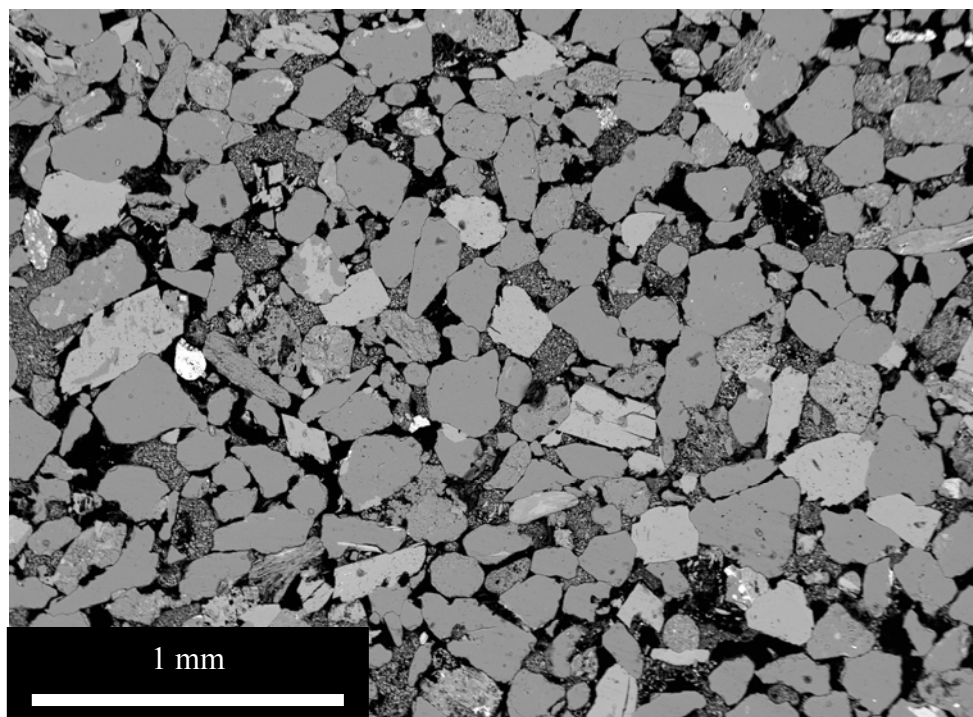
Plate 1. BSEM image of fine to medium sandstone, showing close-packed grain fabric with angular to subangular grains of major quartz and minor albite (mid-grey). K-feldspar (light grey) with deformed ferruginous mudstone lithic clasts or pellets (dull grey with white specs of iron oxide) forming a clay pseudomatrix. Sample CLSH1, Sherwood Sandstone Group, 1111.94 m, Cleethorpes No.1
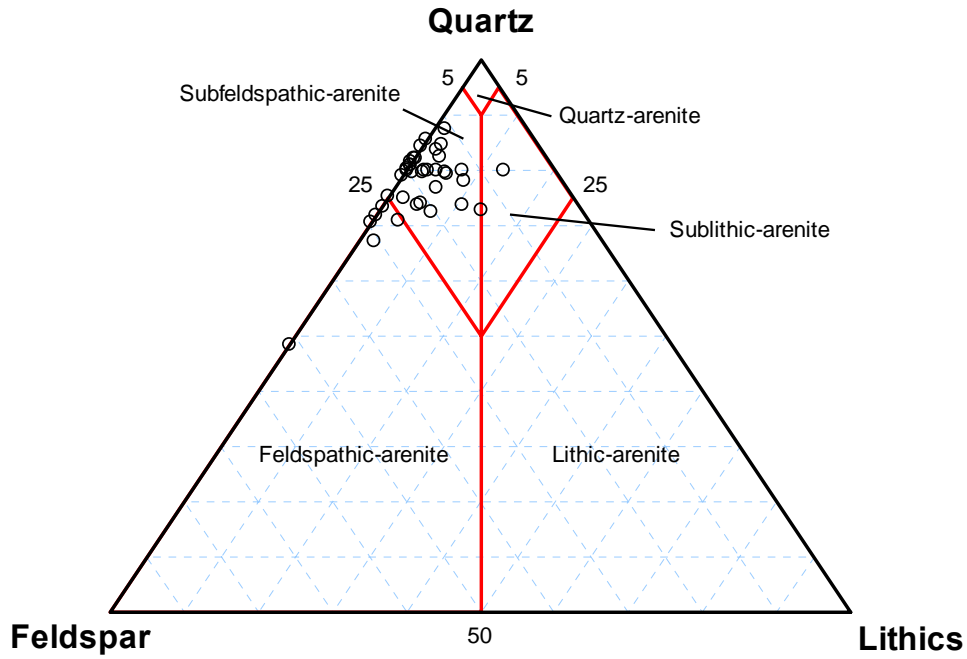
Figure 5. Classification of sandstone samples from the Sherwood Sandstone Group on the basis of measured proportions of quartz, feldspar and lithic clasts (classification after Pettijohn et al., 1987)
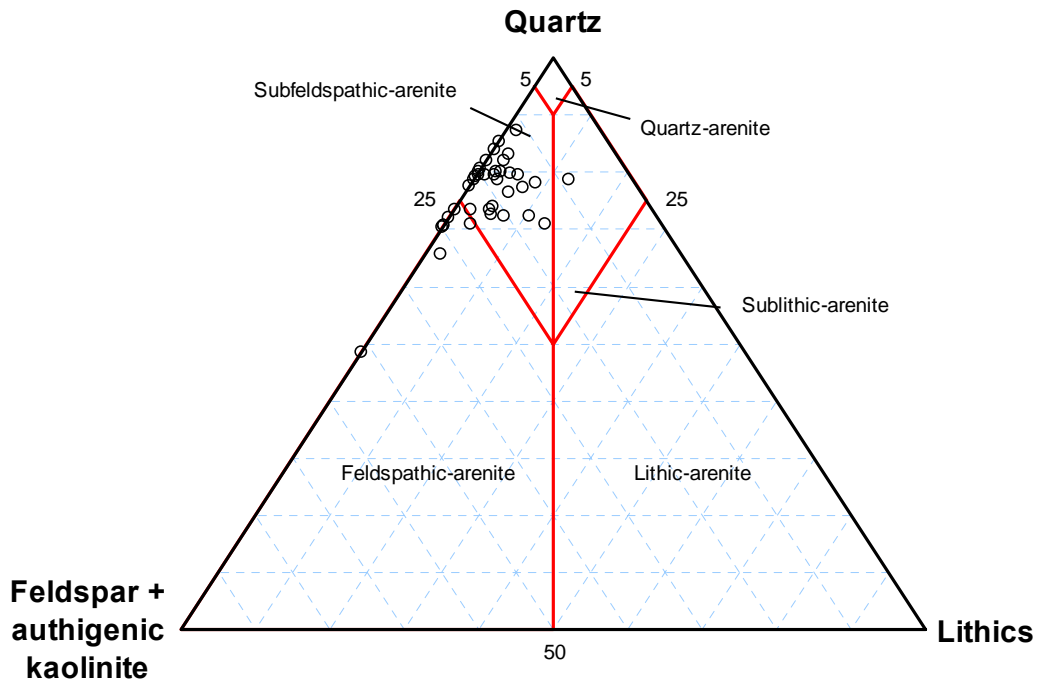
Figure 6. Classification of sandstone samples from the Sherwood Sandstone Group on the basis of estimated original proportions of quartz, feldspar and lithic clasts after accounting for authigenic kaolinite replacement of feldspars (classification after Pettijohn et al., 1987)

Primary detrital components are dominated by a major quartz component, with subordinate to minor amounts of K-feldspar, albite, lithic clasts (including chert, siltstone, mudstone, quartz-felsic rock fragments), minor to trace amounts of muscovite, biotite, chlorite. Accessory detrital minerals include magnetite, altered iron-titanium oxides, rutile, tourmaline, zircon and apatite. Detrital clay with disseminated fine iron oxide is commonly present as fine grain-coating rims. Discrete patches of clay are also present forming an apparent matrix squeezed between compacted detrital quartz and feldspar and filling intergranular pores. The patchy nature of this clay and the recognition of partially-deformed clay and mudstone pellets suggest that much of this intergranular clay is "pseudomatrix" rather than true detrital clay, and results the compactional deformation of plastic, clay-rich lithic grains. EDXA suggests that much of the clay is illitic in composition.

Modal data indicate that most sandstones should be classified as subfeldspathic arenites, with subordinate feldspathic arenites and occasional sublithic arenites (Figure 5). Petrographic observations show that some of the detrital feldspar has been replaced or partially replaced by minor authigenic kaolinite. This implies that the sandstones were originally more feldspathic but even if account is taken of this (as shown in Figure 6) the sandstone classification would remain unchanged. As discussed in Section 3.1.4.2, these modal analyses are likely to have underestimated the amount of lithic clasts, and therefore the proportion of sublithic arenites may actually be greater than initially suggested by the modal data.

1 mm
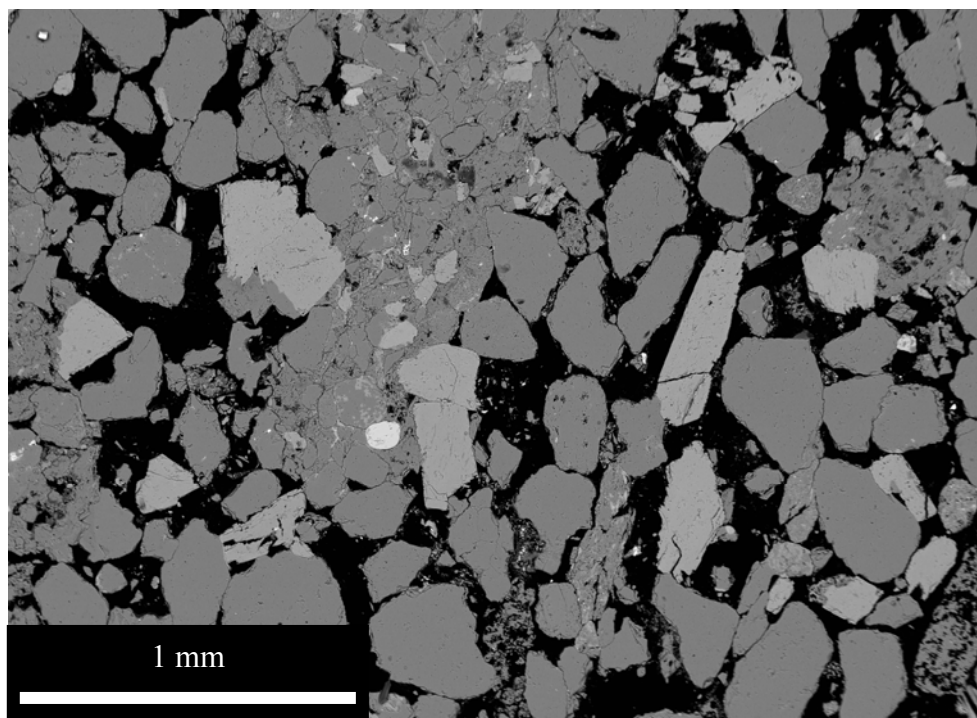
Plate 2. BSEM image of fine to medium sandstone, showing heterogeneously-packed grain fabric with locally tightly-packed detrital grains and areas with open uncompacted grains and oversized intergranular pores. Patchy or micronodular dolomite (dull grey) can be seen cementing areas of uncompacted (expanded fabric) sandstone (top centre). Sample CLSH5, Sherwood Sandstone Group, 1114.40 m, Cleethorpes No.1.

Diagenetic fabrics are very similar to those described previously from these rocks (Bath et al., 1987; Milodowski et al., 1987). Fine pellicles of ferruginous illitic clay coat grain surfaces and probably represent early diagenetic clay infiltrated from the surface shortly after burial. Early diagenetic (eodiagenetic) non-ferroan dolomite cement is an important phase in most sandstones, occurring as irregular patchy or micronodular pore-filling and grain-replacive cement (Plate 2).

21

This may also be surrounded by infiltrated clay or contain inclusions of infiltrated clay. This dolomite cement also may preserve an open uncompact grain fabric, which indicates that it formed before significant burial and compaction. Minor overgrowth of later ferroan dolomite was also observed in some samples.

Anhydrite may also be a significant cement in some sandstones in the Cleethorpes No.1 borehole sandstones (Plate 3), particularly in sandstones from the upper cored section (1105-1121 m) of the borehole. It occurs as intergranular, pore-filling cement, and its relationships to compaction fabrics suggest that more than one generation of cement may be present. In some cases anhydrite cements an open uncompacted grain framework – suggesting it is eodiagenetic in origin. In other cases, it fills residual pores between tightly compacted sand grains implying that this cement is late diagenetic and formed after burial compaction. Traces of halite and sylvite were also identified as trace cements in sandstones from Cleethorpes No.1 borehole. Anhydrite, sylvite and halite cements often show evidence of corrosion and etching in sandstones from the Cleethorpes No.1 borehole and are entirely absent in the samples from shallower boreholes to the west. This suggests that these cements may have originally been more extensive within the sandstones, and that a significant amount of the present intergranular porosity is secondary or rejuvenated, as a result of the dissolution of these evaporite minerals.

Gypsum is present as the major intergranular cement tightly cementing the sandstone sample SSK2552 from the Fulbeck Airfiled No.1 borehole. This has possibly been remobilised from the immediately adjacent gypsiferous mudstones of the overlying Mercia mudstone Group.

1 mm
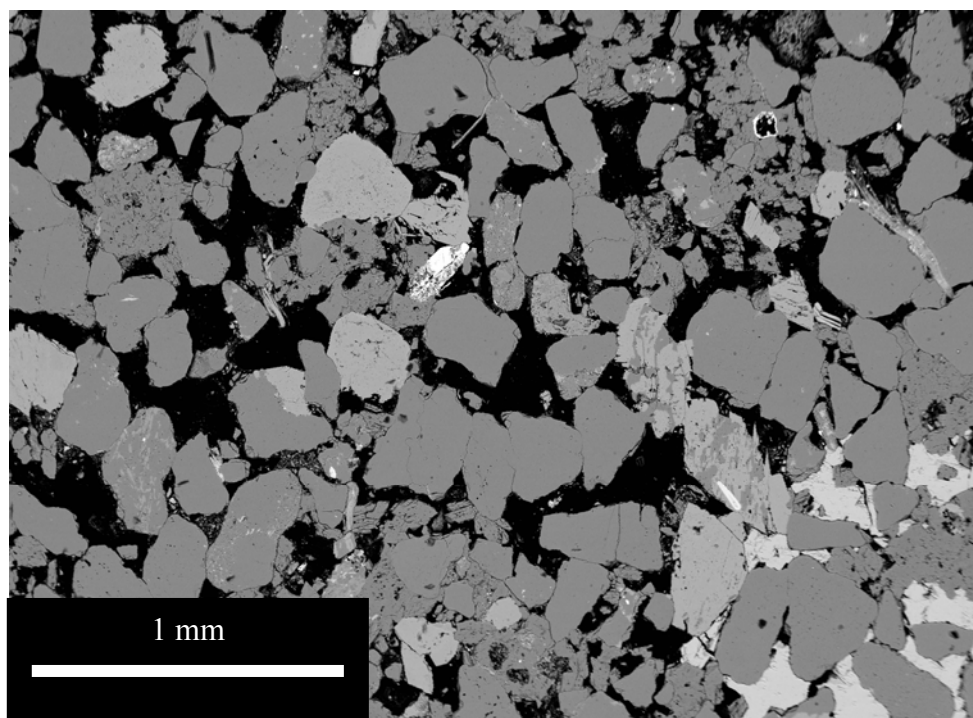
Plate 3. BSEM image of sandstone, showing heterogeneously-packed grain fabric with locally tightly-packed detrital grains and areas with open uncompacted grains and oversized intergranular pores. Patchy or micronodular dolomite (dull grey) can be seen cementing areas of uncompacted (expanded fabric) sandstone (bottom centre) and pore-filling anhydrite cement (white) is also present (bottom right). Sample CLSH7, Sherwood Sandstone Group, 1116.31 m, Cleethorpes No.1.

Calcite and barite occur sporadically as very minor cements in small isolated patches in some samples. Weakly-developed syntaxial and euhedral overgrowths of authigenic quartz and K-

feldspar were observed on detrital grains in some sandstone samples. However, these overgrowths are very limited and do not form significant cementing phases.

The sandstones also display significant evidence of secondary porosity formed as a result of the dissolution of primary detrital grains (framework grain dissolution). This is evident from the abundant presence of large oversized pores (Plate 2 and Plate 3) that are out of keeping with the compaction state and grain size of the sandstones, and which is characteristic of framework grain dissolution secondary porosity (Schmidt and McDonald, 1979b). Close examination often reveals the presence of relict fragments of feldspar grains, particularly albite within framework grain dissolution sites. In contrast, most K-feldspar grains show only minor evidence of corrosion. Minor authigenic kaolinite formation is closely associated with the feldspar alteration. Comparison of the quartz-K-feldspar-albite ratio shows that the deep sandstones from the Cleethorpes No.1 borehole have a significantly greater amount of albite than sandstones from the shallower aquifer (Figure 7).
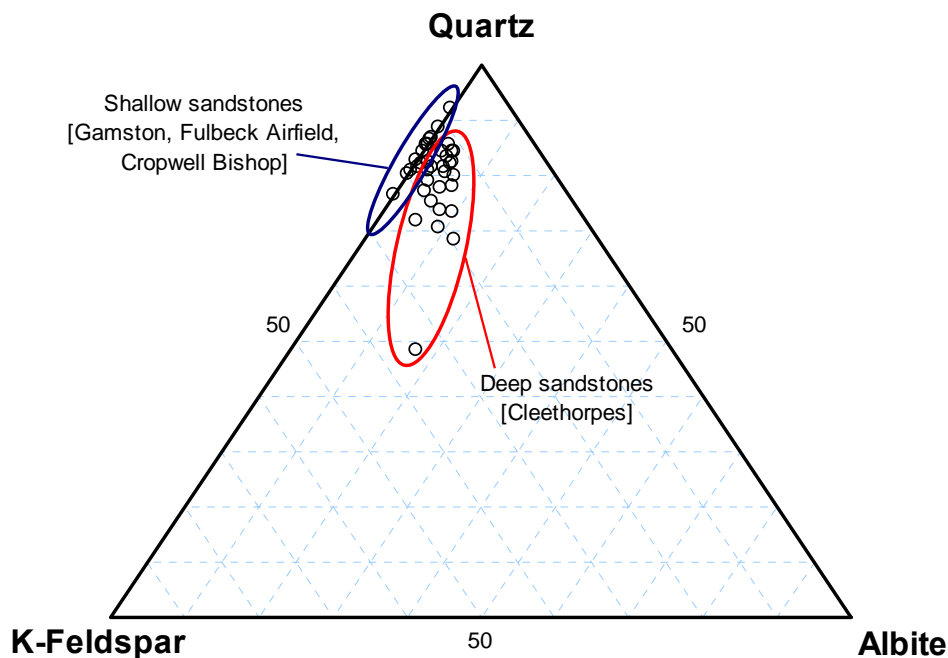
Figure 7. Quartz-K-feldspar-albite ratio plot showing the difference in composition between the deep Sherwood Sandstone Group samples from the Cleethorpes No.1 borehole and samples from the shallower aquifer to the west.

These observations suggest that secondary porosity (including both cement dissolution porosity after anhydrite, and framework grain dissolution after albite and plagioclase) will increase to the west as a result of fresh meteoric groundwater invasion at outcrop, and support conclusions from earlier observations (Bath et al., 1987; Milodowski et al., 1987). However, the relationship between total porosity and sandstone mineralogy is not straightforward. Modal analysis data show that, overall, there is no systematic relationship between total macroporosity and the amount of anhydrite cement (Figure 8). Carbonate cementation may be a more important influence on the present distribution of porosity within the samples. Although there is a wide scatter in data, the modal data suggest that there may be a broad overall trend of decreasing porosity with increasing carbonate (Figure 9).
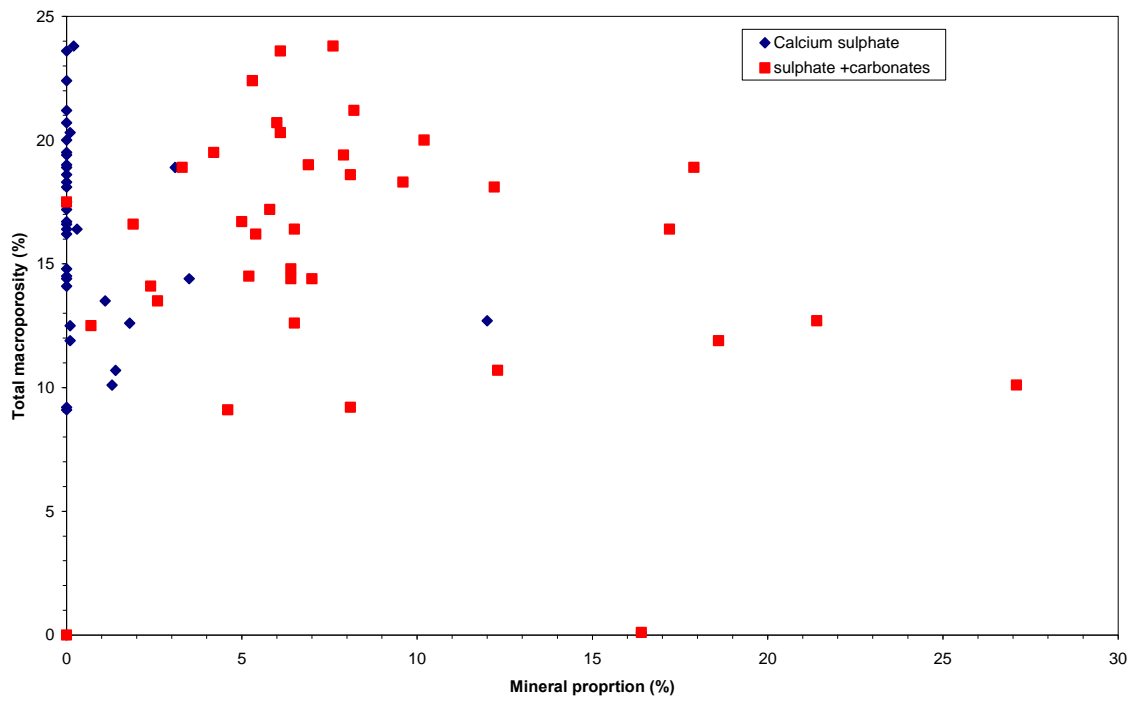
Figure 8. Comparison between total macroporosity, and anhydrite (calcium sulphate) cement and total anhydrite + carbonate cement in the Sherwood Sandstone Group.
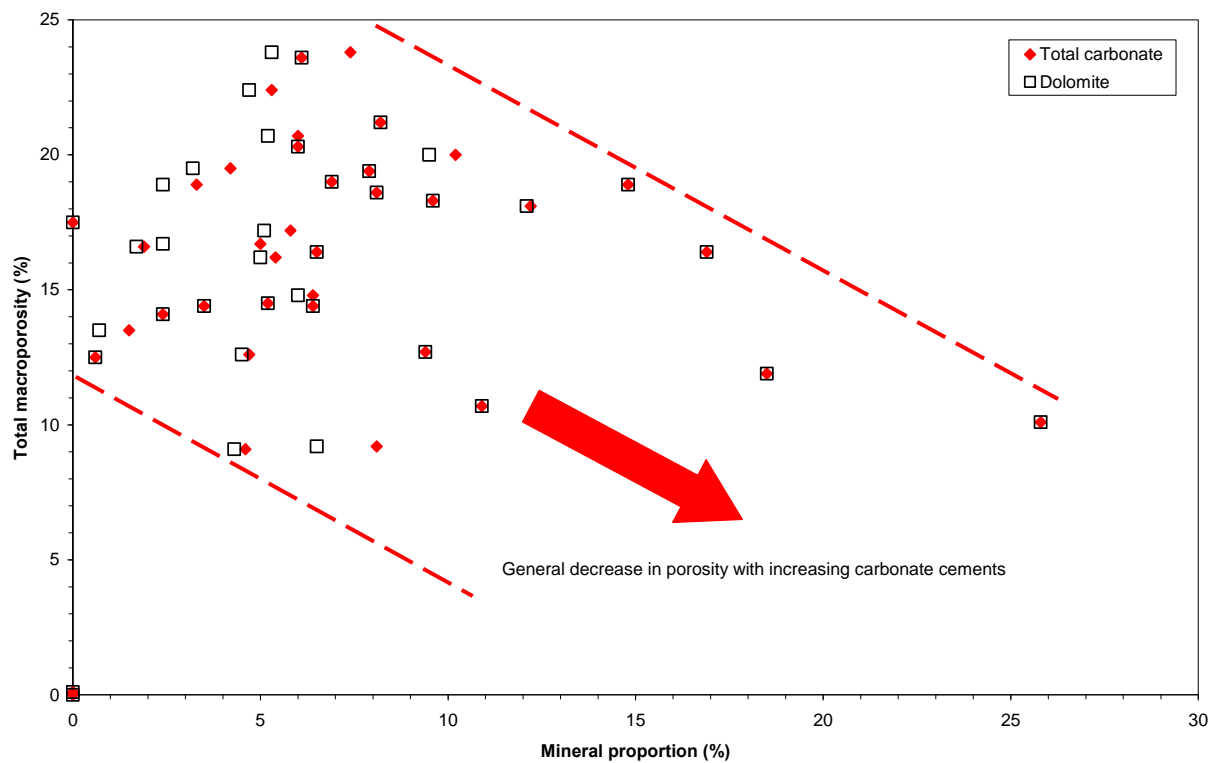
Figure 9. Comparison between total macroporosity and carbonate cement in the Sherwood Sandstone Group.
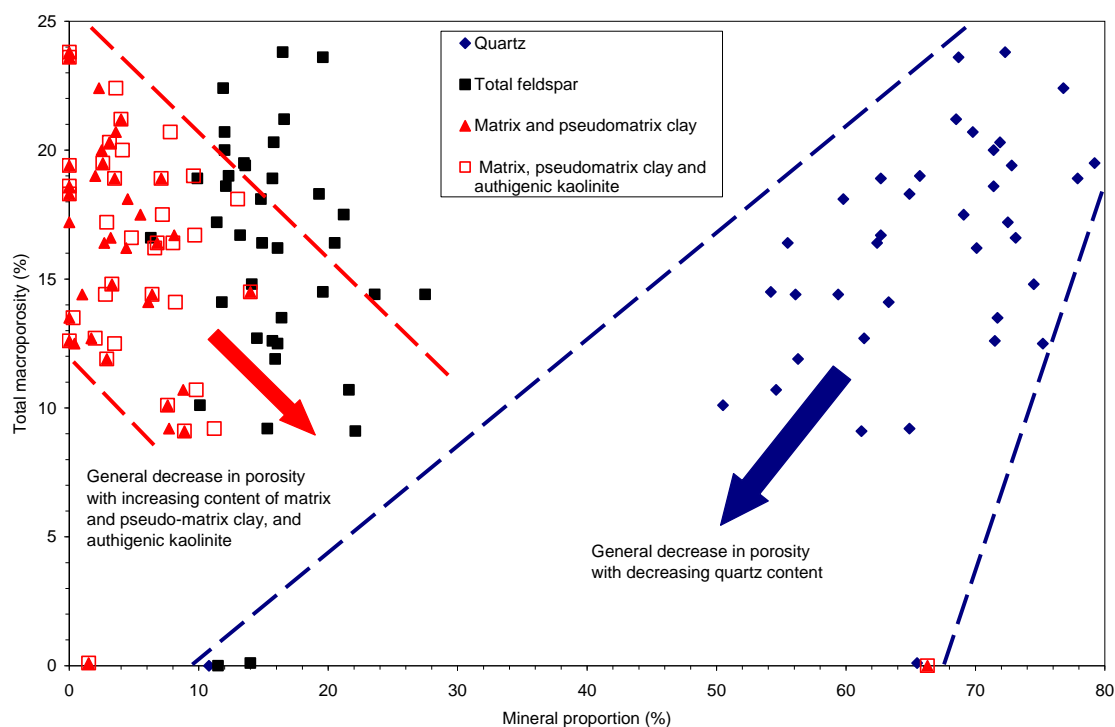
Figure 10. Comparison between total macroporosity carbonate cement in the Sherwood Sandstone Group.

The degree of sorting, and content of detrital quartz, clay and plastic lithic grains also probably exert some influence on the porosity and permeability of these sandstones. Figure 10 shows that sandstones with the highest quartz content tend to correspond to the highest total porosity. Conversely, there appears to be a broad trend of decreasing porosity with increasing clay content (determined as matrix clay and pseudomatrix clay, combined).

The presence of authigenic fibrous illite may also be an important influence on the permeability of the deep Sherwood Sandstone Group. Fibrous illite is often not observed in thin section or routine SEM analysis because the delicate illite fibres collapse on drying and resin-impregnation of the samples (McHardy et al., 1982). However, even very small amounts of fibrous illite can have a very significant effect on permeability because the growth of fine intergrown fibres within the intergranular pore space dramatically reduces effective pore throats (Seeman, 1979). Although it was not observed in thin sections studied for the CASSEM Project, it was previously reported by Milodowski et al. (1987) from SEM observations on samples of sandstone from the Cleethorpes No.1 borehole that were preserved in formation brine and subsequently prepared by critical point drying with CO_2. These samples were recently re-examined as part of a BGS exercise to evaluate environmental SEM equipment, which showed pore surfaces to be extensively coated with fibrous illite (Plate 4).

Published studies of the Rotliegendes of the southern North Sea (Marie, 1975; Glennie et al., 1978) concluded that authigenic fibrous illite is encountered in sandstones that have undergone deep burial. Its presence in much shallower sandstones from the Cleethorpes No.1 borehole is perhaps surprising, and suggests that it may have a more widespread distribution, and occurs at shallower depths, than previously thought. Therefore, the effects of the potential presence of authigenic fibrous illite must be considered in predictive modelling and evaluation of porosity and permeability of the Sherwood Sandstone Group at depths suitable for CCS.
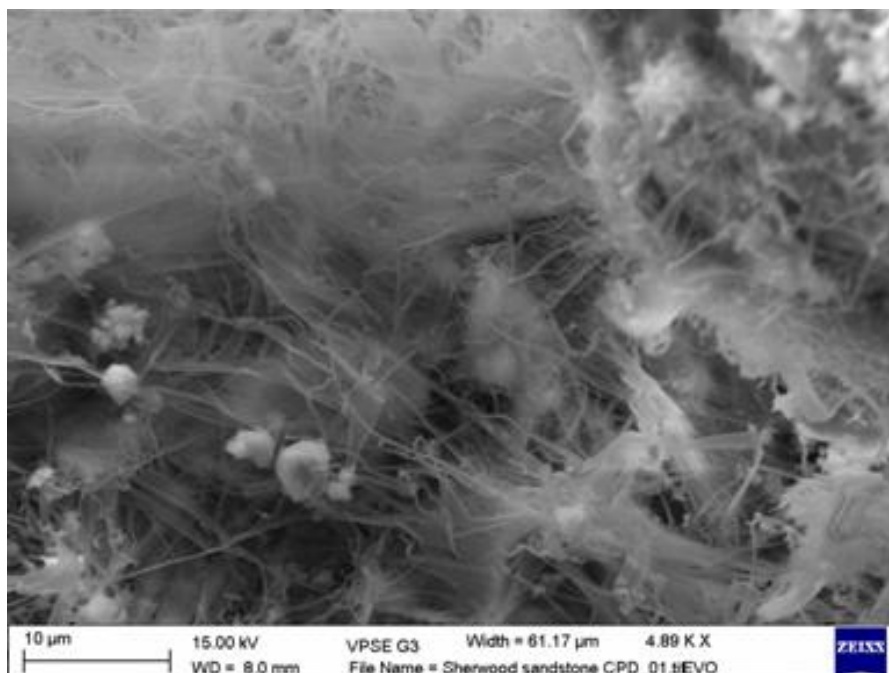
Plate 4. Environmental SEM photomicrograph of authigenic fibrous illite lining pore surfaces in sandstone sample prepared by CO$_2$ critical point drying of core samples preserved in formation brine immediately after recovery. Sherwood Sandstone Group

4.1.1.2 Basal Permian (Rotliegendes) sands and breccias – secondary target aquifer

The Basal Permian sands and breccias were only studied in samples from the Cleethorpes No.1 borehole. They comprise a complex assemblage of poorly-sorted conglomerates with silt and coarse sand matrix, massive sandstones (with traces of low angle cross-bedding), and minor intercalations of siltstone or mudstone. Pebbles in the conglomerates comprise pink and white quartzite, red, grey and green sandstones, siltstones and mudstones, dolomitised limestone and fine grained felsic volcanic rocks.

The sandstones contain a mixture of well-rounded aeolian grains and angular to subrounded quartz grains. Grain packing is highly variable. Finer and poorer sorted (muddier) sandstones have strongly compacted fabrics, and display significant plastic deformation of less competent argillised lithic clasts, and mudstone clasts to produce a clay pseudomatrix. This compaction has produced a significant loss of intergranular porosity (Plate 5). Coarser, cleaner, better-sorted sandstones tend to display a more open fabric, often with large, uncompacted intergranular pores (Plate 6) that might be indicative of the removal of relatively early diagenetic pore-filling cement that prevented compaction during burial (Schmidt and McDonald, 1979b). In many cases the compaction is variable within adjacent laminae at the thin section scale (Plate 7).

The mineralogy of the Basal Permian sandstones is dominated by major detrital quartz, with subordinate to minor K-feldspar and lithic clasts, with minor to trace muscovite, biotite, chlorite flakes. The sandstones can be classified as dominantly subfeldspathic arenites bordering on sublithic arenite. (Figure 11), although the significance and proportion of lithic components is probably underestimated in the modal data (see Section 3.1.4.2). Authigenic kaolinite is a significant component in some samples, and can be seen to have replaced both feldspar grains and some lithic clasts (Plate 7). Taking this into the account the rocks are likely to have originally been more feldspathic, as indicated by Figure 12. Comparison of quartz-K-feldspar-albite ratios shows that the Basal Permian sandstones (Figure 13) contain a much smaller proportion of albite than sandstone of the overlying Sherwood Sandstone Group rocks from same borehole (Figure 7). This relatively low albite content may in part result from the diagenetic dissolution of albite and its replacement by authigenic kaolinite.
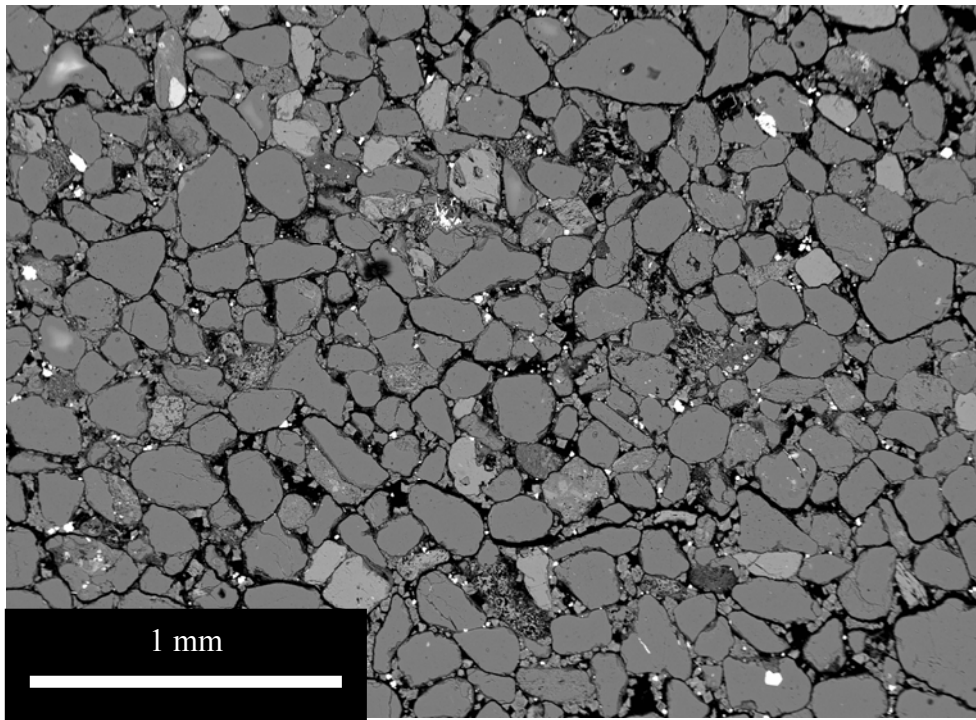
Plate 5. BSEM image of fine to medium sandstone, showing tightly-packed grain fabric with angular to subangular grains of major quartz (mid-grey) and minor K-feldspar (light grey), with deformed ferruginous mudstone lithic clasts (dull grey with white specs of iron oxide). Sample CLPB1, Basal Permian aquifer, 1865.80 m, Cleethorpes No.1
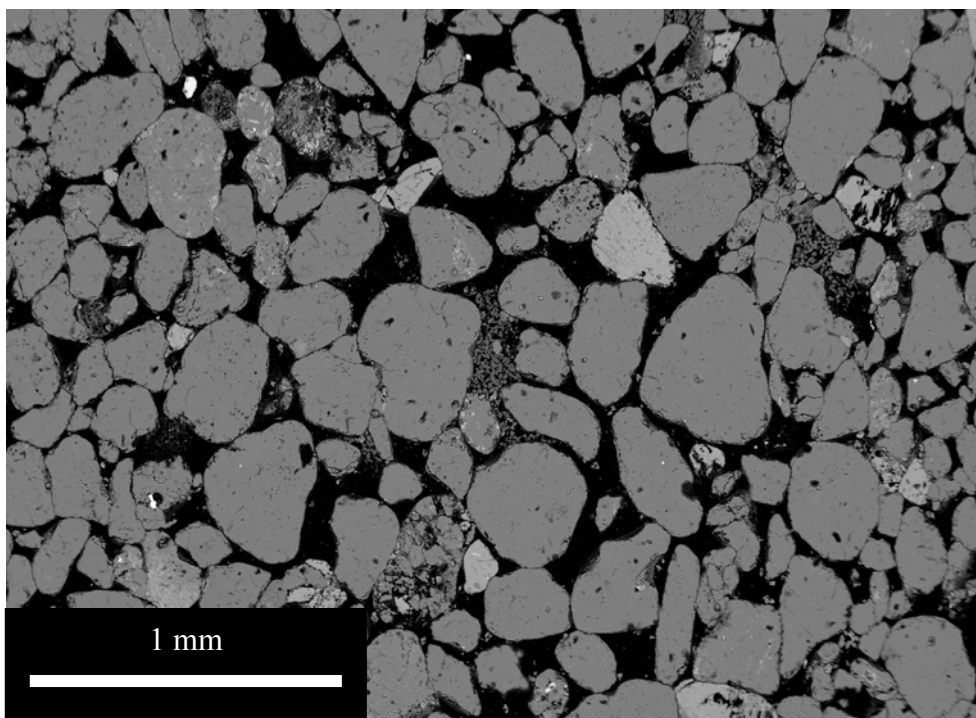
Plate 6. BSEM image of fine to medium sandstone, showing relatively open grain-packing rpunded grains of major quartz (mid-grey) and minor K-feldspar (light grey). Authigenic kaolinite (dark grey) locally fills oversized intergranular pores. Sample CLPB2, Basal Permian aquifer, 1868.20 m, Cleethorpes No.1
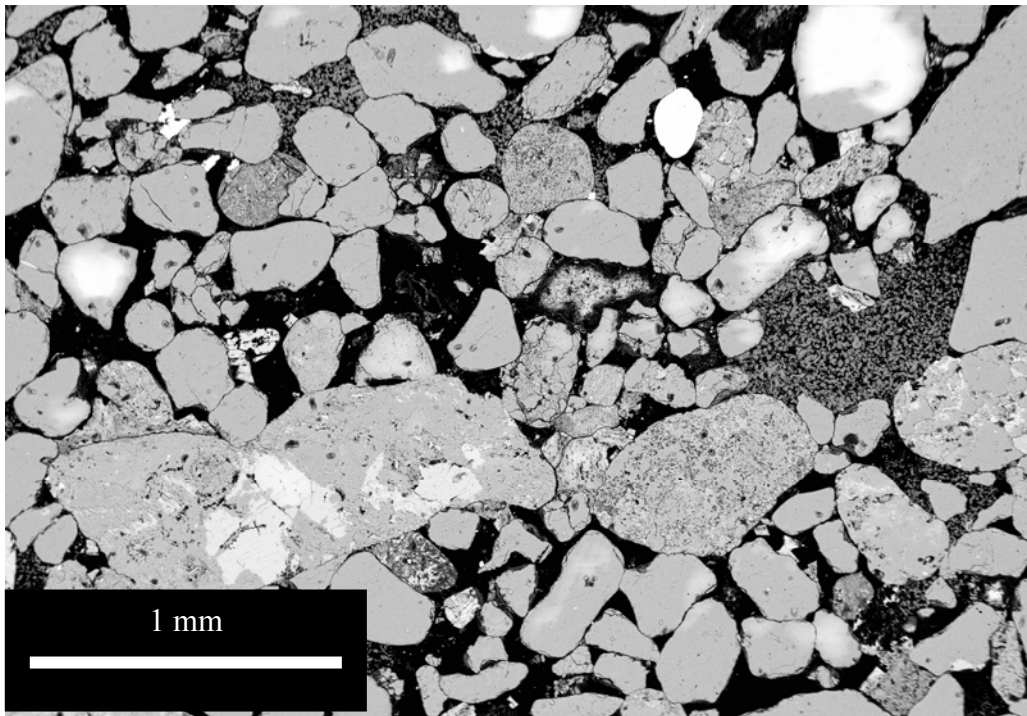
Plate 7. BSEM image of poorly-sorted sublithic arenite showing large felsic lithic clasts and major quartz (mid-grey) and minor K-feldspar (light grey). The rock is variably compacted with some grains showing sutured grain contacts, while other areas of the sample display a relatively open grain framework. Authigenic kaolinite (dark grey) locally fills oversized intergranular pores, indicating replacement of former detrital framework grains. Sample CLPB5, Basal Permian aquifer, 1871.88 m, Cleethorpes No.1
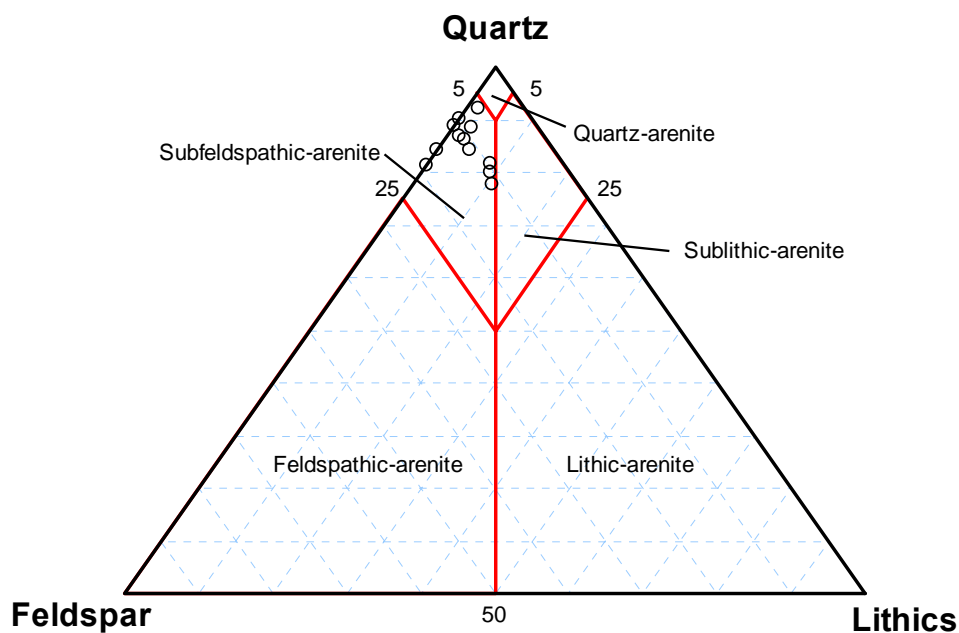
Figure 11. Classification of sandstone samples from the Basal Permian aquifer on the basis of measured proportions of quartz, feldspar and lithic clasts (classification after Pettijohn et al., 1987)
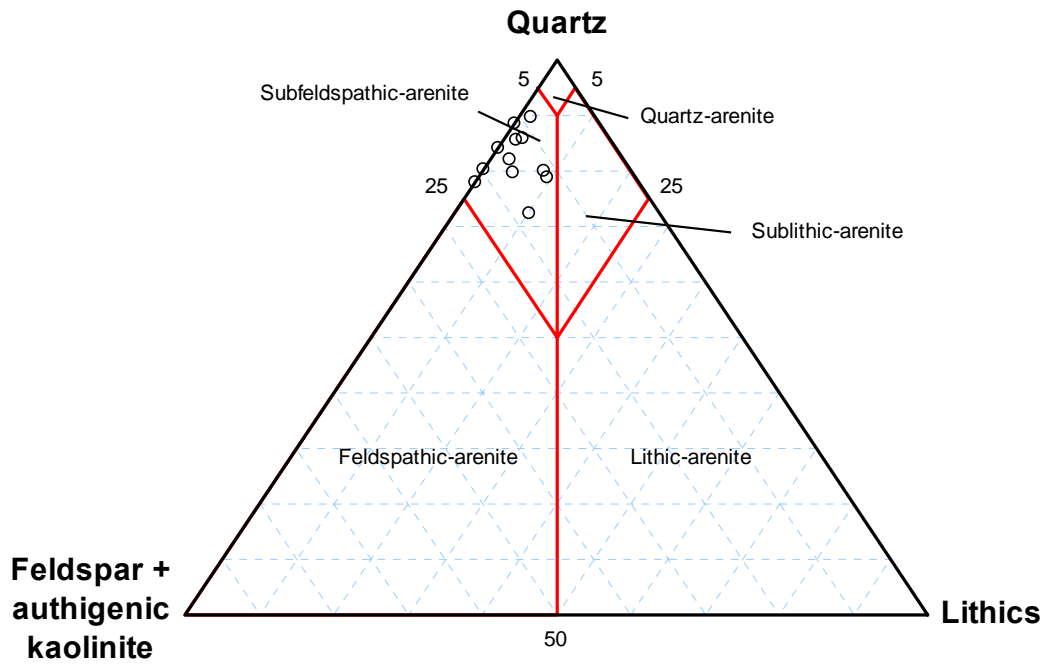
Figure 12. Classification of sandstone samples from the Basal Permian aquifer on the basis of estimated original proportions of quartz, feldspar and lithic clasts after accounting for authigenic kaolinite replacement of feldspars (classification after Pettijohn et al., 1987).
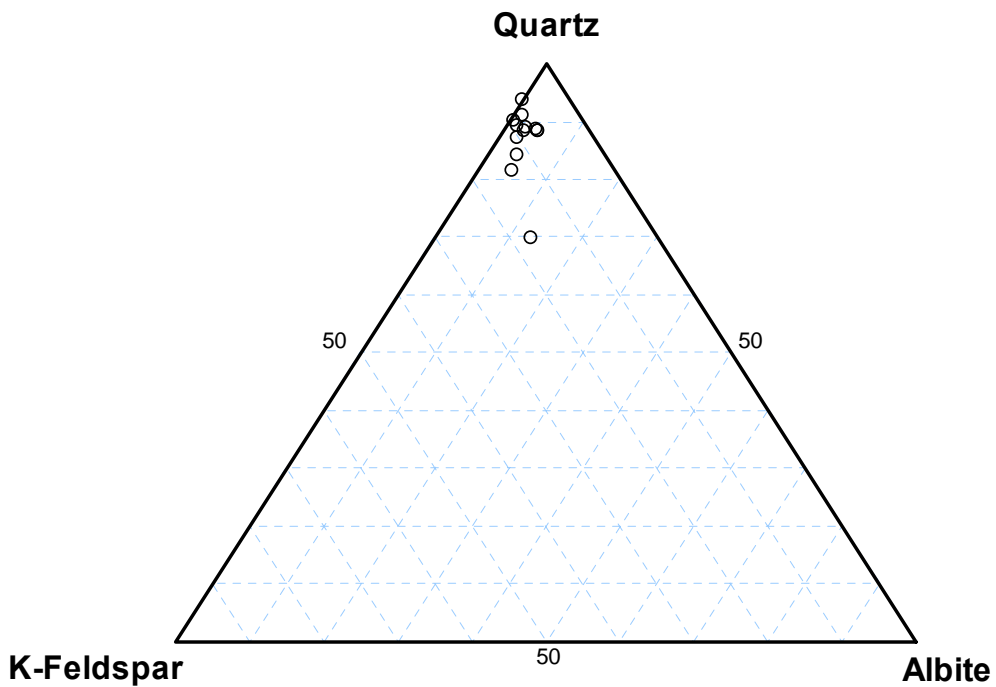

Figure 13. Quartz-K-feldspar-albite ratio plot showing the difference in composition between the Basal Permian aquifer samples from the Cleethorpes No.1 borehole

The rocks have been significantly modified by diagenesis and many features are similar to those observed in the Sherwood Sandstone aquifer. Dolomite cement is a common component but dolomite content varies considerably from <0.1% in some poorly cemented friable sandstones to 19% in well-cemented sandstones. The dolomite occurs as displacive patches or micronodules (up to 0.5 mm diameter) preserving an uncompacted grain fabric and indicating a near-surface eodiagenetic origin. These nodules are similar to those observed in the Sherwood Sandstone Group (cf. Plate 3). In some cases, the dolomite replaces detrital silicate framework grains. Loose aggregates of fine grained, idiotopic dolomite and occasional isolated coarser crystals of dolomite may also partially fill intergranular pore spaces forming a microporous cement binding the sand grains. The dolomite is interpreted to represent pedogenic dolocrete or dolomitised calcrete (cf. Burley, 1984; Bath et al., 1987; Milodowski et al., 1987). The conglomerates may be more tightly cemented by dolomite (Plate 8), with up to 58% of the matrix comprised of dolomite in some samples (e.g. sample CLPB4). The dolomite is both pore-filling and replacive; replacing detrital silicate grains in the sand matrix and replacing limestone clasts. In both sandstone and conglomerate lithologies, later diagenetic (mesodiagenetic) ferroan dolomite and ankerite are present as minor cements, usually occurring as syntaxial overgrowths seeded on the earlier dolomite (Plate 8), further reducing porosity to a minor extent. Ankerite and ferroan dolomite also heal microfractures formed by compactional deformation in the earlier dolomite.
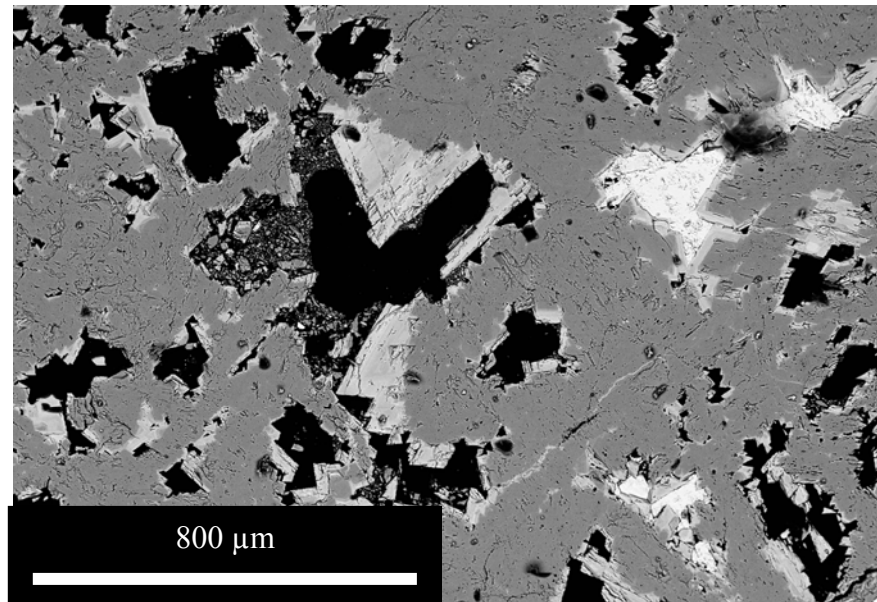
Plate 8. BSEM image of dolomite-cemented matrix of conglomerate bed. The dolomite (dull grey) contains vuggy cavities lined by euhedral overgrowths of ankerite (light grey). Locally, corroded relicts of anhydrite (white) can be seen filling some isolated cavities. Sample CLPB4, Basal Permian aquifer, 1870.70 m, Cleethorpes No.1

Anhydrite is minor cement (0─4%) in the sandstones and conglomerates. Anhydrite may be present as a patchy intergranular cement, often preserving a relatively uncompacted grain fabric (Plate 9). This indicates that this anhydrite is eodiagenetic and formed before the main burial compaction. Anhydrite may also fill isolated residual porosity within the earlier dolomite cement, enclosing (and therefore post-dating) mesodiagenetic ankerite and ferroan dolomite (e.g. Plate 8). It can also be found as minor cement partially filling residual intergranular porosity between highly compacted sand grains. These observations imply that at least two generations of anhydrite are present: an early (eodiagenetic) anhydrite that formed before significant burial; and a later (mesodiagenetic) anhydrite that formed after the main compaction.
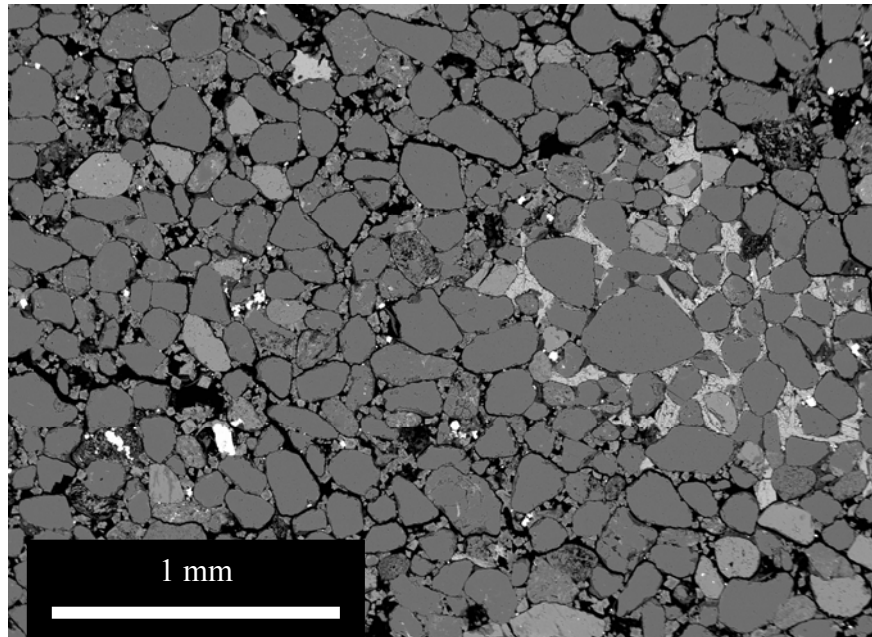
Plate 9. BSEM image of generally tightly-compacted sandstone composed of quartz and minor lithic clasts, containing a patch cemented by intergranular anhydrite cement (light grey, centre right). The anhydrite-cemented area preserves a relatively uncompacted grain fabric. Traces of intergranular barite cement are also present (very bright grains). Sample SSK2389, Basal Permian aquifer, 1865.94 m, Cleethorpes No.1
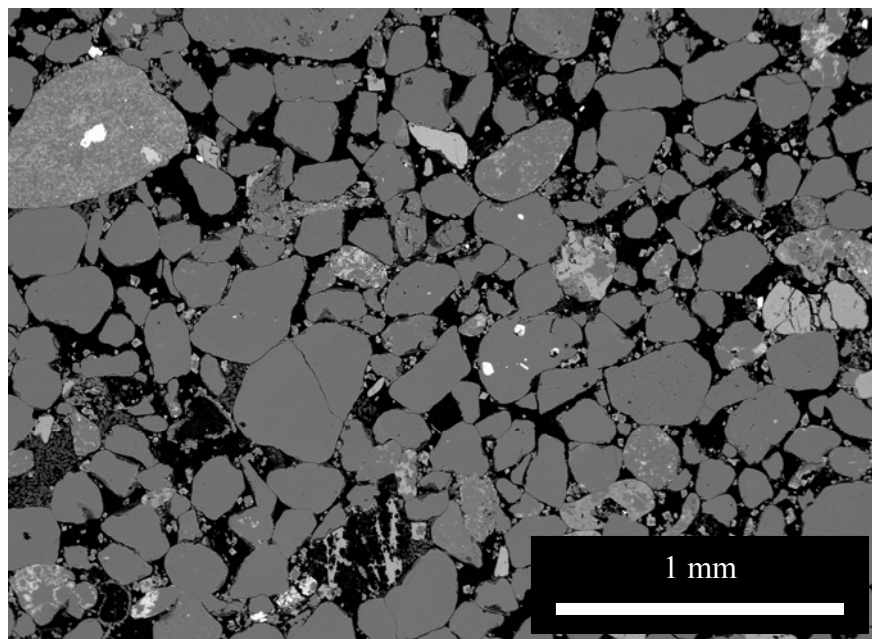
Plate 10. BSEM image of heterogeneously-compacted sandstone with close-packed and open-packed grain fabrics. Large oversized pores (black), with corroded skeletal relicts of K-feldspar are indicative of detrital framework grain dissolution. Sample SSK2388, Basal Permian aquifer, 1868.74 m, Cleethorpes No.1

Other minor to trace diagenetic minerals include halite, sylvite and barite. These occur as late (mesodiagenetic) cements partially filling intergranular porosity. Traces of pyrite were also observed in one sample (CLBP8).

Petrographical evidence suggests that much of the present porosity in these rocks is of secondary origin. Large oversized pores (e.g. Plate 9 and Plate 10) dominate the porosity in many of the samples, and are characteristic of primary framework grain dissolution (Schmidt and McDonald, 1979b). The presence of corroded and skeletal relics of K-feldspar, albite and fine-grained silica associated with many of these oversized pores suggests that they result from the dissolution of detrital feldspars, felsic lithic fragments, and chert grains. Similarly, the heterogeneous packing of the sandstones, with both highly compacted uncompacted grain framework domains present in the same thin section, suggest that the porosity in uncompacted domains is rejuvenated intergranular porosity resulting from the late-stage removal of an eodiagenetic (pre-compaction) cement phase that had preserved the open grain fabric during subsequent burial (Schmidt and McDonald, 1979b). Both anhydrite and dolomite have been identified as pre-compactional eodiagenetic cements. The anhydrite commonly shows signs of etching and corrosion, occurring as relics in isolated pores, indicating that the anhydrite was probably originally much more extensive. In contrast, eodiagenetic dolomite shows no significant evidence of dissolution. Therefore, the dissolution of anhydrite cement would seem to be the most likely candidate to account for the secondary rejuvenation of the intergranular porosity in these rocks.

4.1.1.3 MERCIA MUDSTONE GROUP – PRIMARY TARGET SEAL

The Mercia Mudstone Group is highly variable in lithology.

The Tarporley Siltstone Formation (represented by samples SSK2492, SSK2496, SSK2498 and SSK2502) encountered in the Cropwell Bishop borehole comprises dominantly fine to very fine sandstones and siltstones, interbedded with silty mudstones. Mineralogically, the sandstones are similar to the underlying Sherwood Sandstone Group and represent a transitional facies into the overlying mudstone-dominated sequence.

1 mm
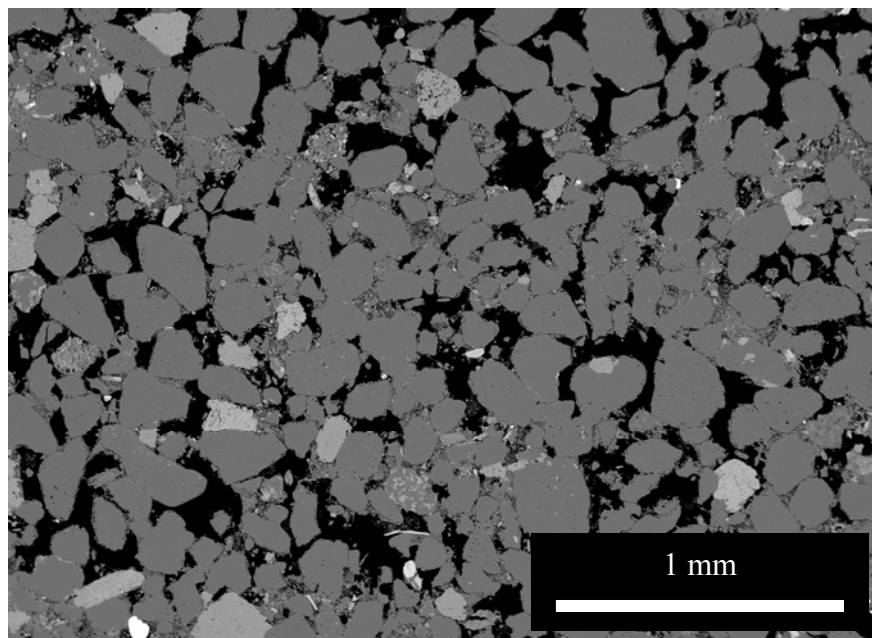
Plate 11. BSEM of porous fine sandstone from the Tarporley Siltstone Formation, with large oversized pores and patches cemented by dolomite. Sample SSK2492, Mercia Mudstone Group, 201.98 m, Cropwell Bishop borehole.

The cleaner sandstones comprise dominantly angular quartz with minor K-feldspar and deformed mudstone pellets or clasts (Plate 11). Grain packing at the thin section scale is very variable, ranging from highly compacted sandstone to areas with relative uncompacted grain fabrics. This

suggests that a significant amount of the present porosity in the very porous rocks at the base of sequence is secondary after the dissolution of an early diagenetic intergranular cement (Schmidt and McDonald, 1979b). These rocks also display large oversized pores characteristic of framework grain dissolution (Schmidt and McDonald, 1979b). Patchy or micronodular, dolomite cementing uncompacted grain fabrics, is also present. This is similar to the eodiagenetic (pedogenic) described from the Sherwood Sandstone Group (Section 4.1.1.1), and is therefore interpreted to be of similar origin. The dolomite shows evidence of dissolution in the Cropwell Bishop borehole samples. Euhedral calcite cement is present as late pore-filling cement. It appears to be very similar to the late (telodiagenetic) calcite described by Bath et al. (1986) and Milodowski et al. (1987) from the Sherwood Sandstone Group in the region, and which has been attributed to precipitation in association with incongruent dissolution of dolomite under the present groundwater regime (Bath et al., 1986). Higher up the sequence the intergranular porosity may be significantly to tightly cemented by pervasive pore-filling gypsum (e.g. sample SSK2502). Late-stage barite cement may be present as a minor component in some sandstones.

Muddier poorly-sorted sandstones and siltstone layers comprise a closely packed fabric of detrital quartz with minor K-feldspar, muscovite, biotite and chlorite flakes in a matrix of very fine grained illitic silt and clay (Plate 12). Much of this clay appears to display a relict primary pelleted fabric and represents 'pseudomatrix' formed by compactional deformation rather than a true primary clay matrix. Fine grained dolomite cement may also be present as matrix-replacive (or matrix-displacive) cement. The intergranular macroporosity in these layers in very low.
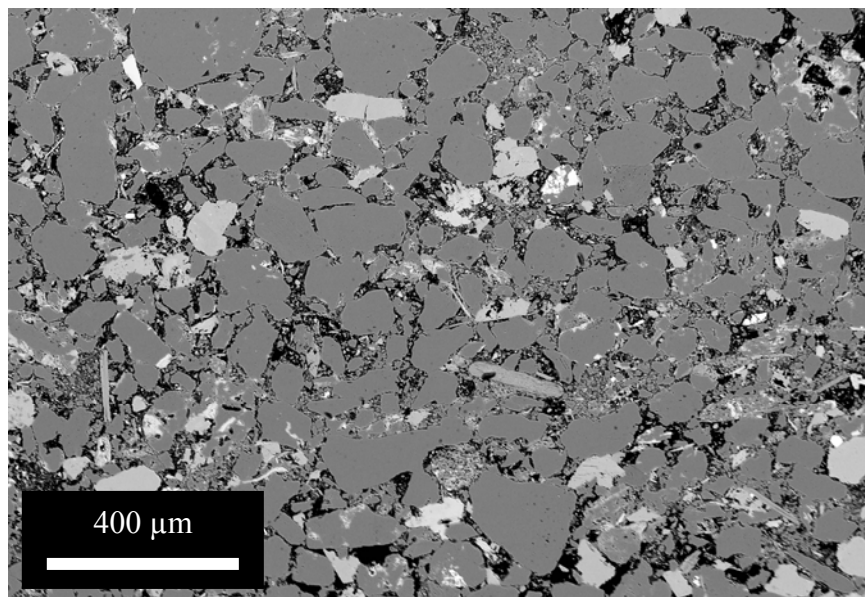
Plate 12. BSEM of poorly-sorted very fine sandstone from the Tarporley Siltstone Formation, with close-packed fabric and interstitial pseudomatrix clay. Minor barite cement is present (bright areas). Sample SSK2498, Mercia Mudstone Group, 192.61 m, Cropwell Bishop borehole.

Higher up the sequence the Tarporley Siltstone Formation passes into more argillaceous strata dominated by units of finely laminated red-brown siltstone, mudstone (Plate 13) interbedded with more massive grey-green dolomite- and anhydrite (now partly gypsified)-cemented siltstones, and structureless red-brown silty mudstones. These laminated rocks are very dolomitic with some laminae represented by discrete dolomicrite. The more massive red-brown siltstones and silty mudstone often contain nodules and irregular discontinuous thin layers of grey anhydrite (Plate 14). The macroporosity in these rocks is very low, although occasional thin

porous laminae of siltstone may present where anhydrite or gypsum cements may have been dissolved
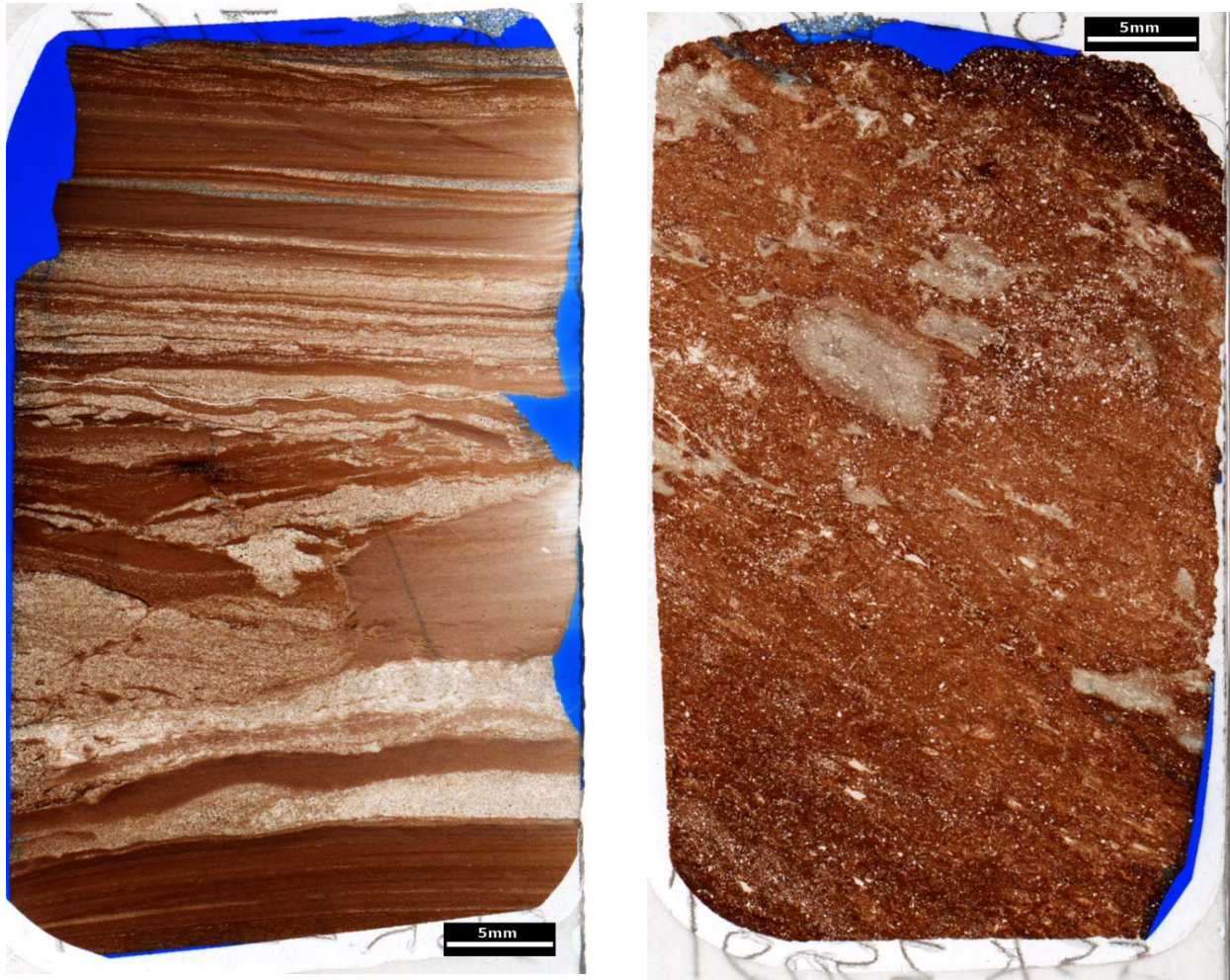
Plate 13. (Left) Transmitted light image showing finely interlaminated, brown mudstone and siltstone layer. Low-amplitude, ripple lamination within discontinuous siltstone laminae is evident. Some layers are disrupted by synsedimentary dewatering structures (irregular sand and silt structures intruded into overlying mudstone laminae. Sample SSK2504, Mercia Mudstone Group, 166.98 m, Cropwell Bishop borehole.

Plate 14. (Right) Transmitted light image of more massive anhydritic red-brown siltstone with faint bed bedding lamination and displacive patches of grey anhydrite. Sample SSK2509, Mercia Mudstone Group, 100.66 m, Cropwell Bishop borehole.

The Mercia Mudstone Group sequences examined in both Cropwell Bishop and Fulbeck Airfield No.1 boreholes is strongly affected by late-stage alteration and gypsification of primary anhydrite fabrics. This has resulted in extensive fracturing and veining by displacive fibrous gypsum veins, and localised brecciation of mudstone fabrics where it appears that wholesale dissolution of anhydrite and gypsum may have occurred, resulting in collapse. Gypsification was observed to occur both from: (a) the near surface, decreasing in downwards, and; (b) from the contact with the underlying Sherwood Sandstone Group aquifer, decreasing upwards. Undisturbed mudstone fabrics are therefore only preserved within a thin zone located between these two alteration zones.

These petrographic observations suggest that the very sandy basal part of the Mercia Mudstone Group (i.e. that part which is referred to as the Tarporley Siltstone Formation) should not be

regarded as a part of the seal. In fact, these rocks are more likely to contribute to the storage volume within the Sherwood Sandstone Group, given the presence of significant porous sandstone and siltstone. Supporting for this conclusion is provided by the fact that these lower Mercia Mudstone Group strata are known to be water-bearing and hence their old statigraphic name – the Keuper Waterstones (Howard et al., 2008). Furthermore, models of groundwater abstraction from the Sherwood Sandstone Group aquifer have to take account of a significant contribution of groundwater to the Tarporley Siltstone Formation in order to the maintain regional water balance (Dr G. Wealthall, 2008, personal communication).

4.1.1.4 ZECHSTEIN GROUP – SECONDARY TARGET SEAL

The Zechstein Group includes a wide range of formations and lithologies, including halite, gypsum, anhydrite, limestone and mudstones. However, only a very limited number of samples could be studied within the project. Furthermore, the only samples available are from relatively shallow depths near outcrop where they might have been altered by fresh groundwater penetration. Consequently, only a few examples of potential seal lithologies are included here to provide some indication of their likely character.

Roxby Formation

The lower boundary of the Sherwood Sandstone Group is transitional into the siltstone and mudstone dominated Zechstein (Permian) Roxby Formation. Two samples were analysed from the Whitemoor (sample SSK2609) and North Selby No.2 (sample SSK2613) boreholes in the Selby area, and reflect two distinct mudstone lithologies.

Sample SSK2613 comprises finely laminated micaceous siltstone (Plate 15) and structureless fine illitic mudstone (Plate 16). The micaceous siltstone lithology is composed dominantly of tightly-compacted angular quartz silt, and flakes of muscovite, biotite and chloritised biotite. An illite-rich clay with very minor disseminated very fine iron oxide fills between these particles. Much of this clay matrix appears to occur in discrete 'clots' that probably represent originally pelleted clay that has been compactional deformed to form a pseudomatrix. Minor auithigenic dolomite is present as scattered rhombs. No significant porosity is present except for traces of microporosity that possibly represent dissolution of traces of anhydrite or gypsum.
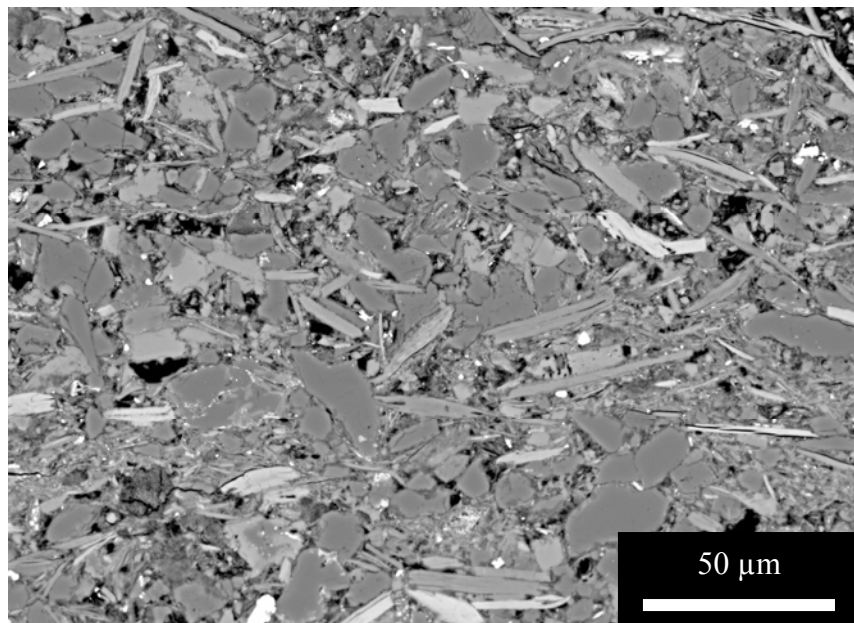
Plate 15. BSEM image of micaceous siltstone with close packed angular detritalquartz grains and subparallel flakes of muscovite and chloritised biotite. Sample SSK2613, Basal Roxby Formation, 262.37 m, North Selby No.1.

Sample SSK2609 represents highly compacted, massive structureless red siltstone or very fine sandstone. It is composed of scattered angular quartz with minor K-feldspar and albite with a fine illitic matrix (Plate 17). Patchy fine anhydrite cement is present and partially altered to gypsum. The clay matrix appears to contain ghost outlines of original pelleted forms, suggesting that it now represents a pseudomatrix formed by the compaction of clay originally deposited in pelleted form. No significant porosity is except for traces of microporosity associated with possible dissolution of minor anhydrite and gypsum grains.
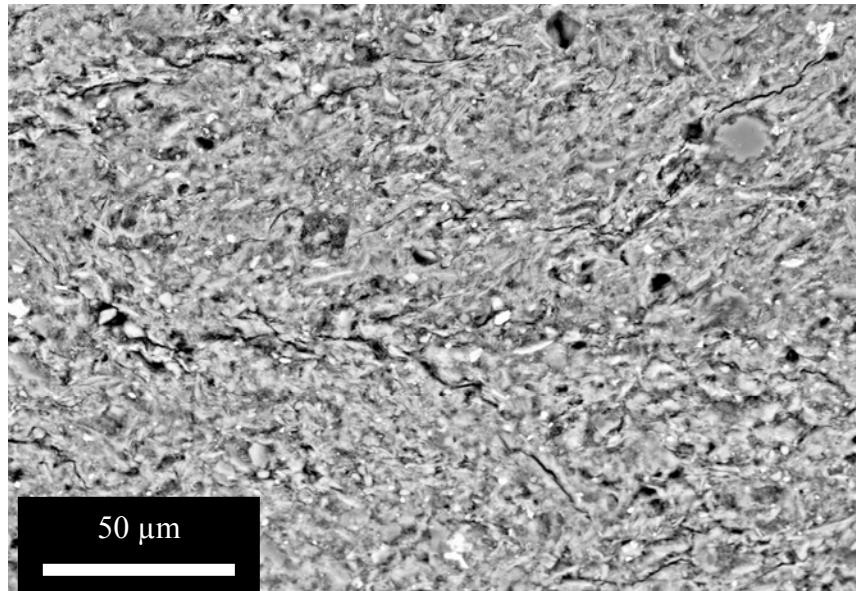
Plate 16. BSEM image of structureless mudstone with tight clay matrix. Sample SSK2613, Basal Roxby Formation, 262.37 m, North Selby No.1.
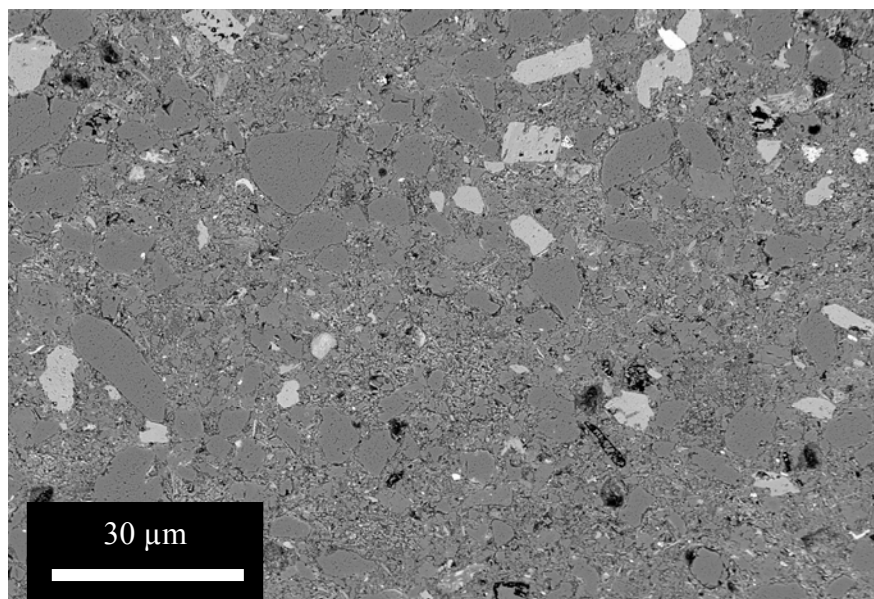
Plate 17. BSEM image of highly compacted siltstone containing quartz (dull grey) and K-feldspar (bright) grains in a tight pseudomatrix of illitic clay. Sample SSK2609, Basal Roxby Formation, 310.16 m, Whitemoor borehole.

Sherburn Anhydrite Formation (Roxby Formation Equivalent)

One sample of an anhydrite layer from the Sherburn Anhydrite in the Whitemoor borehole (sample SSK2611) was examined. The sample comprises largely fine grained, crystalline anhydrite with scattered minor inclusions of quartz silt and fine idiotopic dolomite rhombs. The cystal boundaries of the anhydrite are tightly interlocking and no visible porosity is present

Marl Slate Formation

Two samples of Marl Slate were examined from the Cleethorpes No.1 borehole. They are represented by finely laminated dark grey mudstone and siltstone, with occasional thin laminae of very fine sandstone. The laminae display wavy bedforms indicating fine ripple lamination. Silstone and very fine sandstone laminae comprise grains of angular quartz with fine ragged outlines, minor K-feldspar and felsic lithic clasts composed of quartz-K-feldspar intergrowths. Minotr to trace amounts of detrital mica may also be present. The clay matrix of the siltstone is illitic, and appears to have originally been deposited as discrete silt-sized pellets that have been deformed by compaction to form the present pseudomatrix. The clay-rich laminae comprise very fine silt and clay grade mica and illitic clay, with scattered very fine quartz silt. Authigenic dolomite is a major component, occurring as fine grained patchy cement replacing the clay matrix. Minor to trace amounts of fine anhydrite and pyrite are also present.

No porosity was visible in thin sections from these samples.

Plate 18 Transmitted light image showing finely interlaminated, ripple-laminated, brown mudstone and siltstone layers with scattered grains of quartz sand. Sample SSK2388, Marl Slate Formation, 1865.45 m, Cleethorpes No.1.

4.1.2   Forth area

The mineralogical analyses of the Carboniferous and Devonian aquifer and seal samples from the Forth area are presented in the digital dataset *Modal Mineralogy Data - MIDLAND VALLEY v1.0.xls* (provided on the CDROM enclosure). An overview of the mineralogical and diagenetic characteristics of these rocks is presented in the following sections.

4.1.2.1 KNOX PULPIT SANDSTONE FORMATION – PRIMARY TARGET AQUIFER

The Knox Pulpit Sandstone Formation, together with the Kinnesswood Formation, is regarded as the primary target aquifer unit (Monaghan et al., 2008). It has an extensive outcrop in Fife, where it may be up to 180 m thick, and is likely to be present at suitable depths for CCS within the Firth of Forth (Browne et al., 1987; Monaghan et al., 2008). The Knox Pulpit Sandstone Formation comprises predominantly soft, weakly cemented, white and cream-coloured, very fine- to coarse-grained feldspathic sandstones, and is considered to be of largely aeolian origin (Chisholm and Dean, 1974). The characteristic features of these rocks (Monaghan et al., 2008) are: a marked variation in grain-size between adjacent laminae which may be 1–10 mm thick, referred to as 'pin-stripe' lamination; a rarity of pebbles; the development with small concretionary masses of caliche/calcrete (cornstone) near the top of the formation, and; greenish grey silty claystone near the base. A range of cross-stratification forms and flat lamination occur with reactivation surfaces within sets of cross strata. Ripple lamination is rare except near the top. Well-rounded millet seed grains are common in coarser laminae.

Petrographic analyses for the Knox Pulpit Sandstone Formation were undertaken on representative samples of sandstone from the Glenrothes geothermal borehole (5 samples) supplemented by material from Balreavie No.3 water borehole (1 sample) and from outcrop at Arraty Crags (2 samples; Figure 2, Appendix 1).

The sandstones comprise moderately well sorted very fine, fine and medium grained subfeldspathic arenites (Figure 14). In thin section, they may display a bimodal distribution of grain, with large rounded to subrounded (aeolian) sand grains (predominantly quartz), and finer angular to subangular grains (Plate 19). Primary detrital components comprise major detrital quartz and subordinate K-feldspar, with very minor to accessory muscovite, and traces of apatite, tourmaline, zircon, rutile and iron oxides. Detrital lithic clasts are rare but may have been underestimated in the modal analytical data (Section 3.1.4.2). Detrital plagioclase and albite are absent or present only in traces. The rocks are characterised by tightly-compacted grain fabrics, with long edge grain contacts dominant, common compaction fracturing of feldspars, and plastic deformation of detrital micas and more labile lithic grains (Plate 19). Intergranular clay is common.

The rocks exhibit significant diagenetic modification of the mineralogy and porosity. Micas are typically splayed and detrital feldspars are partially dissolved. Scattered oversized pores are grain-shaped and suggest local detrital framework grain dissolution (Schmidt and McDonald, 1979a,b) (Plate 19 and Plate 20). Etching and corrosion of K-feldspar grains display is common. Ferroan dolomite or ankerite cement is a major component in samples from Glenrothes (Plate 21). Oversized ferroan dolomite/ankerite patches were also observed, indicating that the carbonate mineral has also partially replaced some of detrital framework grains (Schmidt and McDonald, 1979b). It may display euhedral crystal terminations in open pores. Some of the ferroan dolomite has filled residual space between highly compacted detrital grains, demonstrating that it is mesodiagenetic and formed after the main burial compaction. In other cases, it can be seen locally to preserve domains of uncompacted or 'expanded' grain fabric , suggesting it has replaced a near-surface eodiagenetic (pre-compaction) cement, possibly after pedogenic dolocrete or calcrete (cf. similar fabrics in the Sherwood Sandstone Group described in Section 4.1.1.1). Traces of calcite are also present.
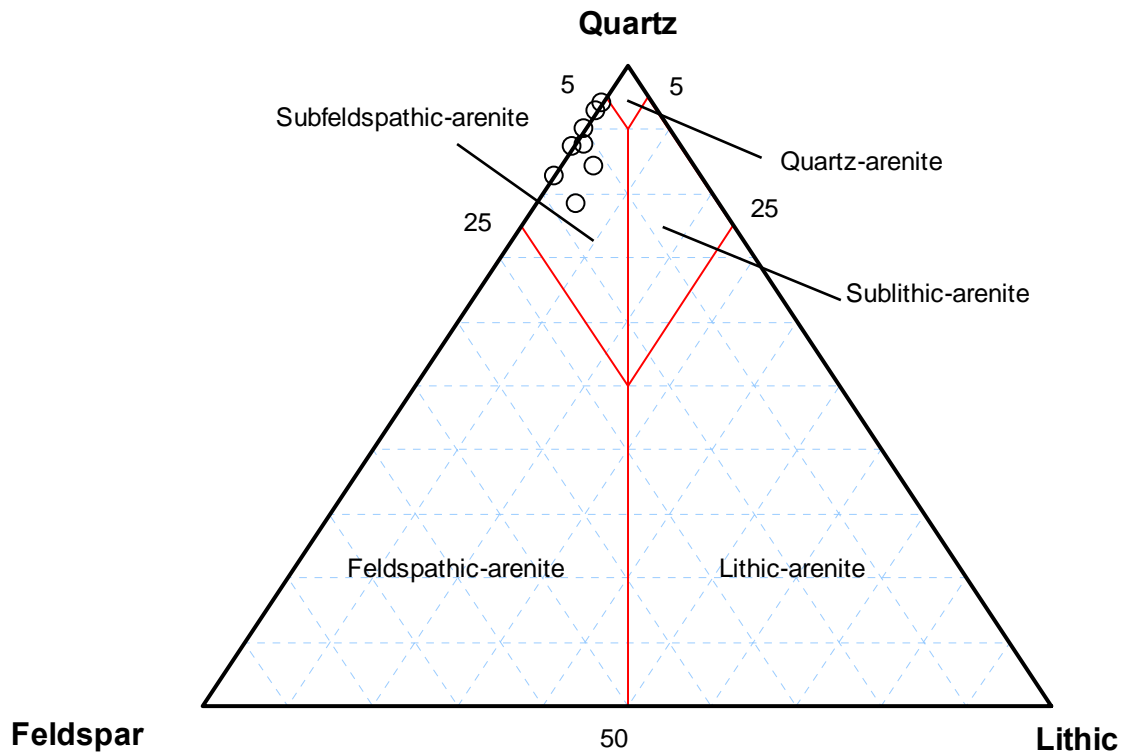
Figure 14. Classification of sandstone samples from the Knox Pulpit Sandstone Formation on the basis of measured proportions of quartz, feldspar and lithic clasts (classification after Pettijohn et al., 1987)
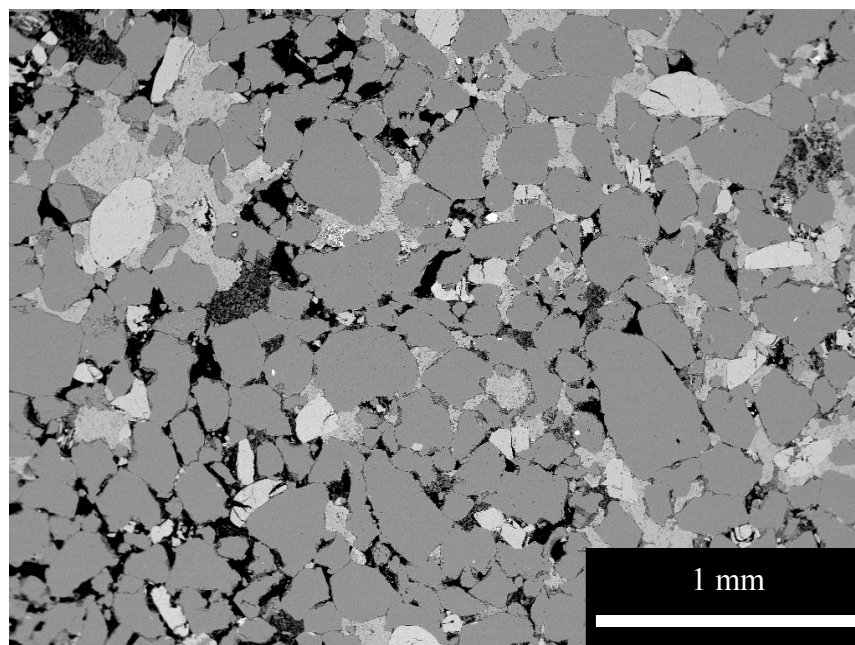
Plate 19. BSEM image of very fine to medium sandstone composed of major detrital quartz (dull grey) and minor K-feldspar (white), with patches of ferran dolomite cement (mid grey). The rock has a compacted grain fabric with rounded to subrounded coarser quartz grains and more angular finer sand grains. Oversized pores are present and may contain authigenic kaolinite. Sample SSK2524, Knox Pulpit Sandstone Formation, 584.38 m, Glenrothes borehole.
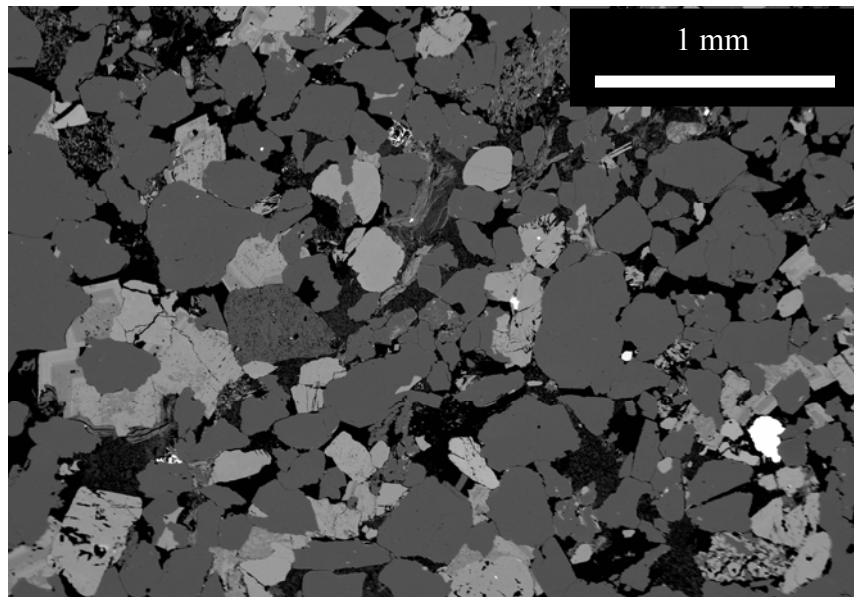
Plate 20. BSEM image of clean, fine to medium sandstone composed of major detrital quartz (dull grey) and minor K-feldspar (white), with patches of ferroan dolomite cement (mid grey). The rock has a compacted grain fabric with rounded to subrounded coarser quartz grains and more angular finer sand grains. Oversized pores are present and may contain authigenic kaolinite. Euhedral crystal faces on some quartz grains represent authigenic quartz overgrowth cement. Detrital muscovite is exfoliated and replaced by kaolinite along cleavage. Sample SSK2526, Knox Pulpit Sandstone Formation, 584.38 m, Glenrothes borehole.
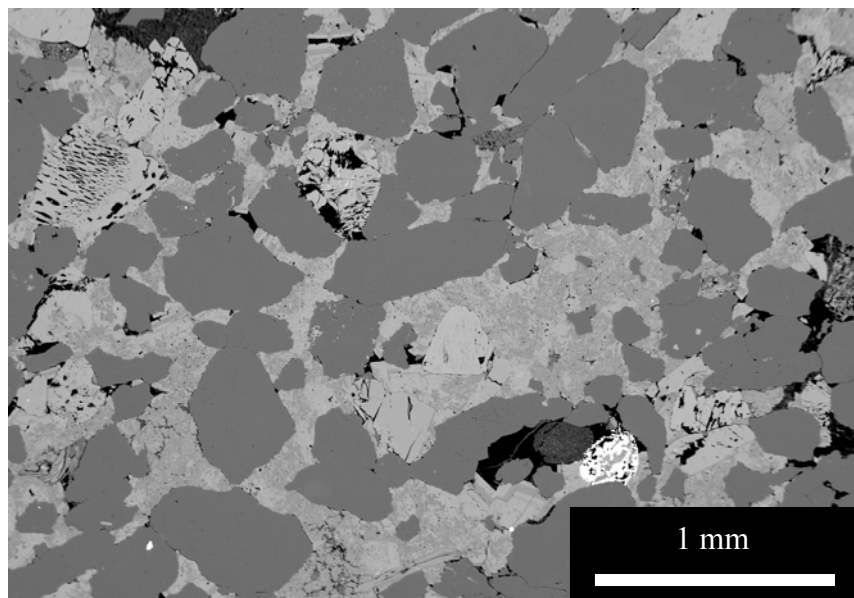
Plate 21. BSEM image of ferroan dolomite-cemented area of fine to medium sandstone. The ferroan dolomite cement (mid grey) fills intergranular spaces between compacted quartz (dull grey) grains and also occupies oversized areas. Sample SSK2526, Knox Pulpit Sandstone Formation, 584.38 m, Glenrothes borehole.

Authigenic syntaxial quartz overgrowths occur on detrital quartz grains in cleaner sand laminae. Authigenic kaolinite is present in most samples (0-5%). It also occupies oversized areas and thus appears to have replaced original detrital grains (possibly feldspars), preferentially replacing grains that were in the fine/very fine sandstone fraction. Detrital muscovite grains are often altered, displaying splaying and exfoliation, with replacement along cleavage by kaolinite (Plate 20).

Modal analyses indicate the highest porosities (16-21%) in the samples from outcrop and shallow depth in the Balreavie borehole. Significantly lower porosities (4-13%) were recorded from the deeper samples in the Glenrothes borehole. The higher porosities in the shallow and outcrop samples coincides with an absence of ferroan dolomite cement. These very porous rocks also preserve of patches of large open intergranular porosity in an otherwise strongly-compacted grain fabric (Plate 22) suggesting that much of the porosity is secondary - possibly as a result of the dissolution and removal of the ferroan dolomite by weathering and shallow groundwater alteration.
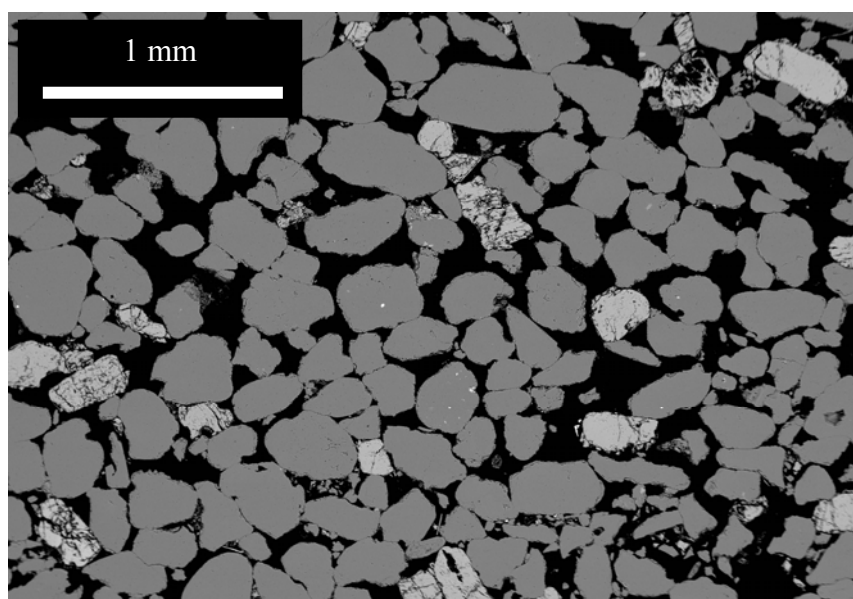
Plate 22. BSEM image of very porous, fine to medium sandstone composed of major sub-rounded to well-rounded grains of detrital quartz (dull grey) and minor K-feldspar (white), with patches of ferroan dolomite cement (mid grey). The rock has a variably-compacted grain fabric with areas of open packing and other areas with close-packed quartz grains with long and triple-point grain contacts. Oversized pores are present and may contain authigenic kaolinite. Sample ASW427, Knox Pulpit Sandstone Formation, from outcrop at Arraty Crags.

4.1.2.2 KINNESSWOOD FORMATION – PRIMARY TARGET AQUIFER

The Kinnesswood Formation, together with the Knox Pulpit Sandstone Formation, is regarded as part of the primary target aquifer unit (Monaghan et al., 2008). It is between 100-200 m thick within much of the area but reaches up to 640 m in the Edinburgh area. The Kinnesswood Formation comprises predominantly purple-red, yellow, white and grey-purple, fine- to coarse grained sandstones which are mostly cross bedded and arranged in upward-fining units. Fine-grained, planar or poorly bedded sandstones, red mudstones and nodules and thin beds of calcrete also occur. The cross-bedded sandstones were deposited in river channels and the fine-grained sandstones and mudstones represent overbank deposits formed on the associated floodplains. The calcretes, which characterise the formation, were developed in soil profiles on

the floodplains under the influence of a fluctuating water table in a semiarid climate (Chisholm and Dean, 1974; Monaghan et al., 2008).

Petrographic analyses for the Kinnesswood Formation were undertaken on representative samples of sandstone from the Glenrothes geothermal borehole(4 samples, including sandstones that appear to be transitional facies into the muddier Ballagan Formation) supplemented by material from Balreavie No.3 water borehole (1 sample) and from outcrop at Maspie Den (1 sample; Figure 2, Appendix 1).

Petrographic analyses show that the sandstones are mineralogically similar to those of the Knox Pulpit Formation. They comprise moderately well sorted, fine to medium (Glenrothes and Maspie Den samples) and medium to coarse (Balreavie sample) subfeldspathic arenites (Figure 15). Primary detrital components comprise major detrital quartz and subordinate K-feldspar, with very minor to accessory muscovite, and traces of apatite, tourmaline, zircon, rutile and iron oxides. Detrital lithic clasts are relatively minor components but the Balreavie sample (BEB7503) is more lithic–rich (lithic-feldspathic arenite) and may approach a sublithic arenite composition, although this is not reflected in the modal mineral data since lithic clasts are probably underestimated (see Section 3.1.4.2). Detrital plagioclase and albite are absent or present only in traces. The rocks are characterised by angular grains with tightly-compacted grain fabrics, with long edge grain contacts dominant, common compactional fracturing of quartz and feldspars, and plastic deformation of detrital micas and more labile lithic grains (Plate 23). Intergranular clay is common, and clay may also be present as discrete clay lamina, particularly in the samples that are from the interval in the Glenrothes borehole that is transitional to the Ballagan Formation.
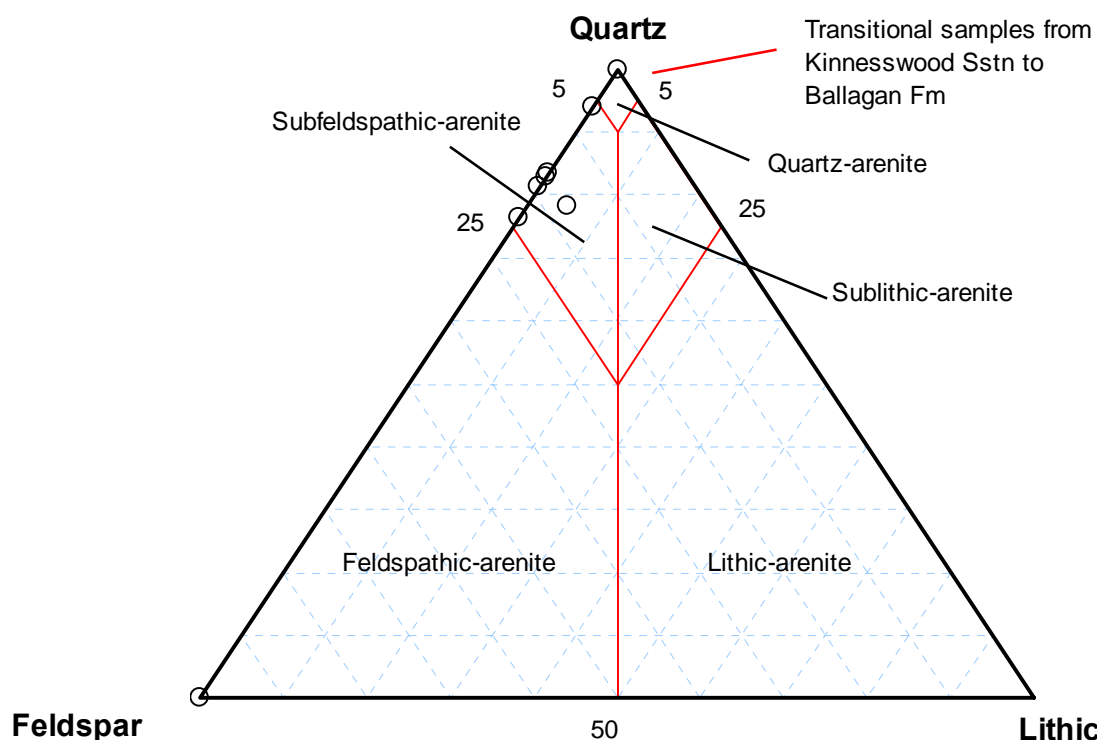
Figure 15. Classification of sandstone samples from the Kinneswood Formation on the basis of measured proportions of quartz, feldspar and lithic clasts (classification after Pettijohn et al., 1987)

The rocks exhibit significant diagenetic modification of the mineralogy and porosity. Etching and corrosion of K-feldspar grains display is common. The sandstones contain large oversized pores (Plate 23) that are indicative of secondary framework grain dissolution porosity (Schmidt and McDonald, 1979b). These pores commonly contain microporous authigenic kaolinite fills that replaces the original detrital silicate grain. Some grains are coated with a fine hematitic film. Quartz grains in cleaner patches and laminae may display 'serrated' quartz outlines possibly representing minor syntaxial overgrowth cement. Minor K-feldspar overgrowths with euhedral faces into open pores were also observed locally cementing adjacent grains.

As in the Knox Pulpit Sandstone Formation, mesodiagenetic ferroan dolomite and ankerite cement are major cements in the Glenrothes samples but are present as minor phases in the Balreavie sample, and are absent in the outcrop sample from Maspie Den. The ankerite occurs as a later overgrowth on earlier ferroan dolomite lining open pores (Plate 24). These carbonate minerals replace detrital framework grains, fills residual space between highly compacted detrital grains, and occur as larger areas or patches that locally preserves an uncompacted or 'expanded' grain fabric indicative of replacement of pedogenic dolocrete or calcrete. Mesodiagenetic calcite is significant in the Balreavie well. Other authigenic minerals include traces of fine grained pyrite and very minor pore-filling barite.

1 mm
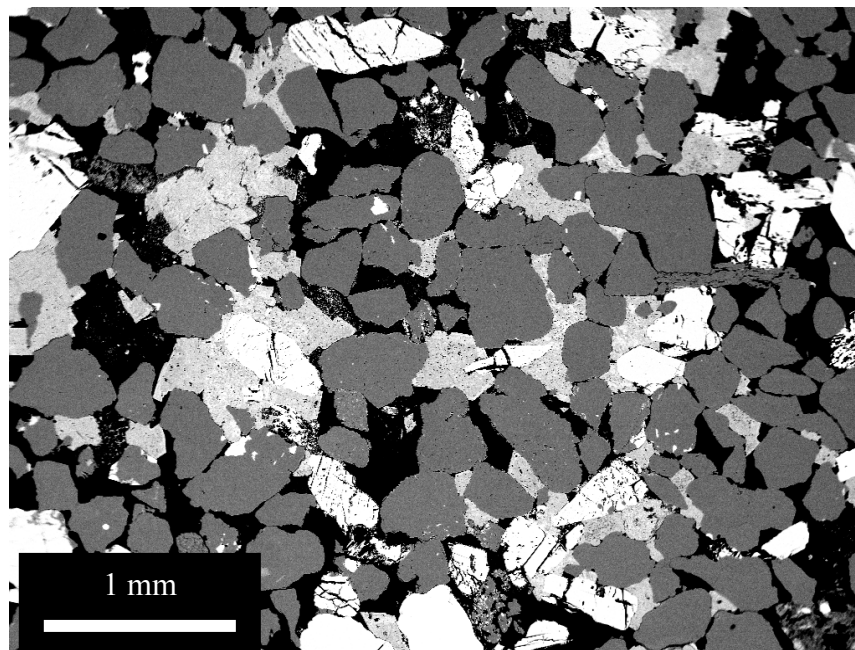
Plate 23. BSEM image of clean, fine to medium sandstone composed of major detrital quartz (dull grey) and minor K-feldspar (white), with patches of ferroan dolomite/ankerite cement (light grey/white). The rock has a compacted grain fabric with angular quartz grains and locally oversized pores produced by framework grain dissolution. Sample SSK2536, Kinnesswood Sandstone Formation, 388 m, Glenrothes borehole.

Modal analyses indicate the highest porosities (16-19%) in the two samples from outcrop and shallow depth in the Balreavie borehole. Significantly lower porosities (1-10%) were recorded sandstones from the deeper samples in the Glenrothes borehole. As seen in the Knox Pulpit Sandstone Formation, the higher porosities seen in the shallow and outcrop samples coincide with an absence of ferroan dolomite cement, suggesting that much of the porosity results from the dissolution and removal of the ferroan dolomite by weathering and shallow groundwater alteration.
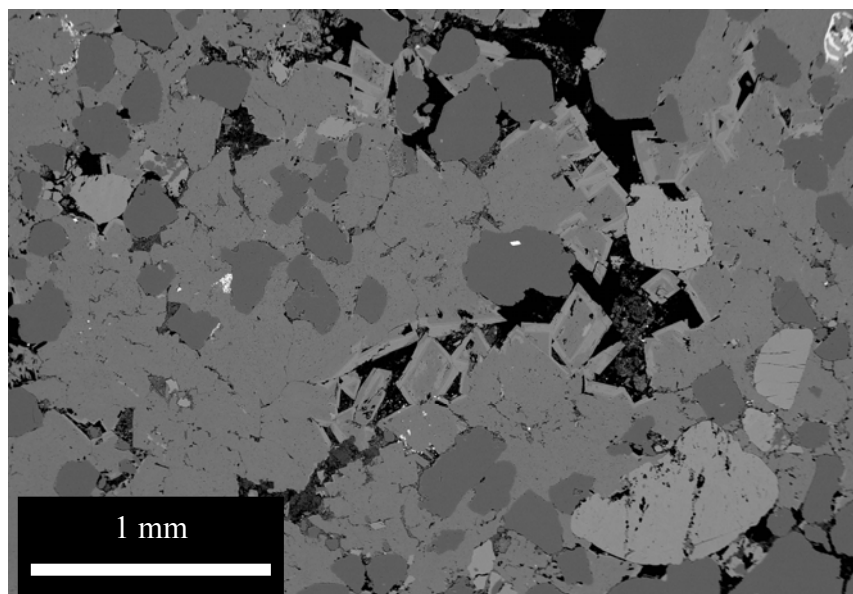
Plate 24. BSEM image of ferroan dolomite-cemented area preserving an uncompacted or 'expanded' grain fabric. The brighter fringes of ankerite can be seen as overgrowths on the ferroan dolomite lining open pores. Sample SSK2532, Kinnesswood Sandstone Formation, 428.4 m, Glenrothes borehole.

4.1.2.3 BALLAGAN FORMATION – PRIMARY TARGET SEAL

The Ballagan Formation overlies the Kinneswood Sandstone Formation, and forms the potential top seal to the Upper Devonian-Lowermost Carboniferous aquifer (Monaghan et al., 2008). It is characterised by generally grey mudstones and siltstones, with nodules and beds of ferroan dolomite (cementstone), the beds are generally less than 0.3 m thick. Gypsum, and to a much lesser extent anhydrite, and pseudomorphs after halite occur. Desiccation cracks are common and the rocks frequently show evidence of brecciation during diagenesis. Both these features are associated with reddening of the strata (Monaghan et al., 2008).

Petrographic analyses for the Ballagan Formation were undertaken on 4 samples from the Glenrothes geothermal borehole. he formation in this borehole is highly variable. The main lithologies include dolomicrite/dolomicritic mudstone, laminated mudstone and siltstone, and muddy sandstone. Because of the very limited number of samples that could be allocated for analyses, the samples were selected to provide an example of the principal lithological variants and should not be regarded as statistically representative of the whole formation

Dolomicrite and dolomicritic mudstone

Dolomicritic horizons are represented by samples SSK2540 and SSK2544.

Sample SSK2540 comprises finely crystalline microdolosparrite representing diagenetically-recrystallised dolomicrite (Plate 25). It is composed of about 72% ferroan dolomite forming a dense matrix of tightly intergrown crystals of ferroan dolomite. Silt-sized grains of minor quartz and trace K-feldspar and mica are disseminated through the dolomicrite..

Sample SSK2544 is more clay-rich than SSK2540. This consists of a tight matrix of highly-compacted illitic clay with scattered grains of quartz and feldspar silt, within which idiomorphic or hypidiomorphic crystals of ferroan dolomite have grown replacively (Plate 26). Minor ferroan calcite is also present and appears to replace the dolomite matrix in small patches.

Both samples are tight and no significant porosity can be seen in thin section. Any porosity seen in BSEM images is probably an artefact of grain plucking during section preparation.
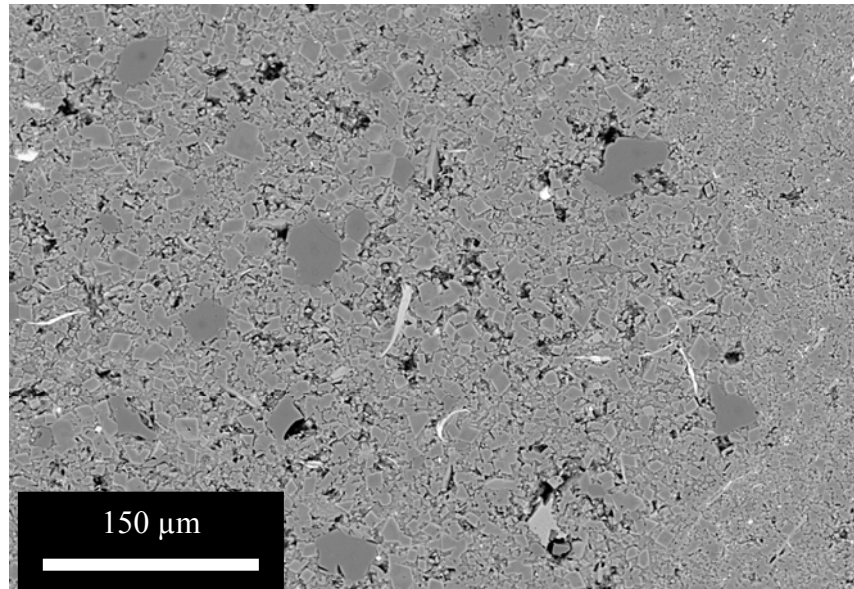
Plate 25. BSEM image of recrystallised dolomicrite (microdolosparrite) showing tight, matrix of intergrown fine ferroan dolomite crystals, with scattered quartz silt and very sparse mica grains. No macroporosity is present. Sample SSK2540, Ballagan Formation, 335.15 m, Glenrothes borehole.
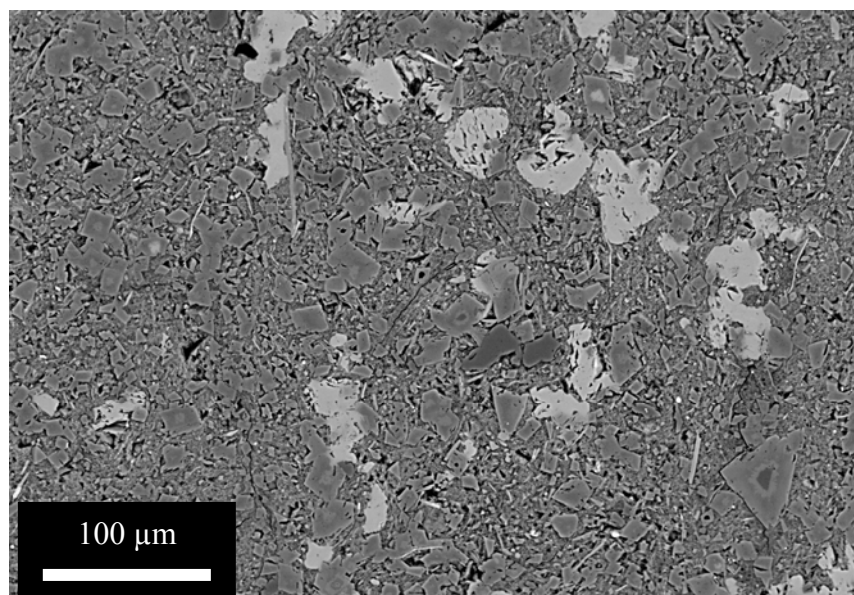
Plate 26. BSEM image of recrystallised dolomicritic mudstone displaying a tight, compact clay matrix with hypidiomorphic to idiomorphic crystals of ferroan dolomite. The dolomite has grown replacively within the matrix of clay. Minor calcite (light grey) is also present and appears to replace the dolomite. Sample SSK2544, Ballagan Formation, 259.88 m, Glenrothes borehole.

Laminated mudstone and siltstone

Sample SSK2542 represents an example of finely laminated calcite-cemented siltstone and mudstone (Plate 27). It comprises a matrix of illite-rich clay with disseminated silt-sized quartz, K-feldspar and mica, with scattered coal fragments. Calcite is the major cement in this rock with only trace amounts of ferroan dolomite.
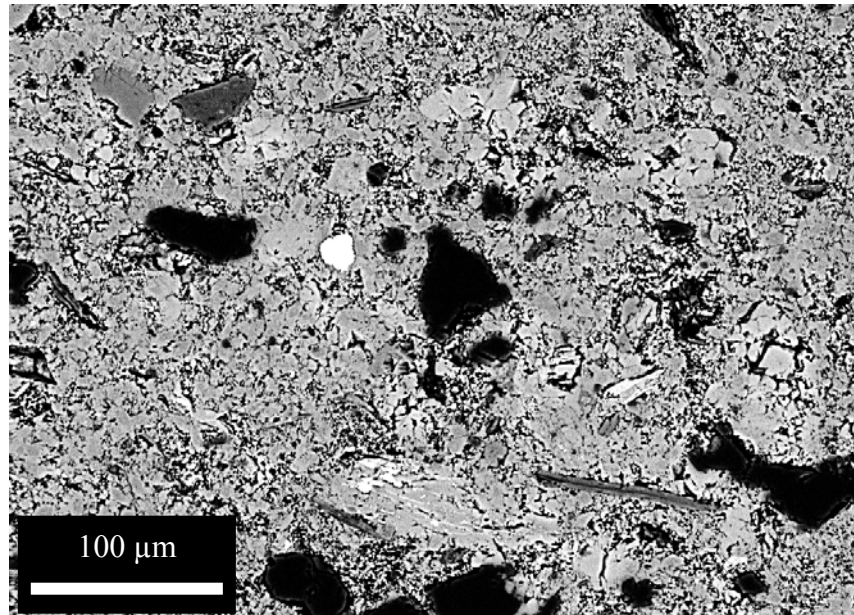
Plate 27. BSEM image of calcite-cement mudstone. Scattered grains of quartz (dark grey), K-feldspar (light grey) and coal fragments (black) are disseminated through a very tight, compact clay matrix that is largely replaced by ferroan calcite. Sample SSK2542, Ballagan Formation, 312.89 m, Glenrothes borehole

Micaceous sandstone

Sample SSK2546 represents a finely laminated mica-rich argillaceous sandstone with common coal fragments (Plate 28). The sand component is dominated by major quartz with minor K-feldspar muscovite and chlorite. Plagioclase is absent. Clay is present in discrete patches that were probably pellets or mudstone clasts that have been deformed by compaction to form a clay-rich pseudomatrix
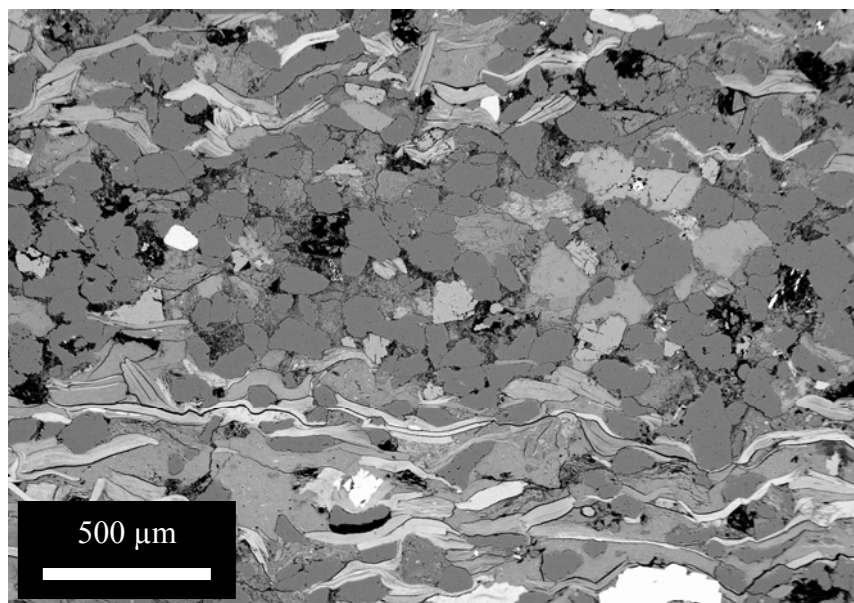
Plate 28. BSEM image of micaceous sandstone showing quartz and K-feldspar sand with thin laminae rich in muscovite and chlorite. The quartz and feldspar grains are highly compacted with sutured grain boundaries. The micaceous grains are bent and plastically-deformed by compaction around more competent quartz and feldspar grains. Sample SSK2546, Ballagan Formation, 221.77 m, Glenrothes borehole

The rock is highly compacted with well-developed sutured grain boundaries and consequently very low intergranular porosity. Clay, mica and chlorite grains are concentrated in thin laminae 100-200 μm thick, where they are oriented parallel to bedding and plastically deformed by the compaction.

No primary intergranular porosity remains and most of the porosity present appears to be secondary, resulting from the dissolution of framework grains (probably after feldspars and lithic clasts.

4.1.2.4 MINOR POTENTIAL AQUIFER AND SEAL UNITS

Passage Formation – aquifer unit

Siliceous sandstones of the Passage Formation at the top of the Clackmannan Group would likely be the most significant aquifer for geothermal prospectivity if deeply enough buried, and are considered to have potential as a minor aquifer unit for CCS in the region (Monaghan et al., 2008). One sample of sandstone from this unit was analysed from the Kincardine East borehole (Figure 2).

The sandstone comprises clean, fine grained quartz arenite with a patchy dolomite cement. The rock is composed of up to 92% quartz. The grain fabric is closely compacted, being dominated by long grain boundary, concavo-convex and triple point grain contacts (Plate 29). This, together with the dolomite cement has dramatically reduced the primary intergranular porosity. However, significant secondary porosity is present as a result of framework grain dissolution (after feldspars and possibly some lithic clasts).
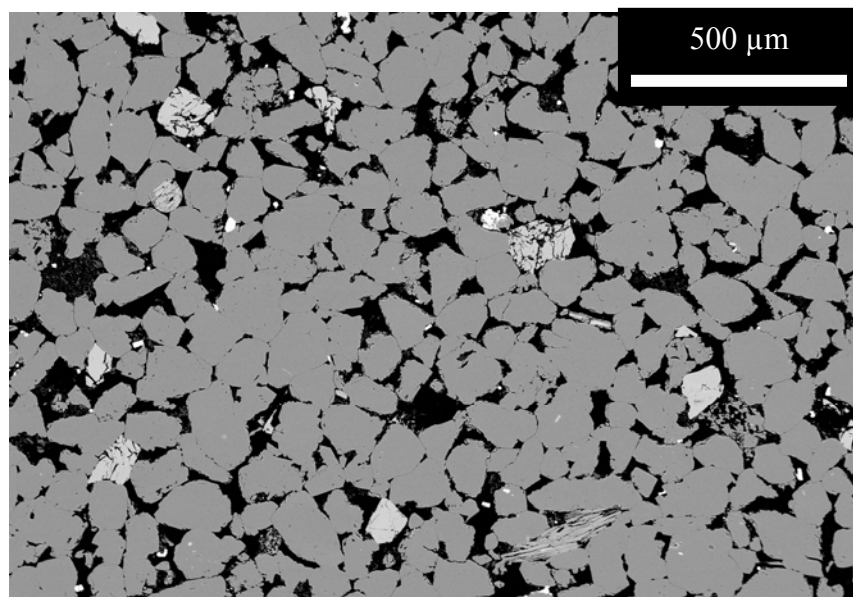
Plate 29. BSEM image of fine grained quartz arenite, with minor corroded K-feldspar grains (light grey). The grain fabric is strongly compacted with large oversized pores representing framework grain dissolution sites. Sample SSK2575, Passage Formation, 221.71 m, Kincardine East borehole.

Upper Limestone Formation –aquifer unit

The Upper Limestone Formation is characterised by repeated upward-coarsening cycles comprising grey limestone overlain by grey to black mudstones and calcareous mudstones, siltstones and paler sandstones capped by seatrocks and coal (Monaghan et al., 2008). This is considered to have some aquifer potential for CCS in the region. One sample of siltstone-

mudstone (sample SSK2562) and one sample of sandstone (sample SSK2573) were examined from the Kincardine East borehole.

Sample SSK2562 is a finely dominantly laminated mudstone to siltstone (Plate 30) with thin (0.1-5 mm) discontinuous lenticular fine lithic sandstone laminae representing 'starved' ripples. Illitic clay is the dominant component, with minor to subordinate silt-grade quartz, muscovite,biotite and chlorite. Dolomite is a very minor cement, fine grained disseminated pyrite is present as a trace phase. Coal organic fragments are common. The rock has been tightly compacted with very low microporosity (Plate 30).

250 μm
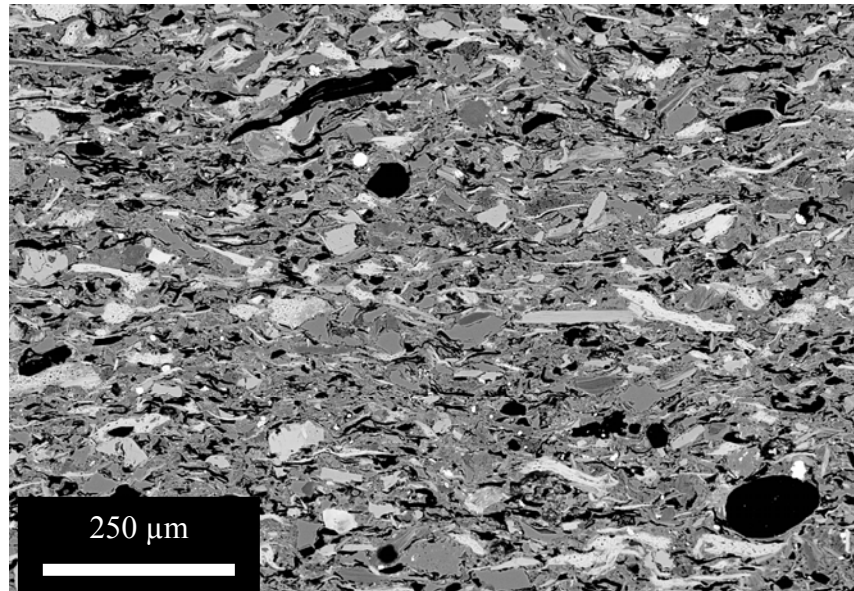
Plate 30. . BSEM image of micaceous mudstone-siltstone, showing silt sized grains micas and quartz, and dark coal grains in a tightly compacted clay matrix. Sample SSK2562, Upper Limestone Formation, 406.00 m, Kincardine East borehole.

Sample SSK2573 is medium to fine, cross-bedded subfeldspathic to sublithic arenite, with occasional siltstone or mudstone laminae <1 mm thick, forming current fore-set laminae. It is dominated by detrital quartz with minor to subordinate K-feldspar, muscovite, biotite and chlorite (Plate 31). The rock has a highly compacted grain fabric dominated by sutured grain boundaries and triple-point grain contacts (Plate 31), plastic deformation of mica, and K-feldspars that are commonly fractured at point-contacts.

The rock is markedly different to the other sandstones described in the previous sections, in that it contains abundant authigenic chlorite. Most of the chlorite has replaced mudstone or clay pellets and laminae. Dark brown laminae seen in thin section are more muddy laminae that are entirely cemented or replaced by authigenic chlorite. Chlorite also partially replaces exfoliated detrital mica fragments. Locally, syntaxial quartz overgrowth cements on detrital quartz has produced well-developed euhedral quartz faces. Quartz cement and kaolinite, closely associated with euhedral quartz crystals and locally enclosing fine kaolinite crystals, suggest quartz may be coeval with, or slightly later than, kaolinite. Most chlorite appears later and generally rests on top of euhedral quartz. However, very occasionally some chlorite may be included within quartz cement, suggesting that some quartz cementation formed simultaneously with chlorite authigenisis. Minor ferroan dolomite-ankerite cement is present. Accessory anatase is associated locally with altered detrital Ti-Fe oxides or ferromagnesian minerals.

Compaction has largely destroyed the primary intergranular porosity. Most of the porosity is now present as large oversized secondary pores, resulting from the dissolution of feldspar

framework grains (Plate 31). Large oversized pores filled by microporous authigenic kaolinite cement, which appears to have replaced framework grains (probably feldspars). Authigenic pyrite crystals occur disseminated within kaolinite cements. Micas are usually exfoliated and degraded, with exfoliated regions being replaced by authigenic kaolinite. Exfoliation occurs into residual pore space between compacted competent quartz grains, indicating exfoliation occurred after the main burial compaction phase. Later diagenetic chlorite overprints and replaces kaolinite cements locally.
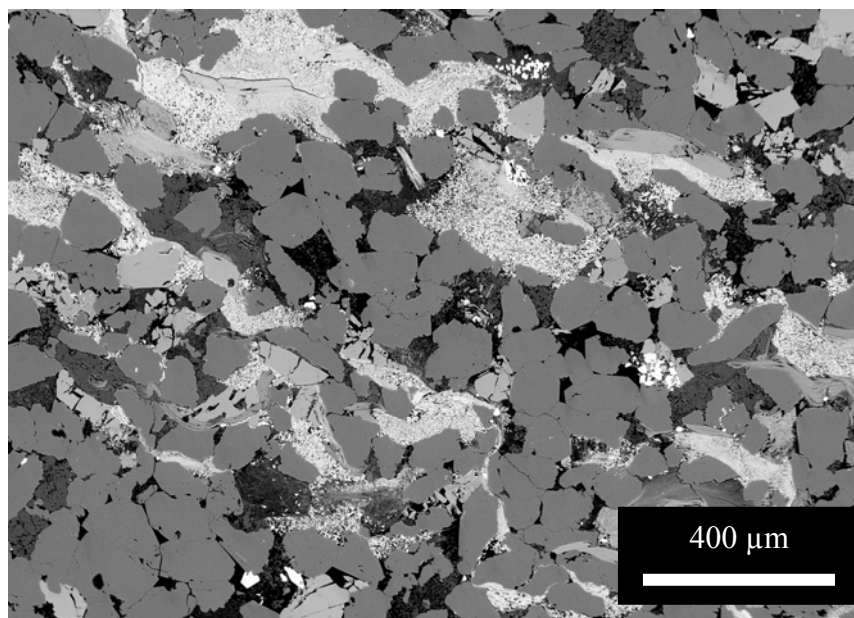
Plate 31. BSEM image of medium to fine grained micaceous sandstone displaying a highly compacted grain fabric with relatively large oversized secondary pores formed by framework grain dissolution. Authigenic chlorite (light grey) replaces pseudomatrix clay formed by the plastic deformation of mudstone clasts and clay pellets. Sample SSK2573, Upper Limestone Formation, 343.56 m, Kincardine East borehole.

Pathhead Formation – aquifer unit

The Pathhead Formation consists predominantly of mudstone and siltstone with beds of limestone and dolomite (Monaghan, et al., 2008). Pale coloured, fine to medium-grained sandstone is subordinate to the argillaceous rocks but may represent some minor aquifer potential. Thin beds of coal and ironstone also occur. Samples from this unit were examined from the Glenrothes (1 sample) and Milton of Balgonie No.2 (2 samples) boreholes (Figure 2).

Sample SSK2550 (Glenrothes) is a fine to medium subfeldspathic arenite, the detrital components are dominated by angular quartz, with subordinate K-feldspar, albite and chlorite. Detrital clay is present in discrete laminae (often micaceous) and as a minor intergranular clay. The grain fabric is tightly compacted, and compaction has destroyed most the primary intergranular porosity. The porosity now present is largely secondary oversized pores produced by feldspar framework grain dissolution. The oversized pores are often filled by microporous authigenic kaolinite cement, which appears to have replaced the framework grains.

The is evidence of minor microcrystalline quartz overgrow producing 'ragged' grain and for authigenic K-feldspar having replaced plagioclase (intergrown with authigenic albite). Extensive authigenic chlorite (Mg-Al-Fe-rich) cement is pervasive through the interstitial/intergranular areas, replacing altered micas and complexly intergrown with kaolinite. The chlorite inter-fingers with the kaolinite, and in some areas, 'relict books' may represent chlorite-replaced kaolinite. The

chlorite authigenesis is similar to that seen in sandstone from the Upper Limestone Formation in the Kincardine East borehole.

Sample SSK2558 is dominantly medium to fine, cross-bedded sandstone, ranging from silt to coarse sand. Clay-rich laminae are present. The rock is highly compacted, with interlocking quartz grains. Plastic mudstone clasts or clay-rich clasts have largely been replaced by Mg-rich (some Ca is also present) siderite microcrystalline cement. Ferroan dolomite cement also present. Authigenic interstitial grain-replacive and pore-filling kaolinite are present similar to that described in previous samples. Muscovite grain are exfoliated and replaced by kaolinite to form muscovite-kaolinite intergrowths. Kaolinite occurs within corroded siderite crystals, which may be partially replaced by kaolinite. Little or no feldspar or lithic grains remain - probably having all been replaced by kaolinite. Some laminae of sand have a patchy siderite cement whilst other laminae may be tightly cemented by siderite.

SSK2559 (Milton of Balgonie No.2) is a bioclastic limestone composed largely of tightly-packed calcitic shell fragments with minor interstitial clay.. Larger shell fragments locally contain sheltered grain packages. The sample as a whole has a pelleted, sheared and fractured appearance. The rock is tight with little or no porosity.

Lower Coal Measures – seal unit

The Lower Coal Measures comprise sandstone, siltstone and mudstone in repeated cycles which most commonly coarsen upwards, but also fine upwards, with seatearth and coal at the top (Monaghan et al. 2008). These are considered to represent a potential seal unit within the region and 4 samples taken from the outcrop at Earlseat Opencast site were examined for CASSEM.

Samples ASW433, ASW434 and ASW436 are largely weakly-laminated, argillaceous or pelleted clay sandstone and siltstone. They are highly compacted and the clay pellets have been deformed to form an interstitial pseudomatrix. Porosity is negligible. ASW436 contains bands of apatite-cemented siltstone in which microcrystalline apatite has replaced a mudstone or clay matrix.

Sample ASW435 represents a relatively clean quartz arenite (c.97% quartz). This sandstone is much more porous, and displays a compacted grain fabric with significant interconnected secondary framework grain dissolution porosity.

Burnside Sandstone Formation – aquifer

The Burnside Sandstone Formation is up to 160 m thick and could represent a potential minor aquifer unit within the region. It consists predominantly of fine- to very coarse-grained sandstones that are dull red or purplish in colour and contain a variable proportion of calcite cement (Monaghan, et al., 2008). Two samples were examined from this formation in core from the Mawcarse Station water borehole.

The two samples represent tightly compacted fine to coarse grained, poorly-sorted, muddy sublitharenites, with wackestone to packstone fabrics. In part the matrix clay is pseudomatrix after deformed pelloidal grains. They contain angular detrital quartz, with minor K-feldspar, biotite and muscovite, with scattered common large lithic clasts up to very coarse sand and granule size. Lithic clasts include microgranite (quartz-K-feldspar) and altered lava fragments with feldspar laths. Mica flakes are deformed by compaction but randomly orientated with no strong bedding-parallel alignment. Most primary intergranular porosity has been lost by compaction. The sandstones contain thin mudstone interbeds up to 3 mm thick of dark brown, very fine mudstone.

The main cementing mineral is patchy non-ferroan or weakly ferroan dolomite cement or dolomite-replaced grains. Minor patchy barite cement and hematite replacing micas and other detrital grains were also observed.

West Lothian Oil ShaleFormation - aquifer

The West Lothian Oil Shale Formation is comprises seams of oil shale in a cyclical sequence predominantly of pale coloured sandstones interbedded with grey siltstones and mudstones, with subordinate limestone/dolomite, sideritic ironstone, hick, pale green-grey or grey argillaceous beds containing derived volcanic detrital 'marl' are present (Monaghan et al., 2008). It passes eastwards into the Aberlady Formation which consists of a cyclical sequence predominantly of pale coloured sandstone interbedded with grey siltstone and grey mudstone.The sandstones in this formation represent a potential aquifer unit (Monaghan et al., 2008).

One sample of sandstone was examined from this unit in the Cousland Borehole No.6. This comprised a fine grained quartz arenite with a patchy dolomite cement. Framework grains are almost entirely quartz with little or no feldspar. Authigenic quartz overgrowths are developed locally and show well defined forms. Oversized pores, skeletal grain remnants and clusters of microporous kaolinite crystals indicate extensive framework grain dissolution and alteration. The sandstone is also cemented by patches of ferroan dolomite cement, which locally encloses quartz overgrowths.

4.2   TWO DIMENSIONAL POROSITY DATA

The porosity and pore size analyses data for the Permo-Triassic rocks from the Yorkshire-Lincolnshire-Nottinghamshire area, and for the Carboniferous and Devonian aquifer and seal rocks from the Forth area are presented in the digital dataset *SUMMARY BSEM-IMAGE ANALYSIS POROSITY DATA (YORK-LINCS and MVS) FOR CASSEM v1.0.xls* (provided on the CDROM enclosure).

4.2.1   Comparison with existing porosity datasets

The Sherwood Sandstone Group and the Basal Permian (Rotliegendes Group) sandstones from the Cleethorpes Borehole have previously been examined in detail petrographically, as part of an earlier BGS programme of research into the potential of the Sherwood Sandstone Group and Basal Permian (Rotliegendes Group) strata as low-enthalpy geothermal reservoirs (Downing et al., 1985; Milodowski et al., 1987). As a result, there are existing porosity datasets, including both plug derived gas porosity-permeability data and conventional point-count modal analysis derived porosity. Where data had been obtained from identical or very close sample points through both the Sherwood Sandstone Group, Basal Permian Breccia and Yellow Sands Formation comparative data cross-plots have been made. This comparison serves to both validate the image-analysis derived data and to elucidate data set relationships.

Image analysis derived data was simply arithmetically averaged per depth point. No attempt at weighting (for example to account for the different proportions of different textures present at a particular depth) has been made.

Figure 16 shows a cross-plot of modal analysis data from the previous study against the total porosity derived by image analysis in this study. Both of these data sets have been obtained from thin sections and record two dimensional porosity data, in many cases from the same thin sections. Linear regression produces a trend-line with a moderately good fit ($R^2 = 0.56$). A moderately wide spread of points reflects the relatively small areas that both techniques sample for their data sets. A skew at low porosity values is a probable indication of a greater sensitivity of the image analysis technique to the finer pore sizes.

Figure 17 shows a cross-plot of gas derived plug porosities from the previous study against the total porosity derived by image analysis in this study. Whist the image analysis derived data is for two dimensional porosity, the plug data is for three dimensional porosity, and so significant differences are to be expected. The linear trend-line produced by regression, however, has a better fit ($R^2 = 0.62$) than with the preceding comparison and there is overall less scatter. The

slope of the line deviates significantly from unity, indeed nearly being a 2:1 slope. From the graph, for total porosities of <25% the image analysis process significantly and increasingly undervalues total porosity, compared to the 3D plug porosity.

When the previously obtained modal analysis total porosity data is compared to the gas plug total porosity data (Figure 18) there is a poor correlation (R2 = 0.17).

In conclusion, the image analysis process produces total porosity data that compares well with previously collected data sets. In particular the image analysis derived porosities produce a better correlation with plug total porosities than do the conventional point count modal analysis porosities. The comparison, however, suggests that the technique under-detects when porosity is low.
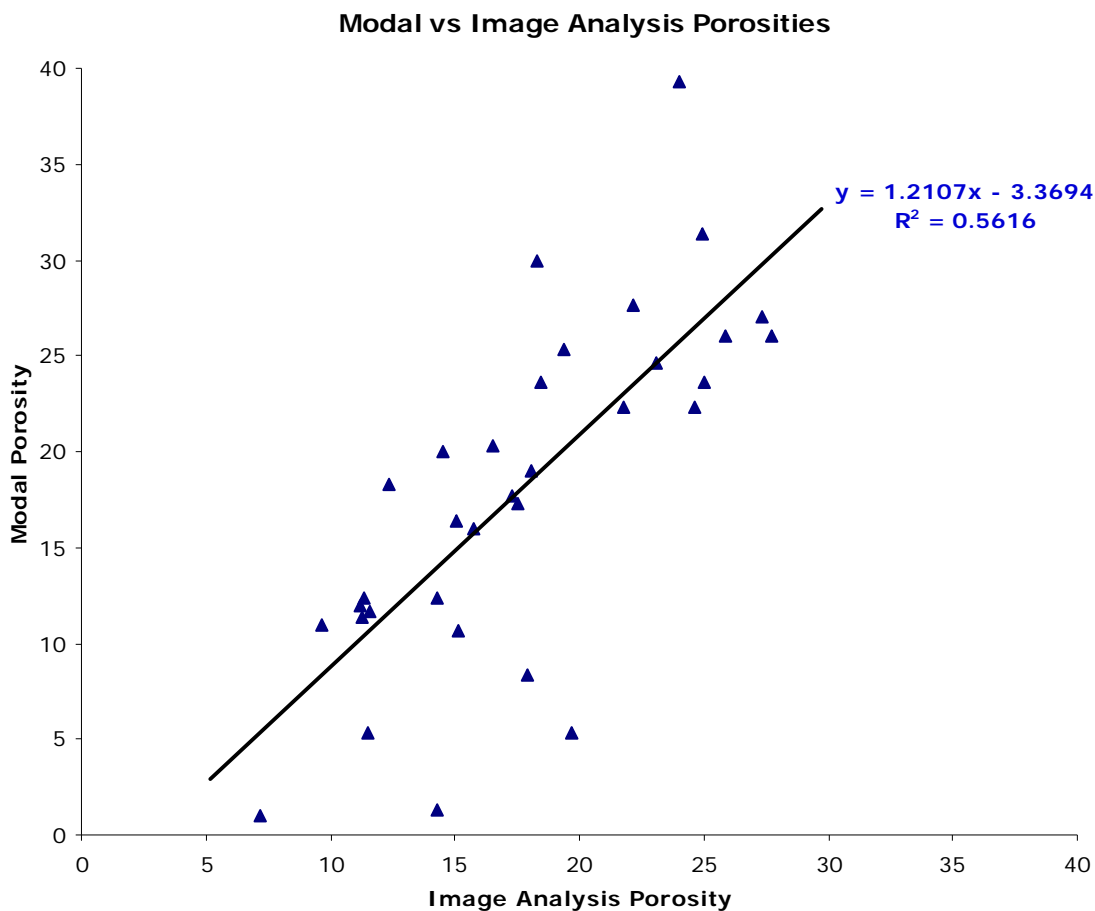
Figure 16. Cross-plot of previously obtained modal analysis total porosity data against image analysis total porosity data from this study, for Cleethorpes Borehole samples.
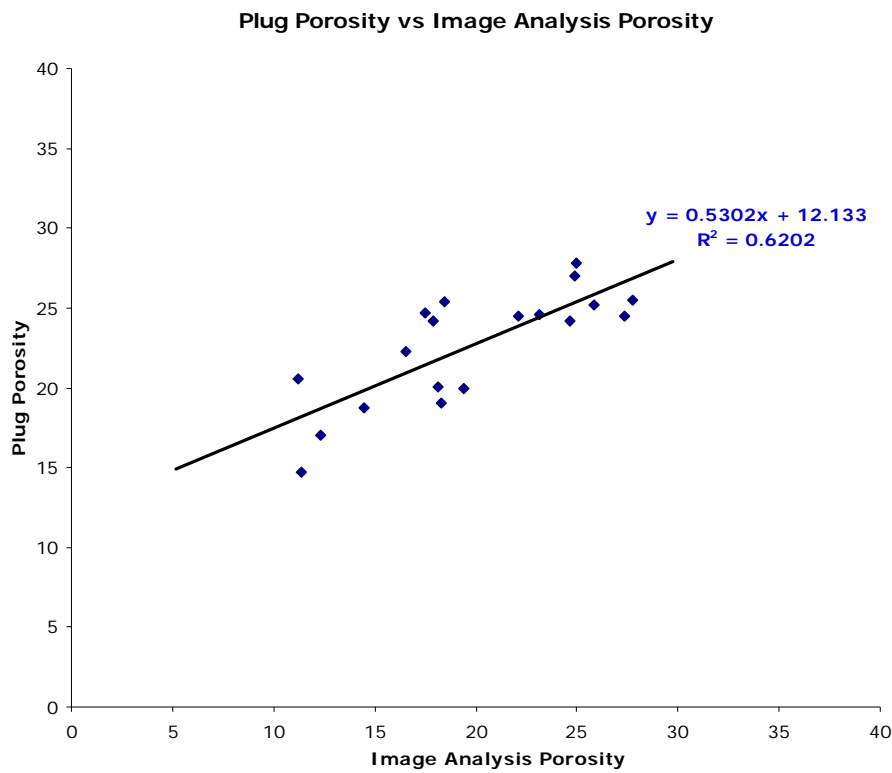
Figure 17. Cross-plot of previously obtained gas-derived total plug porosity data against image analysis total porosity data from this study, from Cleethorpes Borehole samples.
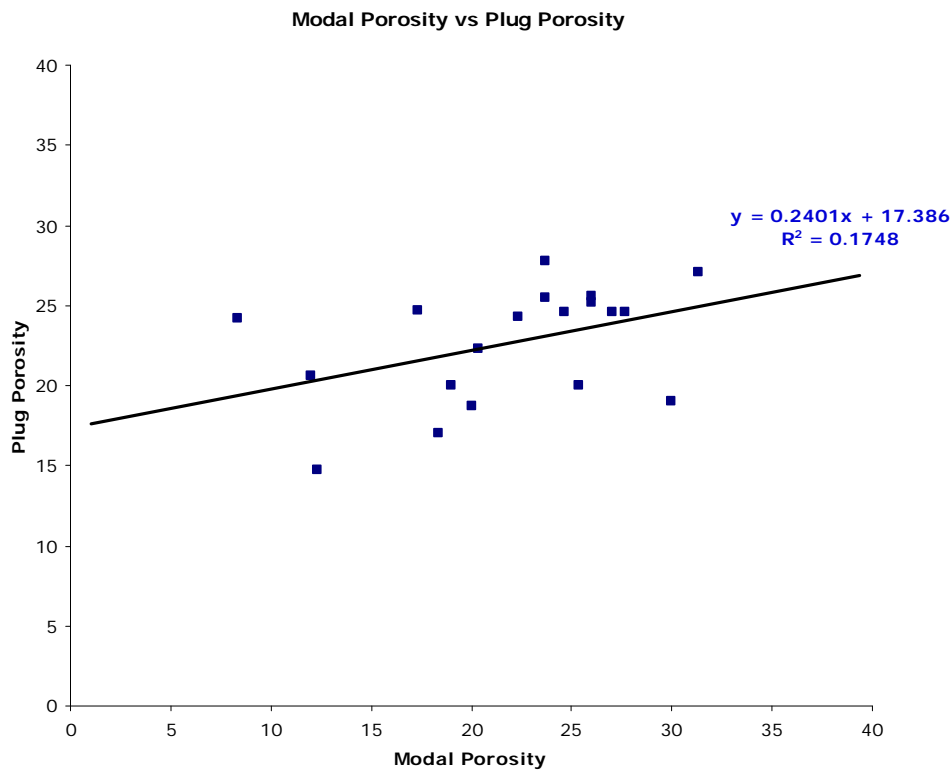
Figure 18. Cross-plot of previously obtained gas-derived total plug porosity data against previously obtained modal analysis total porosity data, from Cleethorpes Borehole samples.

53

4.2.2   Yorkshire-Lincolnshire-Nottinghamshire data

4.2.2.1 BY GEOLOGICAL UNIT

The data collected from the boreholes in the Yorkshire-Lincolnshire-Nottinghamshire study area are summarised below in Figure 19 and Figure 20, and Table 7.

Of the five units sampled, two are considered potential reservoir bodies (Sherwood Sandstone Group, Basal Permian formations) and three are considered potential seals (Mercia Mudstone Group, Marl Slate Formation, Upper Permian Marl= Zechstein Group).

Of the potential seal units, samples from the Marl Slate Formation and Upper Permian Marl record no macroporosity and low total porosities (<10% and <5% respectively).

Samples from the Mercia Mudstone, however, include some that contain significant macroporosity. In some intervals have total porosity values similar to those observed for the potential reservoir bodies (max. 29.5% total porosity, Figure 19, Table 7). The Group is characterised by a wide range of total porosity, reflecting a high degree of lithological, textural and mineralogical heterogeneity, with a relatively high proportion of mesoporosity + microporosity. The samples with high porosities correlate with either the sandstone-rich basal part of the Mercia Mudstone Group (i.e. the Tarporley Siltstone Formation – see also Section 4.1.1.3) or to fine sandstone laminae within the mudstone and siltstone-dominated upper parrt of the sequence. The porosity characteristics of the mudstones and siltstones in upper part of the Mercia Mudstone Group are similar to those of the other potential seal units in that they have low total porosities with no or negligible macroporosity. These lithologies therefore have the potential to provide good low-permeability seals.
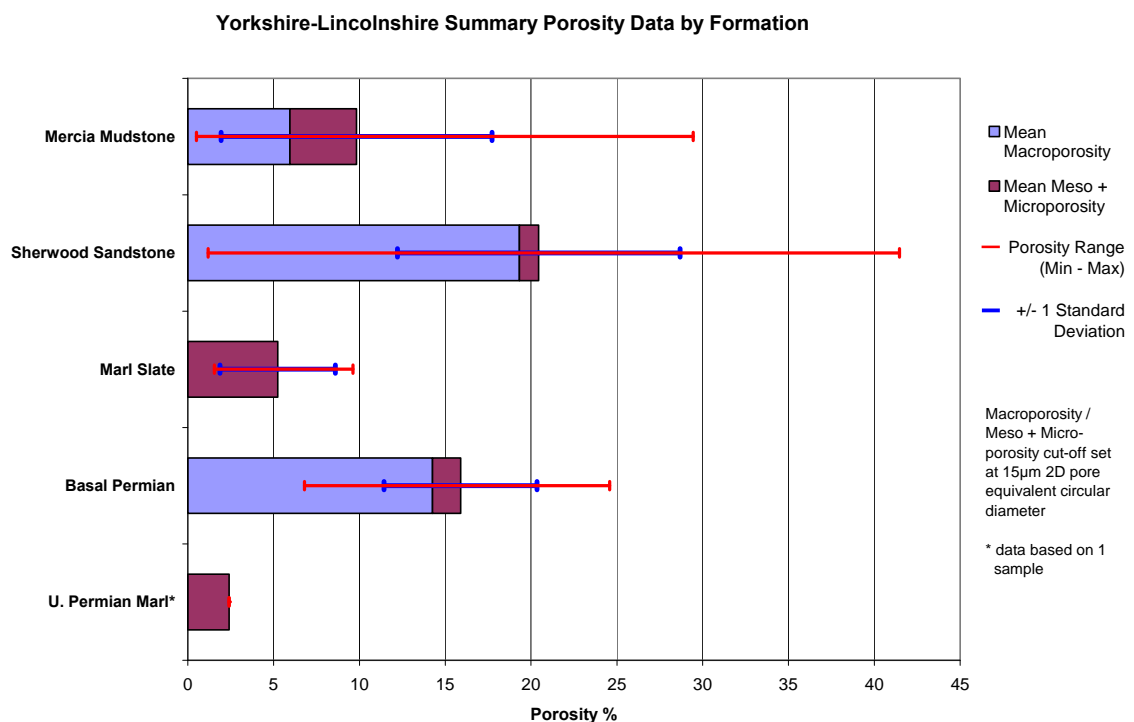
Figure 19. Porosity data by unit from the Yorkshire-Lincolnshire-Nottinghamshire study area.

54
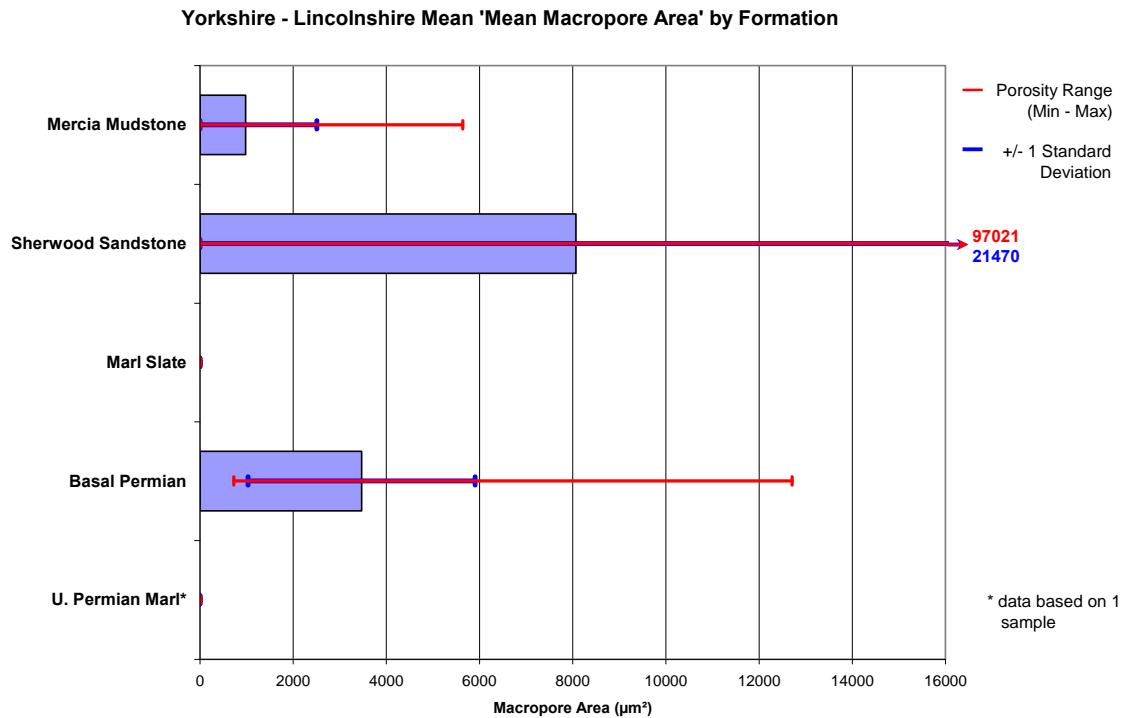
Figure 20. Summary macropore size data by unit from the Yorkshire-Lincolnshire-Nottinghamshire study area.

Of the two potential reservoir units, the Sherwood Sandstone Group has the higher mean total porosity (20.5% compared to 15.9% for the Basal Permian). It also has a lower proportion of mesoporosity + microporosity. A wider range of porosities is also recorded (Figure 19). When looking at the macropore size data (Figure 20), differences between the two formations are greater, with the Sherwood Sandstone Group having higher mean (8000 μm^2 compared to 3500 μm^2) and much higher maximum (97000 μm^2 compared to 13000 μm^2) mean macropore areas. This suggests that not only does the Sherwood Sandstone Group have higher porosity, but also better pore interconnectivity.

The mean macropore elongation data for the three units with macropore content increase with relative depth (Table 7), consistent with expectations from simple compaction considerations. The significantly lower mean Mercia Mudstone elongation may reflect preferential compaction of mudstone units and / or the widespread presence of early cements.

Table 7. Yorkshire-Lincolnshire summary porosity data

Formation	Total Porosity (%)				Macroporosity (>15µm ECD) (%)				Meso+Microporosity (<15µm ECD) (%)				Mean 2D Macropore Area (µm²)				Mean 2D Macropore Elongation			
	Mean	Std Dev.	Max.	Min.	Mean	Std Dev.	Max.	Min.	Mean	Std Dev.	Max.	Min.	Mean	Std Dev.	Max.	Min.	Mean	Std Dev.	Max.	Min.
Mercia Mudstone	9.83	7.90	29.45	0.50	5.95	8.11	27.91	0.00	3.88	2.42	8.11	0.50	982	1529	5638	0	2.15	0.27	2.79	1.75
Sherwood Sandstone	20.45	8.24	41.47	1.18	19.32	8.57	41.40	0.00	1.13	0.68	5.09	0.07	8068	13401	97021	0	2.40	0.17	2.88	1.87
Marl Slate	5.23	3.37	9.62	1.55	0.00	0.00	0.00	0.00	5.23	3.37	9.62	1.55	0	0	0	0	n.a.	n.a.	n.a.	n.a.
Basal Permian	15.89	4.46	24.58	6.79	14.25	4.93	24.02	4.95	1.64	1.25	6.27	0.56	3468	2437	12712	727	2.48	0.22	3.08	2.10
U. Permian Marl [Roxby Fm]*	2.40				0.00				2.40		2.40		0				n.a.	n.a.	n.a.	n.a.

* - Data based on one sample.

4.2.2.2 CLEETHORPES BOREHOLE

The high number of samples and sampling density from the Cleethorpes borehole enables porosity depth profiles to be plotted (Figure 21 for the Sherwood Sandstone Group, Figure 22 for the Basal Permian (Rotliegendes Group) aquifer and the base of the Marl Slate Formation). These confirm that for this borehole, the overall characteristics of these two units are displayed; the Sherwood Sandstone Group has a wider range of total porosities, the highest total porosity and the better mean total porosity.

The depth plot of the Sherwood Sandstone Group (Figure 21) additionally shows that unit has its highest total porosities towards its base and that the deeper samples have lower proportions of mesoporosity + microporosity. As discussed in Section 4.1.1.3 the porosity is influenced by several mineralogical and textural factors. However, the general increase in porosity with depth appears to correlate broadly with a decrease in dolomite and anhydrite cementation. The sample data for the Sherwood Sandstone Group also contains low total porosity intervals with low to negligible macroporosity, corresponding to samples from thin mudstone-siltstone beds

In contrast to this, the Basal Permian aquifer has no strong trend or variation in total porosity with depth, but does tend to have higher proportions of mesoporosity + microporosity in the deeper samples (Figure 22).
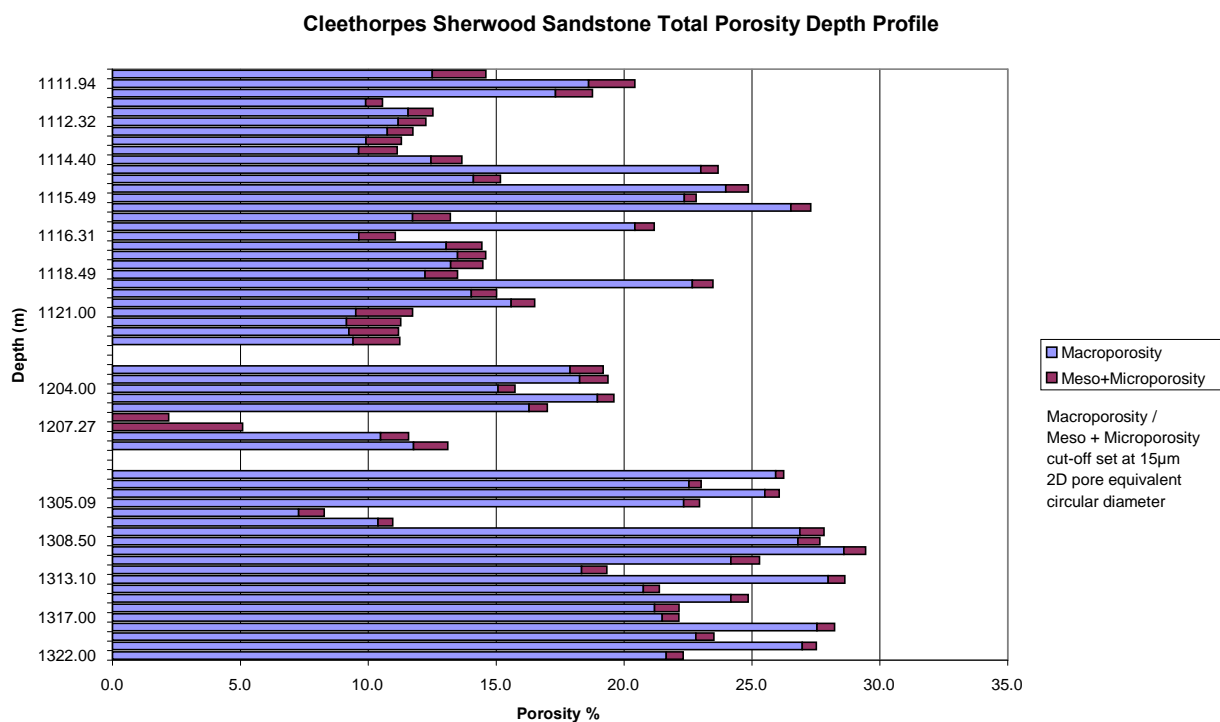
Figure 21. Plot in depth order of porosity data for the Sherwood Sandstone Group interval of the Cleethorpes Borehole.
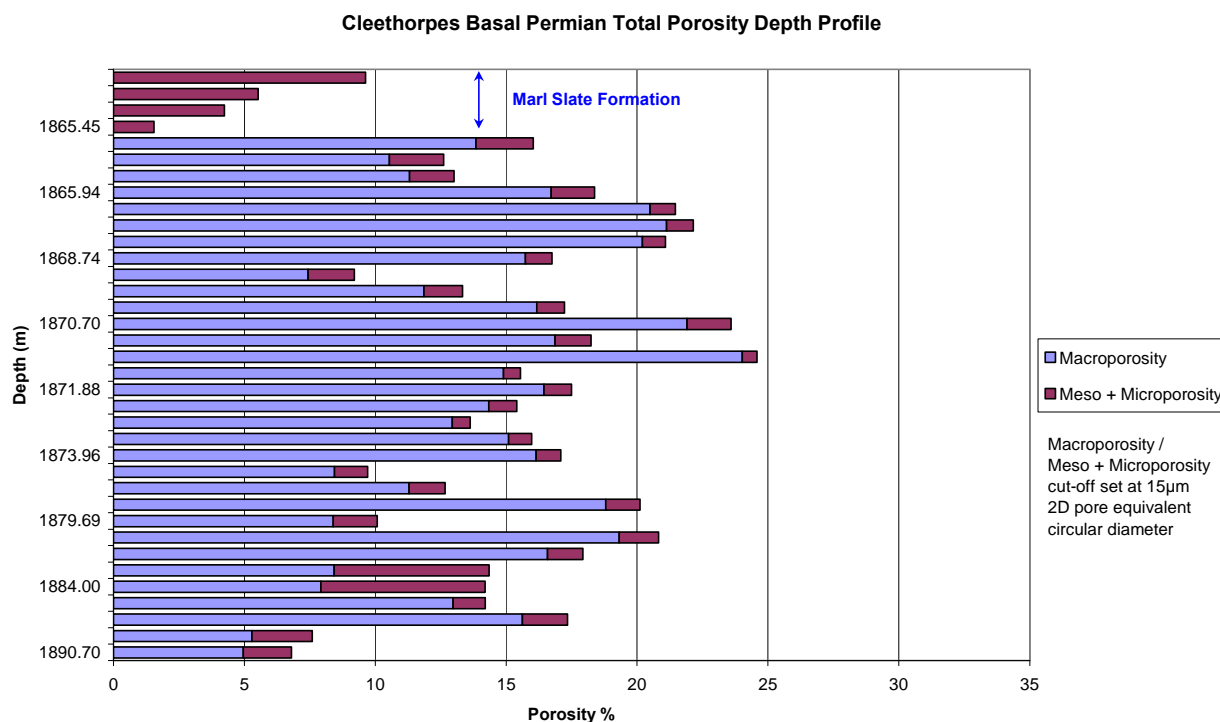
Figure 22. Plot in depth order of porosity data for the Basal Permian aquifer interval of the Cleethorpes Borehole, including the bottom of the Marl Slate Formation.

4.2.3   Forth area data

4.2.3.1 BY GEOLOGICAL UNIT

The data collected from the boreholes in the Forth area are summarised below in Figure 23 and Figure 24, and Table 8.

A total of eleven formations have been sampled in this study area, although six of these (Kinnesswood Sandstone / Ballagan transition, Passage, Upper Coal Measure, Upper Limestone, West Lothian Oil Shale) are only represented by single samples.

Four of the formations have mean total porosities <5%; these are the Ballagan, Burnside Sandstone, Kinnesswood Sandstone / Ballagan transition and Pathhead Formations. Of these, the Ballagan and Pathhead formations have the lowest amounts of average macroporosity (Figure 23). The mean macropore sizes of samples from these formations are low and smallest in the Ballagan Formation, which is the main target seal unit.

Three formations record intermediate values (5-10%) of mean total porosity; these are the Lower Coal Measures, Upper Limestone and West Lothian Oil Shale formations. Of these the Upper Limestone shows the lowest proportion of macroporosity. The Lower Coal Measures Formation is dominated by macropores, but also contains a very wide range of total porosity values, including some of high porosity (21.2%). A wide range in the mean macropore size (Figure 24) matches this range in total porosity and the high maximum porosity is also matched by a high maximum mean macropore size. Consequently, some intervals of the Lower Coal Measures have porosity and interconnectivity properties that are good enough to act as reservoir units. The samples examined for some of these formations were intended to represent both possible seal and aquifer lithologies within the formation (Table 3). For the Lower Coal measures, both a mudstone and a sandstone sample were studied, since this unit includes both potential seal (or baffle) and aquifer lithologies.

Midland Valley Summary Porosity Data by Formation
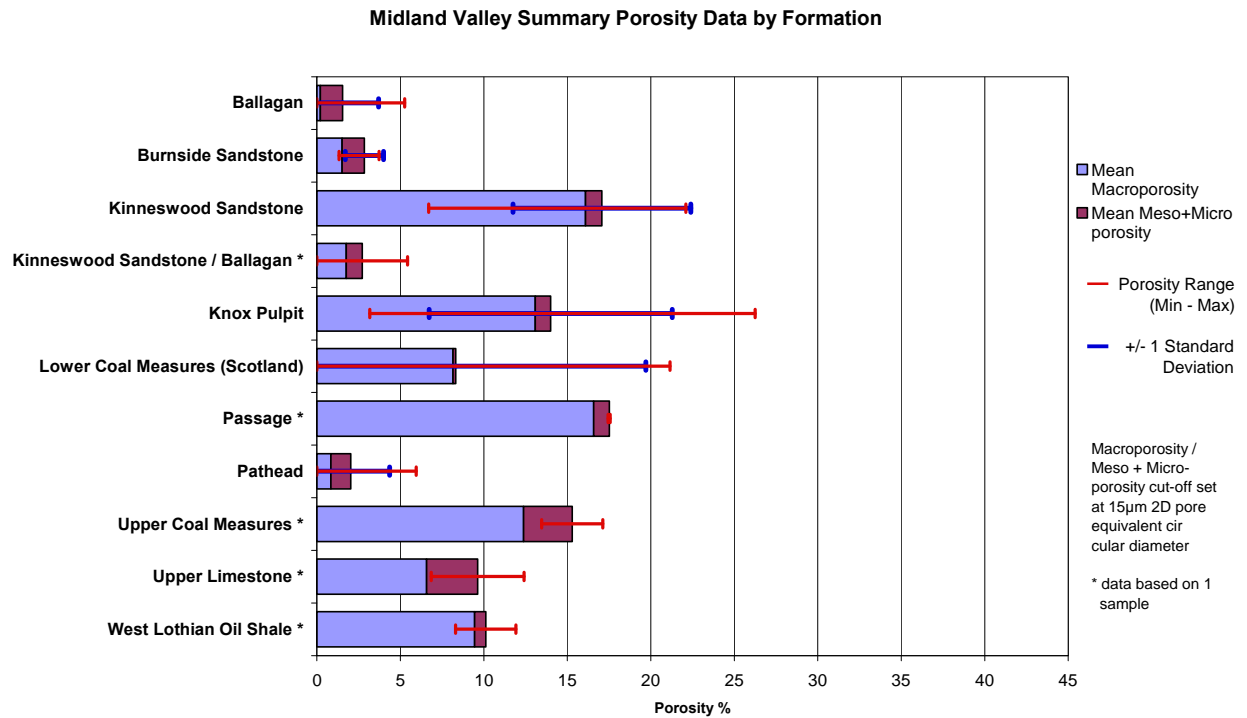
Figure 23. Summary porosity data by formation from the Forth area.

Midland Valley Mean 'Mean Macropore Area' by Formation
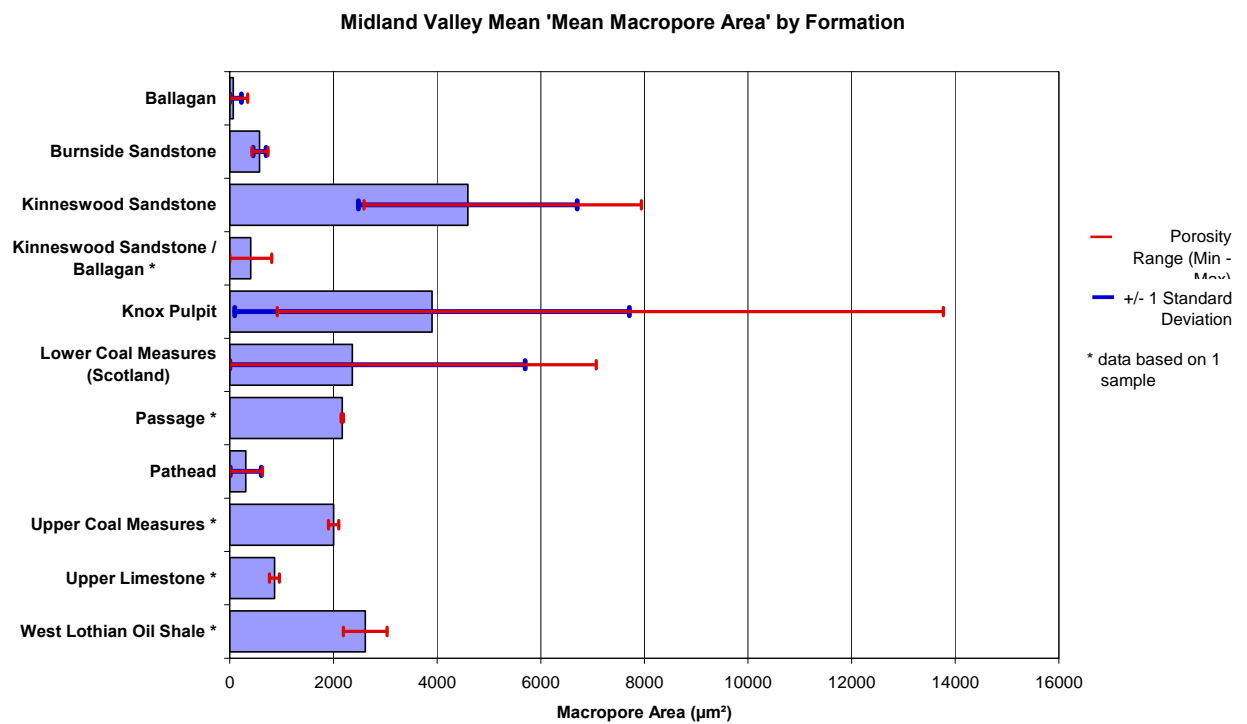
Figure 24. Summary macropore size data by formation from the Forth area.

59

The four formations with the highest mean total porosities, and which are therefore the most likely reservoir units, are the Kinnesswood Sandstone, Knox Pulpit, Passage and Upper Coal Measures (Figure 23). Of these the Knox Pulpit Formation contains the widest porosity range and highest total porosity (26.3%). Of these four, however, the Passage and Upper Coal Measure formations have relatively low mean macropore sizes (Figure 24), suggesting their macropore interconnectivities are limited. The main target aquifer units, Kinnesswood Sandstone and Knox Pulpit formations, on the other hand, have relatively high mean macropore sizes. Again, the Knox Pulpit Formation contains samples with the highest range and maximum mean macropore sizes. Kinnesswood Sandstone Formation samples have more consistent values.

Table 8. Forth area summary porosity data

Formation	Total Porosity (%)				Macroporosity (>15µm ECD) (%)				Meso+Microporosity (<15µm ECD) (%)				Mean 2D Macropore Area (µm²)				Mean 2D Macropore Elongation			
	Mean	Std Dev.	Max.	Min.	Mean	Std Dev.	Max.	Min.	Mean	Std Dev.	Max.	Min.	Mean	Std Dev.	Max.	Min.	Mean	Std Dev.	Max.	Min.
Ballagan	1.53	2.17	5.26	0.00	0.21	0.46	1.03	0.00	1.33	1.73	4.22	0.00	69	155	345	0	2.37		2.37	2.37
Burnside Sandstone	2.85	1.14	3.73	1.33	1.51	0.69	1.96	0.48	1.34	0.53	1.83	0.85	576	126	738	430	2.25	0.06	2.31	2.18
Kinnesswood Sandstone	17.07	5.33	22.10	6.70	16.09	5.37	21.39	5.81	0.98	0.46	1.51	0.37	4592	2109	7943	2591	2.47	0.09	2.63	2.36
Kinnesswood Sandstone / Ballagan*	2.71		5.43	0.00	1.76		3.53	0.00	0.95		1.90	0.00	404		808	0	2.09		2.09	0.00
Knox Pulpit	14.00	7.28	26.25	3.17	13.07	7.45	25.86	2.50	0.93	0.42	1.72	0.30	3902	3808	13772	917	2.38	0.14	2.64	2.23
Lower Coal Measures (Scotland)	8.32	11.39	21.16	0.00	8.15	11.16	20.81	0.00	0.17	0.24	0.50	0.00	2363	3338	7072	0	2.35		2.39	2.31
Passage *	17.51		17.56	17.45	16.58		16.65	16.50	0.93	0.00	0.95	0.91	2171		2192	2151	2.25		2.28	2.22
Pathhead	2.03	2.32	5.95	0.00	0.83	1.20	3.20	0.00	1.19	1.36	3.03	0.00	308	300	627	0	2.20	0.10	2.28	2.09
Upper Coal Measures *	15.30		17.12	13.47	12.37		13.88	10.86	2.93		3.24	2.61	2006		2105	1907	2.48		2.61	2.36
Upper Limestone *	9.63		12.41	6.85	6.57		9.09	4.06	3.05		3.32	2.78	861		959	764	2.23		2.33	2.14
West Lothian Oil Shale *	10.11		11.92	8.31	9.45		11.28	7.62	0.67		0.69	0.64	2615		3037	2194	2.24		2.25	2.23

* - Data based on one sample.

5 Summary and conclusions

5.1   YORKSHIRE-LINCOLNSHIRE-NOTTINGHAMSHIRE AREA

5.1.1   Target aquifer unit characteristics

The Sherwood Sandstone Group is represents the main target aquifer unit in the area of interest (Ford et al., 2008). The samples analysed for the CASSEM Project are predominantly fine to medium grained sandstones, although coarser sandstones also occur within the region.

The Basal Permian (Rotliegendes) sandstone aquifer represents secondary aquifer, which may be of significance because occurs beneath the Sherwood Sandstone Group within the same area, and which may contribute to the storage capacity of a potential CCS site.

5.1.1.1 DETRITAL MINERALOGY

The detrital mineralogy of the Sherwood Sandstone Group and the Basal Permian sandstones are sandstone samples comprises principally: major quartz with subordinate to minor K-feldspar, albite, lithic clasts (including chert, fine grained felsic igneous fragments, siltstone, mudstone), and minor to accessory muscovite, biotite and chlorite, and accessory rutile, magnetite, ilmenite, apatite, zircon, and tourmaline. Thin clays and mudstones may also be present. Modal analyses show that sandstone samples are dominantly subfeldspathic arenites with subordinate feldspathic arenites and occasional for lithic-rich sublithic arenites (classification after Pettijohn et al., 1987). It is likely that the proportion of lithic components is underestimated in the modal analytical data. This is because the modal analysis technique, employing BSEM-EDXA element distribution and phase mapping, does not differentiate the lithic clasts as discrete entities in most cases but determines their component mineral sub-grains separately. However, qualitative visual petrographic observations indicate that the overall rock classification is correct.

5.1.1.2 DIAGENETIC ALTERATION

The sandstones are significantly affected by diagenetic alteration, which has modified the mineralogy, fabric and porosity characteristics. The overall diagenetic characteristics of both formations are very similar, and the CASSEM observations are similar to those described in earlier studies (Burley, 1984; Bath et al., 1987; Milodowski et al., 1987). Observations for the Basal Permian sandstones and breccias are limited to those recorded from samples taken the Cleethorpes borehole.

Authigenic dolomite and anhydrite are important cements and constitute major minerals in some samples. Dolomite occurs as irregular patchy pore-fillings, grain replacements and as small displacive concretions and nodules interpreted as eodiagenetic dolocrete. Anhydrite was observed only in sandstone samples from the >1100m deep sequence in the Cleethorpes borehole, where it occurs as a pore filling cement. The anhydrite-bearing sandstones also contain minor to trace amounts of pore-filling sylvite and halite. These authigenic sulphate and halide minerals were not observed in samples from shallower levels, with the exception of Sherwood Sandstone Group rocks immediately beneath the Mercia Mudstone Group from the Fulbeck Airfield No.1 borehole, where gypsum cement is present. This has probably been derived by remobilisation of gypsum during alteration of the overlying gypsiferous and anhydritic mudstone strata. Calcite and barite cements are also present but are only minor components in most of the samples studied. Quartz and K-feldspar overgrowth were observed in some sandstones, and although they may serve to mechanically 'lock' grains together to form a rigid grain framework, they do not constitute a major pore-filling cement.

Authigenic kaolinite is common and may comprise a significant proportion of the mineralogy. It is microporous and largely replaces detrital framework grains (probably feldspars and lithic clasts) rather than as a pore-filling phase. Occasionally, however, kaolinite precipitation extends into adjacent intergranular regions. The sandstones from the Cleethorpes borehole were also observed to contain evidence of authigenic fibrous illite. This nucleates on pore walls and forms a meshwork of fibres growing across the intergranular pores. Fibrous illite has only been observed by SEM samples preserved at the time of coring in formation fluid and then prepared by critical point drying technique. It is often missed by routine petrographic analyses techniques because normal air-drying of cores, and standard preparation techniques used in thin section preparation, generally destroy these delicate illite fabrics (cf. McHardy et al., 1982).

5.1.1.3 PRINCIPAL CONTROLS ON POROSITY AND PERMEABILITY

Of all the units examined from both study areas the Sherwood Sandstone Group has the highest mean total porosities and mean macropore sizes. Mean porosity determined by PIA is about 20% but some values exceed 40%. The Basal Permian sandstones have a mean porosity of about 16%, with a maximum porosity of about 25%.

Porosity and permeability in the Sherwood Sandstone Group and the Basal Permian sandstones are strongly influenced by diagenetic modification. Burial compaction has reduced the primary intergranular porosity. Clean, well-sorted quartz-rich sandstones show less compaction than muddier sandstones or sandstones with a high proportion of plastic lithic clasts. Sandstones with a large amount of mudstone clasts often have the intergranular pores filled by clay pseudomatrix produced by compactional deformation of those clasts.

Many of the sandstones display evidence for the development of significant secondary porosity. The main secondary porosity generating processes are:

1. Dissolution of anhydrite (and/or gypsum), halite and sylvite cement;

2. Dissolution of dolomite cement;

3. Dissolution of detrital feldspars and lithic grains (framework grain dissolution)

In the Sherwood Sandstone Group the extent of mineral dissolution increases from the east towards outcrop and the groundwater recharge area in the west. This is reflected in a general increase in porosity from deep sandstone in the east to shallow sandstones in the west. Anhydrite, sylvite and halite cements are observed in sandstones in the deep North Sea reservoirs, but are absent in the shallow aquifer. Dolomite cement is appears to be largely unaffected by dissolution in the deep sandstone sequence at Cleethorpes but is corroded and partially removed in shallower samples from the west of the area, and may be removed completely at outcrop (Bath et al., 1987; Milodowski et al., 1987). These cements were probably more widespread throughout the Sherwood Sandstone Group (Milodowski et al., 1987). The regional pattern of alteration and porosity development in the Basal Permian aquifer is unknown because observations are limited only to samples from the deep Cleethorpes borehole sequence. However, given the similarity in diagenetic cements between this unit and the Sherwood Sandstone Group aquifer, a similar pattern of alteration and porosity development might be expected for the Basal Permian aquifer.

Framework grain dissolution influences the porosity of the sandstones in both aquifers, across the region. It results largely from the dissolution of detrital feldspars and lithic grains. Petrographical evidence shows that framework grain dissolution affects mainly albite and lithic clasts in the deepest sandstones in the Cleethorpes borehole. However, at shallower levels to the west, K-feldspar is also affected and albite is essential completely removed by dissolution. Framework grain dissolution, together with the dissolution of eodiagenetic dolomite and anhydrite cements, produces large oversized pores. These are well interconnected with the intergranular pore network, and therefore, would be expected to enhance the permeability of

aquifer unit. However, authigenic kaolinite has replaced the framework grains in some cases, and any increase in porosity is associated with micropores between kaolinite crystallites, and this would probably not be accompanied by increased permeability.

The development of fibrous illite may be a potentially important feature affecting permeability in both sandstones aquifers at depth the east of region. Whilst this authigenic mineral may be a volumetrically small constituent of the rock, it has a dramatic effect on the pore morphology greatly increasing the pore tortuosity. Consequently, potentially microporosity will be increased and permeability significantly decreased, even though the illite has little overall effect on the total porosity. Fibrous illite is encountered in the Rotliegendes of the southern North Sea, where published studies have concluded that it is generally restricted sandstones that have undergone deep burial (Marie, 1975; Glennie et al., 1978). However, its presence in sandstones at shallower depths than offshore from the Cleethorpes No.1 borehole indicates that it may have a more widespread distribution, than previously thought. Therefore, the effects of the potential presence of authigenic fibrous illite must be considered in predictive modelling and evaluation of porosity and permeability of the Sherwood Sandstone Formation at depths suitable for CCS.

5.1.2   Target seal characteristics

5.1.2.1 GENERAL

The principal target seal unit is the Mercia Mudstone Group, which overlies the Sherwood Sandstone Group. The mudstones, siltstones, anhydrite and dolomite strata of the Zechstein Group representing a seal for the secondary aquifer target in Basal Permian sandstones

No samples were available within the study area from depths appropriate to saline aquifer CCS. All the seal lithologies examined come from sequences less than 400 m deep. The mudstones sequences from these relatively shallow depths have been strongly affected by alteration associated with the hydration of anhydrite to gypsum in the shallow groundwater regime near outcrop. This has resulted in disruption of the mudstone fabrics, dissolution collapse, expansive deformation related to the anhydrite to gypsum alteration and displacive gypsum veining. However, the samples taken for the CASSEM project sought to avoid this alteration as far as possible. Nevertheless, the properties determined from these shallow-sourced samples may not be representative of the same units at depth. Therefore, it is recommended that consideration should be given to obtaining and characterising fresh samples of the mudstone seal units from more appropriate depths within the target area. The disruptive gypsification and alteration are likely to be of less importance in the deeper mudstones in the target area to the east of the region, where salinities, pressure and temperature are higher. Anhydrite is more soluble than gypsum at low temperatures and at salinities below halite saturation, and consequently anhydrite hydrates to gypsum (Gustavson and Hovor, 1994). Once groundwater is saturated with respect to gypsum, any further anhydrite hydration and solution results in supersaturation, and the excess $CaSO_4$ carried by ground water flowing from dissolution zones will precipitate as gypsum in open, high-permeability fractures or intergranular porosity. With increasing temperature and salinity, anhydrite becomes less soluble than gypsum and the gypsification process ceases. Thus, as the groundwater becomes more saline and eventually saturated with respect to $CaSO_4$ the dissolution of anhydrite will cease.

5.1.2.2 MERCIA MUDSTONE GROUP

Porosity vales determined by PIA for the Mercia Mudstone Group are generally low (<10% total porosity). Much of this is microporosity but a significant amount of macroporosity is present in the coarser, sandier facies rocks within this unit, where total porosities may be as high as 30% - comparable to those in the Sherwood Sandstone.

The upper part of the Mercia Mudstone Group sequence is more argillaceous. It is dominated by units of finely laminated red-brown siltstone, mudstone interbedded with more massive grey-green dolomite- and anhydrite (now partly gypsified) -cemented siltstones, and structureless red-brown silty mudstones often containing nodules and irregular discontinuous thin layers of grey anhydrite. These laminated rocks are very dolomitic often with discrete laminae of dolomicrite. The macroporosity in these rocks is very low, although occasional thin porous laminae of siltstone may be present where anhydrite or gypsum cements may have been dissolved.

The Tarporley Siltstone Formation, which comprises the lower part of the Mercia Mudstone Group, is particularly porous. These rocks represent a transition from the underlying Sherwood Sandstone lithology. They include a significant component of fine sandstone and siltstone with similar mineralogical characteristics to the underlying Sherwood Sandstone Group. This basal part of the Mercia Mudstone Group is therefore unlikely to provide a seal to the Sherwood Sandstone Group aquifer. Indeed, the old stratigraphical term - 'Keuper Waterstones' – formerly used for this part of the sequence alludes to the fact that they are significantly water bearing and used locally as an aquifer. The Tarporley Siltstone Formation should be regarded as contributing to the storage capacity of the Sherwood Sandstone aquifer, rather than part of the Mercia Mudstone seal.

At shallow depths in the west of the area the Mercia Mudstone Group is strongly affected by the hydration of anhydrite to gypsum. Gypsification results in the disruption of the mudstone fabric, and is accompanied by: expansive disruption (due to increased volume as anhydrite hydrates to gypsum) accompanied by with fracturing and the development of displacive gypsum veining; and dissolution and collapse. This alteration proceeds as a result of interaction with both groundwater penetrating from the surface downwards, and upwards by interaction with groundwater penetrating the base of the Mercia Mudstone Group from the underlying Sherwood Sandstone aquifer. A similar pattern of symmetrical gypsification is also observed the Zechstein anhydrite deposits (e.g. Billingham Main Anhydrite Formation) at shallow depths in the Teeside area of north-east England (Smith and Moore, 1973; Bath et al., 1987). This gypsification process is observed to depths of at least 370 m the Mercia Mudstone Group in the study area (e.g. Fulbeck Airfield No.1 borehole). However, as discussed above this disruptive gypsification and alteration are likely to be of less importance in the deeper sequence where groundwater is very saline, and pressure and temperature are higher. Petrographic observations on samples of mudstones and siltstones, which are largely unaffected by gypsification and anhydrite dissolution, demonstrate these rocks are tight, with no significant interconnected macroporosity. Therefore, the Mercia Mudstone Group may be a very good seal at depth within the target areas further to the east.

5.1.2.3 ZECHSTEIN GROUP

A small number of samples of potential seal lithologies were analysed from the Marl Slate Formation, Roxby Formation, and Sherburn Anhydrite Formation (Roxby Equivalent). The Marl Slate Formation samples were obtained from the deep Cleethorpes geothermal borehole and comprises tightly compacted mudstone and siltstones, with no significant macroporosity. These rocks are likely to be very impermeable and potentially would contribute to the seal to the Permian sandstone aquifer unit. The samples from the Roxby Formation are silty mudstones with anhydrite from shallow depth. They have been affected by gypsification but the unaltered siltstone and mudstone matrix is tight. Similarly, the Sherburn Anhydrite sample comprises dense crystalline anhydrite with no obvious porosity. As discussed above, gypsification and alteration are likely to be less significant in the deeper sequence where groundwater is very saline, and pressure and temperature are higher. Therefore, based on these very limited observations, it seems likely these Zechstein Group lithologies have the potential to be seal rocks where they are present at greater depth in the target areas.

5.2   FORTH AREA

5.2.1   Target aquifer unit characteristics

Samples were analysed from the primary target aquifer units in the Forth area, which are considered to be the Knox Pulpit Sandstone Formation and Kinnesswood Formation. In addition, a small number of samples were examined from minor secondary target aquifers, represented by sandstones in the West Lothian Oil Shale Formation, Burnside Sandstone Formation, Pathhead Formation, Passage Formation and Upper Limestone Formation.

The Knox Pulpit Sandstone Formation samples are characterised by moderately well sorted, very fine, fine and medium grained subfeldspathic arenites. It consists of coarser well-rounded aeolian sand grains and fine angular to subangular grains, often in discrete laminae. The detrital components comprise mainly quartz with subordinate K-feldspar, minor to trace muscovite, and traces of heavy minerals. Plagioclase and albite are rare or absent. Lithic fragments are also rare but may have been underestimated in the modal data. Intergranular clay is present in thin laminae and as pseudomatrix clay produced by the compactional deformation of plastic mudstone clasts or clay pellets. The Kinnesswood Sandstone Formation samples are also dominated by mineralogically-similar subfeldspathic arenites, ranging from fine to medium sandstone. However in these rocks the sand is predominantly angular to subangular.

Ferroan dolomite and ankerite are major cements in both units; partially filling residual intergranular pore space, replacing detrital framework grains, and replacing eodiagenetic (pedogenic) dolocrete or calcrete nodules. Quartz and K-feldspar overgrowths for minor cements and minor calcite and occasional barite may also be present as intergranular cements. Authigenic kaolinite, replacing detrital framework grains (probably largely plagioclase and lithic clasts) is common.

The Kinnesswood Sandstone Formation samples have the highest mean porosity (17%) but porosity ranges from about 7% to 22%. The Knox Pulpit Sandstone Formation has a slightly lower mean porosity (14%) but ranges from 3% to 26 %. The porosity characteristics of these rocks have been significantly influenced by burial compaction and diagenetic processes. Compaction has had a significant effect, reducing the primary intergranular porosity considerably in both formations. Much of the present porosity in these rocks is secondary, and dominated by the dissolution of feldspar (or lithic clast) framework grains, which produced large oversized pores. Some of these framework grain dissolution sites are partially filled by microporous authigenic kaolinite. The highest porosities are found in samples from outcrop where porosity has been enhanced by the removal of ferroan dolomite cement. Where present at depth (e.g. Glenrothese borehole) this cement preserves an uncompacted sandstone fabric. The dissolution dolomite in the shallow aquifer and at outcrop most probably accounts for the production of oversized secondary intergranular pores observed in samples from these areas. Deeper samples such as those from the Glenrothes borehole where the ferroan dolomite cement has not been removed have lower porosities, which is less favourable for aquifer storage at CCS depths.

Mineralogical and porosity data are also provided for samples representing a number of minor potential aquifer units. Broadly similar processes influence the porosity observed in these rocks. However, samples from the Upper Limestone Formation and the Pathhead Formation also contain major authigenic chlorite, which replaces detrital clay, pseudomatrix clay, and reduces pore space. Siderite is also an important cementing phase in the Pathhead Formation. The samples from the Burnside Sandstone Formation represent tightly compacted and poorly-sorted, muddy sublitharenite with wackestone or packstone grain fabrics. Virtually all primary porosity has been lost in these samples through the greater compaction of these much poorer-sorted rocks.

5.2.2   Target seal characteristics

The mineralogy and porosity characteristics were examined for samples from the Ballagan Formation, which is the primary target seal unit in the Forth area. A small number of samples were also studied to provide information on the minor secondary seal target represented by the mudstones and siltstone lithologies in the Upper Coal Measures and Lower Coal Measures.

The Ballagan Formation samples examined were finely laminated siltstone and mudstone, micaceous sandstone and dolomicrite to dolomicritic mudstone. They are highly compacted, and plastic lithic grains such as mudstone clasts and clay pellets have been intensely deformed to form an intergranular pseudomatrix. The total porosity is very low (mean <2%) and essentially represented by microporosity with negligible macroporosity. Petrographic observations suggest that the Ballagan Formation would appear to represent a potentially good seal to the Kinnesswood and Knox Pulpit Sandstone formations, at least with respect to the matrix porosity and permeability of this unit. However, it was noted during core observations that fracturing is present and the petrographic characteristics of fractures has not been included within the present study. These may provide pathways for leakage through the seal and need to be investigated further.

The Upper Coal Measures and Lower Coal Measures samples are mostly represented by weakly laminated, argillaceous or pelleted clay sandstone. These are highly compacted with negligible macroporosity because plastic lithic grains such as mudstone clasts and clay pellets have been deformed to form an intergranular pseudomatrix. One Upper Coal Measures sandstone sample of clean quartz arenite (97% quartz) from 237 m depth in the Briathorne No.4 borehole was found to be quite porous (15% total porosity) with most this (12%) present as macroporosity, even though the sandstone had a highly compacted grain fabric. In this sample the porosity is dominated by secondary framework grain dissolution porosity. The petrographic observations therefore show that there are porous and permeable horizons within thin sandstones in these units that are potential leakage pathways through these minor seal or overburden units.

5.3   OVERALL COMMENTS AND FUTURE WORK

The Cleethorpes and Glenrothes boreholes in particular, have provided a substantial amount of rock material to characterise the mineralogy, petrology and porosity of potential aquifer and seal units at CCS suitable depths. Further samples from borehole core provided good indications on mineralogical and porosity changes at slightly shallower depths, which may be of great use in modelling the up-dip migration of theoretical CO_2 injection and in characterising the overburden to the aquifer and seal.

Future work should focus on analysing more samples of seal rocks from CCS depths and in better characterising the range of lithologies available, as well as the fractures observed in some cores.

Appendix 1 CASSEM borehole and outcrop sample locations

Borehole or outcrop name	Borehole BGS no.	BNG Easting	BNG Northing
GLENROTHES	NO20SE385	325617	703144
MILTON OF BALGONIE 2	NO30SW187	331821	700235
KINCARDINE EAST LONGANNET COLLIERY	NS98NW230	293900	686400
COUSLAND 1	NT36NE222	337810	668020
CROPWELL BRIDGE CROPWELL BISHOP	SK63NE28	467730	335473
GAMSTON	SK77NW29	470330	376550
FULBECK AIRFIELD FB1	SK85SE25	488893	350533
CLEETHORPES 1	TA30NW51	530237	407090
MAWCARSE STATION	NO10NE3	315400	705950
BRIARTHORN NO.4 SEABORE	NT37NE49	335700	678210
NO.6 EASTER LATHRISK	NO20NE19	328370	708020
NO.3 BALREAVIE WATER BOREHOLE	NO20NE17	326900	706640
TOP OF ARRATY CRAGS	outcrop	322530	707790
BASE OF ARRATY CRAGS	outcrop	322555	707809
W END OF ARRATY CRAGS	outcrop	322454	707761
WATERFALL MASPIE DEN NR FALKLAND	outcrop	323484	706863
IN SMALL GORGE MASPIE DEN NR FALKLAND	outcrop	323592	706929
IN SMALL GORGE MASPIE DEN NR FALKLAND	outcrop	323614	706948
EARLSEAT OPENCAST SITE	outcrop	332265	697803
EARLSEAT OPENCAST SITE	outcrop	332286	697805
COUSLAND 6	NT36NE241	338345	668035

Glossary

Aeolian sandstone - sandstones produced by the movement of sand grains by wind power

Anhedral – term to describe the texture of a rock in which the mineral grains have no crystal form. Synonymous with ***xenotopic***

Anticline - a fold that is convex up and has its oldest beds at its core.

Aquifer - an underground layer of water-bearing permeable rock or unconsolidated materials (gravel, sand, silt, or clay) from which groundwater can be usefully extracted using a water well.

Argillaceous -said of rock or sediment that contains, or is composed of, clay-sized particles or clay minerals

Authigenic – pertaining to a secondary or neoformed mineral that is formed in situ in a sediment or sedimentary rock or sediment after its deposition and during subsequent burial (see also ***Diagenetic, Diagenesis***). For example, a mineral (e.g. calcite or anhydrite cements) precipitated within the intergranular pore spaces, or a secondary mineral formed as a replacement of a primary detrital mineral (e.g. kaolinite replacement of feldspars).

Basalt is a common extrusive volcanic rock. It is usually gray to black and fine-grained due to rapid cooling of lava at the surface of a planet.

BSEM – backscattered scanning electron microscopy.

Caprock (roof rock, seal) impermeable rock overlying an oil or gas reservoir that tends to prevent migration of oil or gas out of the reservoir. Commonly is it shale, anhydrite, mudstone or salt,

Carbon capture and storage (CCS) is an approach to mitigating global warming based on capturing carbon dioxide ($CO2$) from large point sources such as fossil fuel power plants and storing it deep underground instead of releasing it into the atmosphere

Claystone - sedimentary rock that is composed primarily of clay-sized particles (less than 1/256 millimetre in diameter

Detrital – pertaining to a feature or component of primary sedimentary origin, e.g. primary sedimentary particles such as sand or silt grains, or clay particles (cf. 'detritus').

Diagenesis – the sum of all processes, including both chemical and physical processes that produce changes in a sediment after its deposition. Usually, not all the minerals in a sediment are in chemical equilibrium, so changes in interstitial water composition or in temperature or in both will lead to chemical alteration of one or more of the minerals present. Diagenesis can be divided (cf. Schmidt and McDonald, 1979a) into different stages: (i) ***eodiagenesis (early diagenesis)*** – syndepositional changes or changes occurring before significant burial; ***mesodiagenesis (burial diagenesis)*** - changes occurring during burial and compaction; and ***telodiagenesis*** - late-stage changes (excluding erosion) affecting rocks at outcrop and shallow depths, as a result of meteoric groundwater penetration and weathering following uplift after burial. Diagenesis is considered a relatively low-pressure, low-temperature alteration process that involves such processes as cementation, replacement, crystallization, chemical remobilization/redistribution and leaching. With progressively deeper burial, diagenesis may be transitional into low-grade metamorphism and the boundary between the two is arbitrary but diagenesis is normally differentiated from metamorphism by lower temperatures and pressures.

Diagenetic – adjective to describe a feature or property of a sedimentary rock (e.g. mineralogy, structure, fabric, porosity, pore fluid) which formed or originated during the process of *diagenesis*.

ECD - equivalent circular diameter - morphological parameter defining the of size of particles measured in petrographical section/images

EDXA – energy-dispersive X-ray microanalysis.

Enthalpy- a quotient or description of thermodynamic potential of a system, which can be used to calculate the "useful" work obtainable from a closed thermodynamic system under constant pressure and entropy.

Eodiagenesis - see *Diagenesis*

Euhedral – term to describe the texture of a rock in which the mineral grains display very well-defined crystal form with well developed faces. Synonymous with *idiotopic*

Fluviolacustrine- Sedimentary deposits formed by a combination of fluvial (river) and lacustrine (lake) conditions

Formation -a basic rock unit distinctive enough to be readily recognizable in the field and widespread and thick enough to be plotted on a map. It describes the strata, such as limestone, sandstone, shale, or combinations of these and other rock types

Fossils - are the preserved remains or traces of animals, plants, and other organisms from the remote past

Hypidiotopic – term to describe the texture of a rock in which the mineral grains display some trace crystal of crystal form. Intermediate between *idiotopic* and *xenotopic*. Synonymous with *subeuhedral*

Idiotopic – term to describe the texture of a rock in which the mineral grains display very well-defined crystal form with well developed faces. Synonymous with *euhedral*

Igneous rocks are formed by solidification of cooled magma (molten rock). They may form with or without crystallization, either below the surface as intrusive (plutonic) rocks or on the surface as extrusive (volcanic) rocks).

Limestone is a sedimentary rock composed largely of the mineral calcite (calcium carbonate: $CaCO_3$).

Lithology - description of rocks on the basis of colour, structure, mineral composition, and grain size; the physical character of a rock.

Macropores –pores observed in petrographical sections with ECD >15μm.

Mesodiagenesis - see *Diagenesis*

Mesopores – pores observed in petrographical sections with ECD >5μm and <15μm.

Micropores – pores observed in petrographical sections with ECD <5μm

Mineralogical modal analysis - see *Modal analysis*.

Modal analysis – alternatively referred to as *mineralogical modal analysis* - the percentage by volume of each of the minerals that make up a rock. Usually determined by point-counting of mineral grains and pores recorded from representative traverses observed in petrographical thin section, using an optical petrological (polarizing) microscope. May also be determined by petrographical image analysis (PIA) of petrographical images recorded from thin sections or polished rock slices.

Mudstone (also called *mudrock*) is a fine grained sedimentary rock whose original constituents were clays or muds. Grain size is up to 0.0625 mm (0.0025 in) with individual grains too small to be distinguished without a microscope

Outcrop- referring to the appearance of bedrock or superficial deposits exposed at the surface of the Earth.

Neoformed – pertaining to a feature (usually a mineral) formed in situ within a rock – i.e. a 'newly-formed' phase or feature of secondary origin, as opposed to a feature of primary origin (see also ***Authigenic***).

Pedogenesis – the process or sum of processes, of soil formation. Can also be regarded as **early diagenesis (eodiagenesis)** in relation to syndepositional near-surface subaerial alteration of sediments.

Pedogenic - pertaining to a feature (e.g. mineral, fabric, structure) of a sediment or rock which has its origins in ***pedogenesis***.

Permeability - the ability, or measurement of a rock's ability, to transmit fluids, typically measured in darcies or millidarcies. Formations that transmit fluids readily, such as sandstones, are described as permeable and tend to have many large, well-connected pores

PIA – *petrographic image analysis*. Quantitative analysis of features in petrographical sections using digital (computerised) processing of images.

Porosity - the percentage of pore volume or void space, or that volume within rock that can contain fluids

Sandstone is a sedimentary rock composed mainly of sand-size mineral or rock grains

Saline aquifer - A deep underground rock formation composed of permeable materials and containing highly saline fluids.

Seal Rock - the impervious capping which prevents the upward migration of hydrocarbons from reservoir often comprising clays, shales or evaporites.

Sedimentary rock is formed by deposition and consolidation of mineral and organic material and from precipitation of minerals from solution *SEI* – secondary electron image.

SEM –scanning electron microscopy.

Siltstone is a sedimentary rock which has a composition intermediate in grain size between the coarser sandstones and the finer mudstones and shales.

Stratigraphy- a branch of geology, studies rock layers and layering (stratification).

Subhedral – term to describe the texture of a rock in which the mineral grains display some trace crystal of crystal form. Intermediate between ***euhedral*** and ***anhedral***. Synonymous with ***hypidiotopic.***

Syncline- a downward-curving fold, with layers that dip toward the center of the structure

Syntaxial – term to describe the growth of a mineral in which new growth occurs in optical or crystallographic continuity with that of the underlying mineral substrate.

Telodiagenesis - see ***Diagenesis***

Tight – term used describe low permeability, or a rock fabric in which little porosity is present or visible in thin section.

Tuff - a type of rock consisting of consolidated volcanic ash ejected from vents during a volcanic eruption

*Unconformity-*a surface of erosion or nondeposition that separates younger strata from older strata; most unconformities indicate intervals of time when former areas of the sea bottom were temporarily raised above sea level.

Xenotopic – term to describe the texture of a rock in which the mineral grains have no crystal form. Synonymous with ***anhedral***

References

British Geological Survey holds most of the references listed below, and copies may be obtained via the library service subject to copyright legislation (contact libuser@bgs.ac.uk for details). The library catalogue is available at: http://geolib.bgs.ac.uk.

ALLEN, D.J., BREWERTON, L.J., COLEBY, L.M., GIBBS, B.R., LEWIS. M.A., MACDONALD A.M., WAGSTAFF, S.J. AND WILLIAMS, A.T. 1997. The physical properties of major aquifers in England and Wales. *British Geological Survey Technical Report WD/97/34* 312pp [Also published as *Environment Agency. R&D Report*, **8**,.312pp.]

ATKINS, P.W. 1982. *Physical Chemistry* (2nd Edition). Oxford Univesity Press.

BATH, A. H., DARLING, W. G., GEORGE, I. A. AND MILODOWSKI, A. E. 1987. $^{18}O/^{16}O$ and $^2H/^1H$ changes during progressive hydration of a Zechstein anhydrite formation. *Geochimica et Cosmochimica Acta*, **51**, 3113-3118.

BATH, A.H., MILODOWSKI, A.E. AND STRONG, G.E. 1986. Fluid flow and diagenesis in the East Midlands Triassic sandstone aquifer. *In:* GOFF, J.C. AND WILLIAMS, B.P.J. (editors). *Fluid Flow in Sedimentary Basins and Aquifers*, Geological Society Special Publications, **34**, 127-140.

BATH, A.H., MILODOWSKI, A.E. AND SPIRO, B. 1987. Diagenesis of carbonate cements in Permo-Triassic sandstones in the Wessex and East Yorkshire-Lincolnshire basins, UK: a stable isotope study. *In:* MARSHALL, J.D. (editor). *Diagenesis of Sedimentary Sequences*. Geological Society Special Publication, **36**, 173-190.

BRERETON, R., BROWNE, M.A.E, CRIPPS, A.C., GEBSKI, J.S., BIRD, M., HALLEY, D.N. AND MCMILLAN, A.A. 1988. Glenrothes Borehole: Geological Well Completion Report. Investigation of the Geothermal Potential of the UK, *British Geological Survey TechnicalReport* **WJ/GE/88/2**.

BROWN, H.C.T. 1970. *Examination of the Factors influencing the Hydrology of the Bunter Sandstone in the East Midlands*. Unpublished PhD Thesis, University of Loughborough.

BROWNE, M.A.E., HARGREAVES, R.L. AND SMITH, I.F. 1985. The Upper Palaeozoic Basins of the Midland Valley of Scotland. Investigation of the Geothermal Potential of the UK, British Geological Survey.

BURLEY, S.D. 1984. Patterns of diagenesis in the Sherwood Sandstone Group (Triassic), United Kingdom. *Clay Minerals*, **19**, 403-440.

CHADWICK, R.A., HOLLOWAY, S., BROOK, M.S. AND KIRBY, G.A. 2004. The case for underground CO_2 sequestration in northern Europe. *In:* BAINES, S.J. AND WORDEN, R.H. *Geological Storage of Carbon Dioxide.* Geological Society Special Publication, **233**, 17-28.

CHISHOLM, J I, AND DEAN, J M, 1974. The Upper Old Red Sandstone of Fife and Kinross: a fluviatile sequence with evidence of marine incursion. *Scottish Journal of Geology*, **10**, 1-30.

DOWNING , R.A., ALLEN, D.J., BIRD, M.J. GALE, I.N., KAY, R.L.F. AND SMITH, I.F. 1985. Cleethorpes No.1 Geothermal Well – a preliminary assessment of the resource. *Investigation of the Geothermal Potential of the UK. British Geological Survey.*

DOWNING, R.A., EDMUNDS, W.M. AND GALE, I.N. 1986. Regional groundwater flow in sedimentary basins in the U.K. *In:* GOFF, J.C. AND WILLIAMS, B.P.J. (editors). *Fluid Flow in Sedimentary Basins and Aquifers*. Geological Society Special Publications, **34**, 105-125.

FORD, J R, PHARAOH, T C, HULBERT, A G, VINCENT, C J AND COOPER, A H. 2008. CASSEM Work Package One - British East Midlands and Lincolnshire Geological Modelling. *British Geological Survey Commissioned Report*, **CR/08/152**.

GLENNIE, K.W., MUDD, G.C. AND NAGTEGAAL, P.J.C. 1978. Deposition environment and diagenesis of Permian Rotliegendes sandstones in Leman Bank and Sole Pit areas of the UK southern North Sea. *Journal of the Geological Society*, **135**, 25-34.

GALE, J. 2004. Why do we need to consider geological storage of CO_2? *In:* BAINES, S.J. AND WORDEN, R.H. *Geological Storage of Carbon Dioxide.* Geological Society Special Publication, **233**, 7-15.

GUSTAVSON, T.C. AND HOVOR, S. 1994. Origin of satin spar veins in evaporite basins. *Journal of Sedimentary Research*, A**64**, 88-94.

HALLSWORTH, C.R. AND KNOX, R.W.O'B. 1999. BGS Rock Classification Scheme. Volume 3: Classification of sediments and sedimentary rocks. *British Geological Survey Research Report*, **RR99-03**.

HODGE, T. 2003. The Saltfleetby Field, Block L 47/16, Licence PEDL 005, Onshore UK. *In:* GLUYAS, J.G. AND HICHENS, H.M. (editors). *United Kingdom Oil and Gas Fields, Commemorative Millennium Volume.* Geological Society, London, Memoir, **20**, 911-919.

HOWARD, A.S., WARRINGTON, G., CARNEY, J.N., AMBROSE, K., YOUNG, S.R., PHAROAH, T.C., CHENEY, C.S. 2008. Geology of the Nottingham District. *Memoir for the 1:50 000 Geological Sheet 126 (England and Wales.* British Geological Survey, Keyworth, Nottingham.

MARIE, J.P.P. 1975. Rotliegendes stratigraphy and diagenesis. *In:* Woodland, A.W. (editor). *Petroleum and the Continental Shelf of North-West Europe. Volume 1*, 205-210. Applied Sciences Publishers, Barking.

MCHARDY, W.J., WILSON, M.J. AND TAIT, J.M. 1982. Electron microscope and X-ray diffraction studies of filamentous illitic clay from sandstones of the Magnus Field. *Clay Minerals*, **17**, 23-39.

MILODOWSKI, A.E., STRONG, G.E., WILSON, K.S., HOLLOWAY, S. AND BATH, A.H. 1987. Diagenetic influences on the aquifer properties of the Permo-Triassic sandstones in the East Yorkshire and Lincolnshire Basin. *Investigation of the Geothermal Potential of the UK. British Geological Survey.*

MONAGHAN, A.A., MCINROY, D.B., BROWNE, M.A.E. AND NAPIER, B.R. 2008. CASSEM Work Package One - Forth Geological Modelling. *British Geological Survey Commissioned Report*, **CR/08/151**. 82pp.

PETTIJOHN, F.J., POTTER, O.E. AND SEIVER, R. 1987. *Sand and Sandstone*. New York: Springer.

ROTHWELL, N.R. AND QUINN, P. 1987. The Welton Oilfield. *In:* BROOKS, J. AND GLENNIE, K. (editors). *Petroleum Geology of North West Europe.* Graham & Trottman. pp. 181-189.

SEEMAN, U. 1979. Diagenetically formed interstitial clay minerals as a factor in Rotliegend Sandstone reservoir quality in the Dutch Sector of the North Sea. *Journal of Petroleum Geology*, **1**, 55-62.

SCHMIDT, V. AND MCDONALD, D.A.. 1979a. The role of secondary porosity in the course of sandstone diagenesis. *In*: SCHOLLE, P.A. AND SCHLUGER, P.R. (editors). *Aspects of Diagenesis*. Society of Economic Paleontologists and Mineralogists Special Publication, **26**, 175-207.

SCHMIDT, V. AND MCDONALD, D.A.. 1979b. Texture recognition of secondary porosity in sandstones. *In*: SCHOLLE, P.A. AND SCHLUGER, P.R. (editors). *Aspects of Diagenesis*. Society of Economic Paleontologists and Mineralogists Special Publication, **26**, 209-225.

SCOTT, J. AND COLTER, V.S. 1987. Geological aspects of current onshore Great Britain exploration plays. *In:* BROOKS, J. AND GLENNIE, K. (editors). *Petroleum Geology of North West Europe.* Graham & Trottman. pp. 95-107.

SMITH, D.B. AND MOORE, P.J. 1973. Deposits pg gypsum at Hurworth Place, Darlington. *Report, Institute of Geological Sciences*. **73**, HMSO, London.

STOREY, M.W. AND NASH, D.F. 1993. The Eakring Dukeswood oil field: an unconventional technique to describe a field's geology. *In:* Parker, J.R. *Petroleum Geology of Northwest Europe: Proceedings of the 4th Conference*. Petroleum Geology'86 Ltd. Published by The Geological Society, London, pp. 1527-1537.

STRONG, G.E. AND MILODOWSKI, A.E. 1987. Aspects of the diagenesis of the Sherwood Sandstones of the Wessex Basin and their influence on reservoir characteristics. *In*: MARSHALL, J.D. (editor). *Diagenesis of Sedimentary Sequences*. Geological Society Special Publication, **36**, 325-337.

WARD, J., CHAN, A. AND RAMSAY, B. 2003. The Hatfield Moors and Hatfield West Gas Storage Fields, South Yorkshire. *In:* GLUYAS, J.G. AND HICHENS, H.M. (editors). *United Kingdom Oil and Gas Fields, Commemorative Millennium Volume.* Geological Society, London, Memoir, **20**, 105-125.